

Western  Graduate&PostdoctoralStudies

Western University  
Scholarship@Western

---

Electronic Thesis and Dissertation Repository

---

2-5-2013 12:00 AM

## Synthesis and Spectroscopic Studies of Substituted Pyrrolocytidines

McKenry Charles  
*The University of Western Ontario*

Supervisor  
Robert H. E. Hudson  
*The University of Western Ontario*

Graduate Program in Chemistry  
A thesis submitted in partial fulfillment of the requirements for the degree in Master of Science  
© McKenry Charles 2013

Follow this and additional works at: <https://ir.lib.uwo.ca/etd>

 Part of the [Chemicals and Drugs Commons](#)

---

### Recommended Citation

Charles, McKenry, "Synthesis and Spectroscopic Studies of Substituted Pyrrolocytidines" (2013).  
*Electronic Thesis and Dissertation Repository*. 1125.  
<https://ir.lib.uwo.ca/etd/1125>

This Dissertation/Thesis is brought to you for free and open access by Scholarship@Western. It has been accepted for inclusion in Electronic Thesis and Dissertation Repository by an authorized administrator of Scholarship@Western. For more information, please contact [wlsadmin@uwo.ca](mailto:wlsadmin@uwo.ca).

SYNTHESIS AND SPECTROSCOPIC STUDIES OF SUBSTITUTED  
PYRROLOCYTIDINES

(Spine title: Synthesis And Spectroscopic Studies of Cytidine Analogs)

(Thesis format: Monograph)

by

McKenry Charles

Graduate Program in Chemistry

A thesis submitted in partial fulfillment  
of the requirements for the degree of  
Master of Science

The School of Graduate and Postdoctoral Studies  
The University of Western Ontario  
London, Ontario, Canada

© McKenry Charles 2012

THE UNIVERSITY OF WESTERN ONTARIO  
School of Graduate and Postdoctoral Studies

**CERTIFICATE OF EXAMINATION**

Supervisor

Examiners

\_\_\_\_\_  
Dr. Robert H. E. Hudson

\_\_\_\_\_  
Dr. Martin J. Stillman

Supervisory Committee

\_\_\_\_\_  
Dr. Elizabeth R. Gillies

\_\_\_\_\_  
Dr. James Wisner

\_\_\_\_\_  
Dr. Gilles A. Lajoie

The thesis by

**McKenry Charles**

entitled:

**Synthesis and Spectroscopic Studies of Substituted  
Pyrrolocytidines**

is accepted in partial fulfillment of the  
requirements for the degree of  
Master of Science

\_\_\_\_\_  
Date

\_\_\_\_\_  
Chair of the Thesis Examination Board

## Abstract

This thesis reports work in the area of modified nucleosides for potential use as molecular probes in nucleic acid chemistry. These heterocyclic base surrogates that are capable of canonical base pairing have use in the study of nucleic acid conformation, as reporters of the state of hybridization.<sup>[1]</sup>

The synthesis of a 5-phenylpyrrolocytidine was attempted in order to compare its properties with its 6-substituted pyrrolocytidine counterpart. Unfortunately, the 5-substituted pyrrolocytidine was not achieved.

The synthesis of five nucleosides based on the pyrrolocytidine scaffold was reported. Their synthesis was achieved through the tandem Sonogashira/annulations reaction between 5-iodocytidine derivatives and terminal alkynes to yield the bicyclic nucleoside pyrrolocytidine.

Photophysical studies were performed to determine possible FRET pairs to be used as molecular beacons and Stern-Volmer plots were used to determine how effective each quencher was at reducing the fluorescence intensity of the fluorophores. The molar absorptivity of a 6-DABCYL mimic pyrrolocytidine was determined and compared with the universal quencher DABCYL.

## Keywords

DNA, Organic Synthesis, Modified Nucleobases, Deoxycytidine, Pyrrolocytidine, 5-iododeoxycytidine, Quencher, Fluorophore, Stern-Volmer plot.

## Acknowledgments

I would like to thank my supervisor professor Robert H. E. Hudson for taking me on as a student after many years of inactivity in chemistry, I am very grateful. This work would not have been possible without his support and guidance; I could not have asked for more from a supervisor. Over the years he has been a friend, mentor and as I move forward to the next chapter of my life his teachings will never be forgotten. Thank you.

Thanks to all my lab mates that I have learned from and worked closely with, notably: David, Mohamed, Andre, Mojmir, Mark, Kirby, Dwayne, Sam, Christie, Kelly, Melissa, Adam, Rachael and Augusto. You guys have helped make my experience an educational and memorable one. Also, previous members of the Hudson group who have paved the way and provide valuable products which were used in my photophysical studies.

I also thank Dr. Mark Workentin for his valuable suggestions and comments during the photophysical experiments.

I would like to also thank my committee members and examiners for taking the time to review my thesis and for their helpful discussions along the way.

I can't forget the wonderful staffs in the main office of chemistry, which were always willing and ready to help. Thank you Clara, Sandy, Anna and Darlene, you guys are wonderful and I will miss you.

Thanks to Mr. Mario Otalora for his help with graphic design.

In addition, I would like to thank Mr. Mathew Willans for the maintenance of the NMR facility and Mr. Doug Hairsine for performing HRMS of small molecules, from the department of chemistry at the University of Western Ontario.

Most importantly, I would like to thank my significant other Melissa Van Sas, our daughter McKayla Charles, parents: Nathalie and Johnson, extended family and friends for their support throughout the years; I could not have done it without you.

# Table of Contents

<b>CERTIFICATE OF EXAMINATION</b> .....	ii
Abstract .....	iii
Acknowledgments.....	iv
Table of Contents .....	v
List of Tables .....	viii
List of Schemes .....	ix
List of Figures .....	xii
List of Abbreviations .....	xv
List of Appendices .....	xvii
Chapter 1 .....	1
1 Introduction to nucleic acid chemistry .....	1
1.1 Single nucleotide polymorphisms and their diagnosis .....	4
1.2 Nucleic acid analogues as molecular probes .....	7
1.3 Unnatural nucleic acid analogues .....	10
1.4 Palladium/copper catalyzed reactions.....	11
1.5 6-substituted pyrrolocytidines versus 5-substituted pyrrolocytidines.....	12
1.6 Fluorescence quenching.....	13
1.7 Stern-Volmer plots.....	15
1.8 Overview.....	16
Chapter 2.....	17
2 Towards 5-phenylpyrrolocytidine.....	17
2.1 Chapter Introduction .....	17
2.2 Results and Discussion .....	18
2.2.1 Synthesis of 5-(trimethylsilylethynyl)-3',5'-diacetyl-2'-deoxyuridine ....	18

2.3 Conclusion .....	29
2.4 Future Outlook .....	29
2.5 Experimental .....	29
General experimental procedures.....	29
2.5.1 Synthesis of 3',5'-diacetyl-2'-deoxyfuranouridine.....	30
Chapter 3.....	33
3 Synthesis of 6-substituted pyrrolocytidines .....	33
3.1 Chapter Introduction .....	33
3.2 Results and Discussion .....	34
3.2.1 Synthesis of aromatic alkynes.....	34
3.2.2 Synthesis of 6-substituted pyrrolocytidine nucleobases .....	37
3.3 Conclusion .....	41
3.4 Future Outlook .....	41
3.5 Experimental .....	42
3.5.1 Synthesis of the <i>para</i> -nitrobenzene acetylene ( <b>11</b> ).....	42
3.5.2 Syntheses of the DABCYL mimic alkyne ( <b>14</b> ) .....	43
3.5.3 Synthesis of 6-substituted pyrrolocytidines ( <b>18</b> ) .....	45
Chapter 4.....	50
4 Photophysical Quenching Studies.....	50
4.1 Chapter Introduction .....	50
4.2 Results and Discussion .....	51
4.2.1 Quenching of 1 $\mu$ M pyrene (Fa) fluorophore with 1 mM of the quencher 18a.....	55
4.2.2 Quenching of 1 $\mu$ M pyrene (Fa) fluorophore with 10 mM <i>p</i> -nitrophenylpC moiety (Qb).....	58
4.2.3 Quenching of 5 $\mu$ M pyrene (Fa) fluorophore with 10 mM 5-((4- nitrophenyl)ethynyl) cytosine moiety (Qc).....	61

4.2.4	Quenching of 1 $\mu\text{M}$ Fb fluorophore with 1 mM DABCYL mimic (18a).	63
4.2.5	Quenching of 1 $\mu\text{M}$ Fb fluorophore with 10 mM 6-(4-nitrophenyl)pC ethylester moiety (Qb)	65
4.2.6	Quenching of 1 $\mu\text{M}$ Fb fluorophore with 10 mM 5-((4-nitrophenyl)ethynyl) cytosine ethylester moiety (Qc)	67
4.2.7	Isomerization test for the quencher 18a	69
4.2.8	Determination of the quencher 18a molar absorptivity	73
4.3	Conclusion	75
4.4	Future Outlook	76
4.5	Experimental	77
4.5.1	Preparation of the 5 $\mu\text{M}$ pyrene (Fa) solution	77
4.5.2	Preparation of the 1 $\mu\text{M}$ pyrene (Fa) solution	77
4.5.3	Preparation of the 1 $\mu\text{M}$ phenyl pC acid (Fb) solution	77
4.5.4	Preparation of the 1 mM azopyrrolocytidine (18a) solution	78
4.5.5	Preparation of the 10 mM 6-(4-nitrophenyl) pC moiety (Qb) solution	78
4.5.6	Preparation of the 10 mM 5-((4-nitrophenyl)ethynyl)cytosine moiety (Qc) solution	78
4.5.7	Quenching studies	78
4.5.8	Isomerization test for the 18a quencher	79
4.5.9	Determination of the molar absorptivity of 18a	79
Chapter 5		80
5	Conclusion and Outlook	80
	References	82
	Appendices	85
	Curriculum Vitae	102



## List of Tables

<b>Table 2.1:</b> Summarized table of results for the attempted synthesis of the fU (compounds <b>3</b> and <b>4</b> ) base.....	23
<b>Table 2.2:</b> Unsuccessful attempts towards the synthesis of compound <b>5</b> to <b>6</b> .....	25

## List of Schemes

<b>Scheme 1.1:</b> Information flow in biological systems.....	2
<b>Scheme 1.2:</b> Illustration of a positive response (fluorescence) of a base discriminating fluorophore (BDF) upon hybridization to its match versus its mismatch.....	6
<b>Scheme 1.3:</b> Illustration of FRET mechanism operation used in molecular beacon technology.....	6
<b>Scheme 1.4:</b> Representation of a fluorescent RNase H assay using a dual label system employing a fluorophore and a quencher.....	8
<b>Scheme 1.5:</b> The Castro-Stephens reaction.....	8
<b>Scheme 1.6:</b> Catalytic cycle of the Pd/Cu Sonogashira reaction.....	12
<b>Scheme 2.1:</b> Illustration of the starting material and the 5-phenylpyrrolocytidine nucleoside.....	17
<b>Scheme 2.2:</b> Schematic illustration of the synthesis of 5-(trimethylsilylethynyl)-3',5'-diacetyl-2'-deoxyuridine. Also, the schematic for the attempted synthesis towards two substituted furanouridine nucleobases are shown.....	19
<b>Scheme 2.3:</b> Synthetic scheme of the 5-endo dig cyclization reported by Dembinski.....	20
<b>Scheme 2.4:</b> Illustration of the nucleophilic attack of the alkyne towards the electrophilic source of iodine.....	20
<b>Scheme 2.5:</b> Mechanism for the 5-endo-dig Ag <sup>+</sup> catalyzed reaction proposed by Agrofoglio.....	21
<b>Scheme 2.6:</b> Illustration of the cationic intermediate that would be formed during the 5-endo-dig cyclization product.....	22
<b>Scheme 2.7:</b> Schematic of the desilylation reaction of compound <b>5</b> .....	24

<b>Scheme 2.8:</b> Schematic of the attempted cyclization of compound <b>5</b> using Agrofoglio methodology.....	24
<b>Scheme 2.9:</b> Illustration of the unfavourable intermediate during the formation of compound <b>7</b> .....	25
<b>Scheme 2.10:</b> Schematic illustration for the synthesis of compound <b>6</b> from compound <b>5</b> ....	26
<b>Scheme 2.11:</b> Schematic of the attempted iodination and atom exchange on the fU nucleobase.....	27
<b>Scheme 2.12:</b> Illustration of the iodination at the 3-position of the indole reaction reported by Zolfigol.....	28
<b>Scheme 3.1:</b> Schematic representation of the 5-alkynylcytidine via the 5-endo-dig cyclization to the pyrrolocytidine nucleobase (A) and subsequent removal of the benzoyl group (B)....	33
<b>Scheme 3.2:</b> Schematic of the synthetic methodology used to obtain compound <b>11</b> .....	35
<b>Scheme 3.3:</b> Mechanism for the deprotection of trimethylsilyl in methanol with potassium carbonate.....	35
<b>Scheme 3.4:</b> Synthetic illustrations for the synthesis of the DABCYL mimic alkyne <b>14</b> .....	36
<b>Scheme 3.5:</b> Proposed mechanism for the formation of compound <b>12</b> via the diazonium salt, where 'B' stands for base.....	37
<b>Scheme 3.6:</b> Synthetic scheme towards the various 6-substituted pyrrolocytidine nucleobases.....	39
<b>Scheme 3.7:</b> Synthetic scheme of 2-[6-arylethynyl]pyridin-3-yl]-1H-benzimidazole using microwave technology reported by Raut.....	41
<b>Scheme 3.8:</b> Scheme of the synthesis from the pyrrolocytidine nucleoside to the phosphoramidite derivative.....	42

<b>Scheme 4.1:</b> Trans (left) to cis (right) equilibrium for the isomerization of the azopyrrolocytidine quencher.....	71
<b>Scheme 4.2:</b> Proposed mechanisms for the isomerization of the azopyrrolocytidine quencher (18a) from the trans-cis isomer.....	72
<b>Scheme 4.3:</b> Illustration of FRET mechanism operation used in molecular beacon technology.....	76

## List of Figures

- Figure 1.1:** Schematic of DNA polymer showing the repeating structure (nucleotide), 5'-phosphate group and 3'-hydroxyl group. The 'Base' on the sugar represents any of the four naturally occurring nucleobases.....3
- Figure 1.2:** Schematic illustration of A-, B-, and Z-form DNAs. Also shown are the views of A-, B-, and Z-form DNA down the helical axis.....3
- Figure 1.3:** Illustration of the base pairs hydrogen bonding to each other via their Watson-Crick base pair faces, with adenine (A) to thymine (T) and guanine (G) to cytosine (C). The sugar phosphate backbone of DNA is represented by backbone in this schematic.....4
- Figure 1.4:** DNA strand 2 showing a single nucleotide cytosine (C) to thymine (T) polymorphism from DNA 1.....5
- Figure 1.5:** Comparison of the structures of DNA (top) and PNA (bottom).....7
- Figure 1.6:** Structural example of the parent pyrimidine and purine showing the numbering system of the atoms.....9
- Figure 1.7:** Illustrative examples of arbitrary classes of fluorescent nucleobases. Class I: pendant fluorophore (circled), class II: non base-pairing analogs; class III base-pairing capable analog.....10
- Figure 1.8:** Illustration showing the H-bonding donor (D) and acceptor (A) properties of cytosine (C) and pyrrolocytidine (pC) analogs as well as the numbering system for pC.....11
- Figure 1.9:** Illustration of a 5-substituted pC versus a 6-substituted pC.....12
- Figure 1.10:** Jablonski diagram showing the radiative and non radiative transition between electronic states.....13
- Figure 1.11:** Diagram showing the Stokes shift resulting from the difference between the absorption and emission spectra.....14

<b>Figure 2.1:</b> Structural representation of cytosine (C), pyrrolocytosine (pC), furanouracil (fU) and uracil (U) showing their hydrogen bonding donor (D) and acceptor (A) properties.....	18
<b>Figure 2.2:</b> Illustration of the comparison between the fU and benzofuran as well as the pC and indole ring.....	28
<b>Figure 4.1:</b> Jablonski diagram showing resonance energy transfer between donor and acceptor fluorophore, as well as the spectral overlap for donor emission and absorption spectra of fluorophores.....	50
<b>Figure 4.2:</b> Illustration showing structural components of fluorophores and quenchers used in quenching studies.....	52
<b>Figure 4.3:</b> UV-visible spectra of a 5 $\mu$ M solution of <b>18a</b> (A), <b>Qb</b> (B) and <b>Qc</b> (C).....	54
<b>Figure 4.4:</b> UV-Visible spectra (A), quenching spectra ( $\lambda_{ex} = 334$ nm) (B) and Stern-Volmer plot (C) for 1 $\mu$ M pyrene and <b>18a</b> .....	57
<b>Figure 4.5:</b> UV-visible spectra (A), quenching spectra ( $\lambda_{ex} = 319$ nm) (B) and Stern-Volmer analysis plot (C) for 1 $\mu$ M pyrene and <b>Qb</b> .....	60
<b>Figure 4.6:</b> UV-visible spectra (A), quenching spectra ( $\lambda_{ex} = 334$ nm) (B) and Stern-Volmer analysis plot (C) for 5 $\mu$ M pyrene and <b>Qc</b> .....	62
<b>Figure 4.7:</b> UV-visible spectra (A), quenching spectra ( $\lambda_{ex} = 320$ nm) (B) and Stern-Volmer analysis plot (C) for 1 $\mu$ M phenylpC acid and <b>18a</b> .....	64
<b>Figure 4.8:</b> UV-Visible spectra (A), quenching spectra ( $\lambda_{ex} = 320$ nm) (B) and Stern-Volmer plot (C) for 1 $\mu$ M phenylpC acid moiety and <b>Qb</b> .....	66
<b>Figure 4.9:</b> UV-visible spectra (A), quenching spectra ( $\lambda_{ex} = 320$ nm) (B) and Stern-Volmer plot (C) for 1 $\mu$ M phenylpC acid and <b>Qc</b> .....	68
<b>Figure 4.10:</b> Spectra of a 1 $\mu$ M irradiated sample of <b>18a</b> .....	70
<b>Figure 4.11:</b> UV-visible spectrum of the trans and cis isomer of azobenzene in ethanol at room temperature.....	71

**Figure 4.12:** Plots of absorbance versus concentration to determine the molar absorptivity at 260 nm (A) and 445 nm (B) for **18a**.....74

**Figure 4.13:** Structural representation of DABCY1, SE and cytosine-1-acetic acid reference compounds.....75

## List of Abbreviations

AcOH: acetic acid

br. s: broad singlet

d: doublet

DABCYL: 4-((4-(dimethylamino)phenyl)azo)benzoic acid

dd: doublet of doublets

DMAP: *N, N*-dimethyl-4-aminopyridine

DMF: dimethylformamide

DMTr: 4,4'-dimethoxytrityl

DNA: 2'-deoxyribonucleic acid

dt: doublet of triplet

EDTA: ethylenediamine tetraacetic acid

EtOAc: ethyl acetate

Fa: pyrene

Fb: 6-(phenyl)pyrrolocytidine nucleobase

FCC: flash column chromatography

FRET: Förster resonance energy transfer

h $\nu$ : light

K: Kelvin

K<sub>sv</sub>: Stern-Volmer rate constant

m: multiplet

mM: millimolar

MeOH: methanol

MW: microwave

pC: pyrrolocytosine



Ph: phenyl

*P*-NO<sub>2</sub> Ph-: *para*-nitrophenyl

*P*-MeO Ph-: *para*-methoxyphenyl

PhpC: phenylpyrrolocytidine

ppm: parts per million

Qa: 6-(((4-(dimethylamino)phenyl)azo)benzene)pyrrolocytidine nucleobase

Qb: 6-(4-nitrophenyl)pyrrolocytidine moiety

Qc: 5-(4-nitrophenyl)ethynylcytosine moiety

s: singlet

t: triplet

TBAF: tetra-*n*-butyl ammonium fluoride

THF: tetrahydrofuran

TLC: thin layer chromatography

TMS: trimethylsilyl

## List of Appendices

<sup>1</sup> H NMR of compound <b>1</b> .....	86
<sup>1</sup> H NMR of compounds <b>2</b> .....	87
<sup>1</sup> H NMR of compound <b>5</b> .....	87
<sup>1</sup> H NMR of compound <b>6</b> .....	88
<sup>1</sup> H NMR and <sup>13</sup> C NMR of compound <b>10</b> .....	89
<sup>1</sup> H NMR and <sup>13</sup> C NMR of compound <b>11</b> .....	90
<sup>1</sup> H NMR and <sup>13</sup> C NMR of compound <b>12</b> .....	91
<sup>1</sup> H NMR and <sup>13</sup> C NMR of compound <b>13</b> .....	92
<sup>1</sup> H NMR and <sup>13</sup> C NMR of compound <b>14</b> .....	93
<sup>1</sup> H NMR and <sup>13</sup> C NMR of compound <b>15</b> .....	94
<sup>1</sup> H NMR of compound <b>16</b> .....	95
<sup>1</sup> H NMR and <sup>13</sup> C NMR of compound <b>17</b> .....	96
<sup>1</sup> H NMR and <sup>13</sup> C NMR of compound <b>18a</b> .....	97
<sup>1</sup> H NMR and <sup>13</sup> C NMR of compound <b>18b</b> .....	98
<sup>1</sup> H NMR for compound <b>18c</b> .....	99
<sup>1</sup> H NMR for compound <b>18d</b> .....	99
<sup>1</sup> H NMR and <sup>13</sup> C NMR of compound <b>18e</b> .....	100
<sup>1</sup> H NMR for compound <b>19a</b> .....	101

## Chapter 1

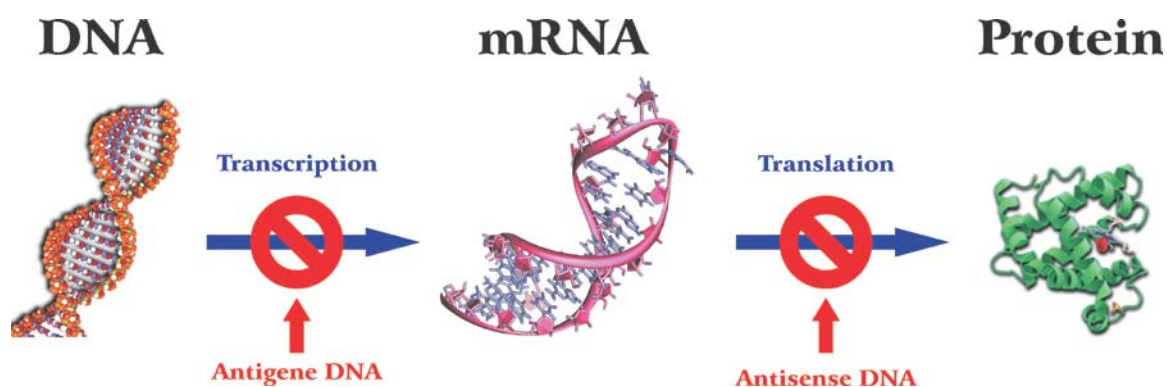
### 1 Introduction to nucleic acid chemistry

Dr. Friedrich Miescher, a Swiss scientist, was the first to isolate a novel non-protein substance from the nuclei of white blood cells in 1869 which he called “nuclein.”<sup>[2]</sup> His original findings were made using puss samples obtained from bandages that were discarded from local hospitals. Over the next 70 years many scientists made very important discoveries regarding nuclein, including: a protein free extract of nuclein prepared by Richard Altmann in 1889, which he called nucleic acid; Jacobs and Levene worked with nucleotides, and identified the phosphate, sugar and nucleobase components.<sup>[2]</sup>

In 1942 Oswald T. Avery, Colin M. MacLeod and Maclyn McCarty indentified Miescher’s original discovery, which we now know as DNA, to be the molecule of genetic inheritance.<sup>[3]</sup> The chemical structure was later elucidated in 1953 by James D. Watson and Francis H. C. Crick. These key findings have since changed how we see biology and have led to numerous advances in the field of biochemistry and in our understanding of molecular biology.<sup>[4]</sup> Over the subsequent decades since the elucidation of DNA, numerous discoveries have been made expanding our knowledge and understanding of molecular biology, including the undertaking of the human genome project. The determination of the sequence of the human genome has paved the way for many more discoveries, including: better understanding of the process of human evolution, the cause of disease and the interplay between environment and heredity in understanding human conditions.<sup>[5]</sup>

DNA contains all the necessary information for life to function and multiply. The method of propagation of DNA in the cell is the main thesis of molecular inheritance and the detailed residue-by-residue transfer of the precise order of nucleotides within a DNA molecule, which are represented by the central dogma of molecular biology; DNA is transcribed into RNA, which is translated into protein (**Scheme 1.1**).

The ability to diagnose mutations in the genome that makes us prone to diseases is therefore a very desirable ability. These advances are being made in the field of molecular biology and biochemistry. Researchers are now capable of targeting DNA and mRNA by synthesizing a complementary oligomeric strand in order to stop transcription and translation respectively; this is the antigene and antisense strategy (**Scheme 1.1**). These strategies have the potential to be used as a genetic drug to “silence” certain genes, hence turning them “off” and preventing certain genetic diseases.



**Scheme 1.1:** Information flow in biological systems

The structure of DNA consists of the four nucleobases and a backbone made of alternating 2-deoxyribose sugar which is connected via phosphodiester bonds. The four nucleobases are thymine (T) and cytosine (C) which are classified as pyrimidines and the purines adenine (A) and guanine (G). The long polymeric units are made up of simpler units called nucleotides (**Figure 1.1**); which are the building blocks of nucleic acids. The joined subunits form an extensive polymer with the 5'-OH at one end and the 3'-OH at the other end (**Figure 1.1**).

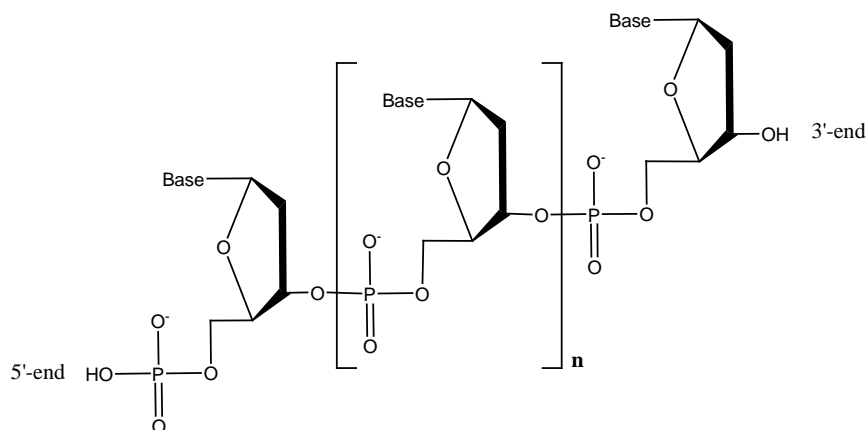


**Figure 1.1:** Schematic of DNA polymer showing the repeating structure (nucleotide), 5'-phosphate group and 3'-hydroxyl group. The 'Base' on the sugar represents any of the four naturally occurring

The two strands run antiparallel to each other and are based paired through hydrogen bonds forming one of either A, B or Z-form DNA (**Figure 1.2**).<sup>[6]</sup> In the B-DNA which contains the helical structure, there are two different types of grooves formed along the backbone when the two strands interact by base pairing. These grooves are designated as the major and minor grooves respectively, due to their sizes (**Figure 1.2**).<sup>[6]</sup>

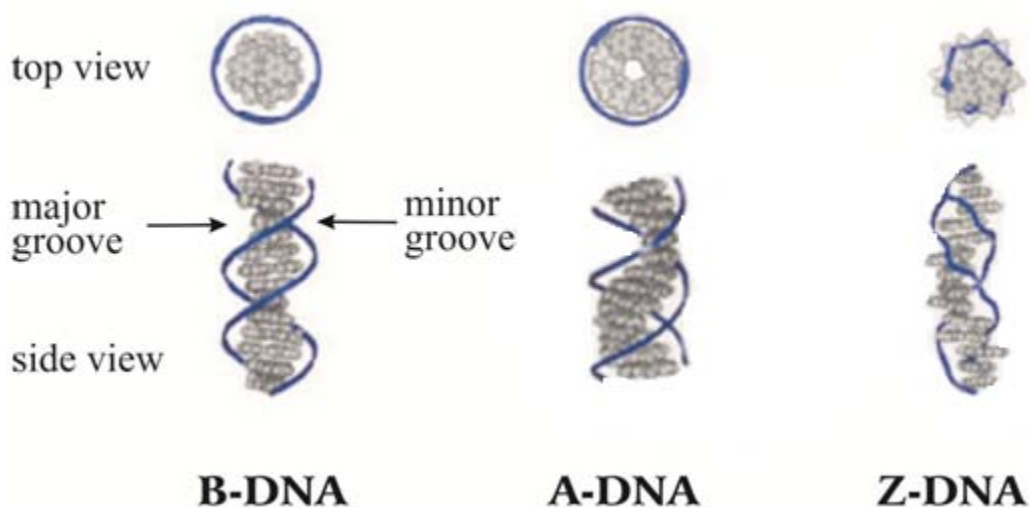


**Figure 1.2:** Schematic illustration of A-, B-, and Z-form DNAs. Also shown are the views of A-, B-, and Z-form DNA down the helical axis.

The repeating phosphate groups in the DNA backbone, gives the polymer an overall negative charge thus making it very water soluble. Due to the high electrostatic charge, there is a repulsive force associated with the binding of the two strands, which occurs by hydrogen bonding between the purine and pyrimidine nucleobases. The pyrimidines and purines hydrogen bond to each other such that the purine adenine forms two hydrogen bonds to the pyrimidine thymine, and the purine guanine forms three hydrogen bonds to the pyrimidine cytosine (**Figure 1.3**).

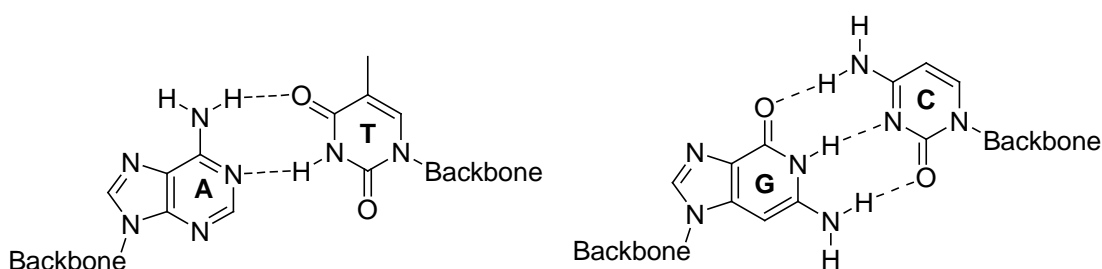


**Figure 1.3:** Illustration of the base pairs hydrogen bonding to each other via their Watson-Crick base pairing faces, with adenine (A) to thymine (T) and guanine (G) to cytosine (C). The sugar phosphate backbone of DNA is represented by 'backbone' in this schematic.

## 1.1 Single nucleotide polymorphisms and their diagnosis

Single nucleotide polymorphisms (SNPs) are a variation of the nucleobase at a single nucleotide. SNPs are the most common known form of human genetic variation and on average occurs once for every thousand nucleotides in the genome.<sup>[7]</sup> **Figure 1.4** shows a cytidine to thymine SNP in DNA.<sup>[8]</sup> SNP that occur within the coding sequence accounts for about 3 – 5% of a person's DNA that is responsible for the translation of protein.<sup>[9]</sup> Most SNP occur outside the coding sequence, however the ones that occur within the coding sequence are of particular interest, because they can alter the biological functions of proteins resulting in desirable or undesirable traits which can make one, or one's progeny susceptible to disease.<sup>[10]</sup> The ability to diagnose these permutations in the genome is therefore desirable.

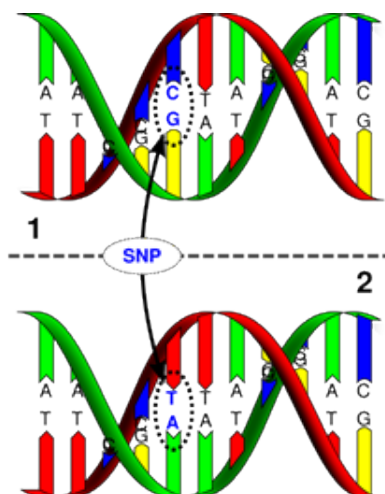
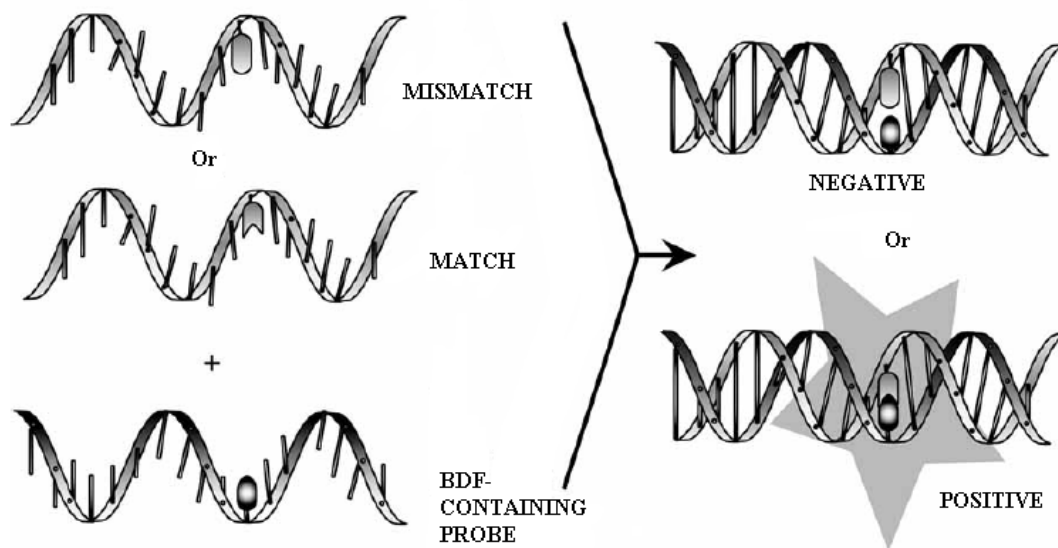


**Figure 1.4:** DNA strand 2 showing a single nucleotide cytosine (C) to thymine (T) polymorphism from DNA 1.<sup>[8]</sup>

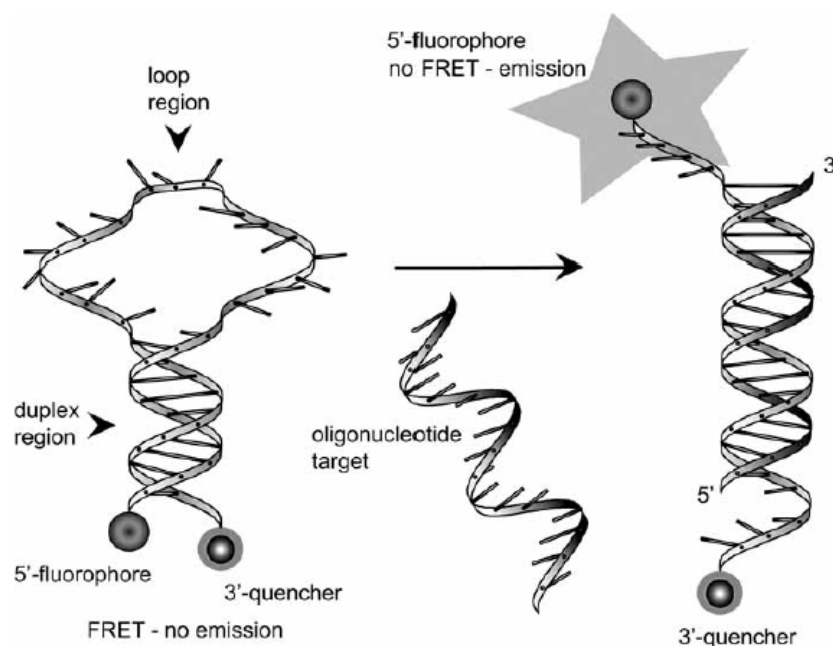
One of the most frequently used methodologies for the diagnosis of SNP employs the use of molecular probes based on Förster Resonance Energy Transfer (FRET) to monitor hybridization. A base discriminating fluorophore (BDF) containing probe that can selectively bind to its target sequence will result in a positive response upon hybridization and a negative response upon hybridization to its mismatch (**Scheme 1.2**). This methodology is preferred over the full sequencing of an amplified polymerase chain reaction (PCR) gene which is the archetypal method of SNP diagnosis; due to this methodology being costly and time consuming it is not preferred.<sup>[10]</sup>

An application for these probes is their potential to be used in antigene and antisense strategies to stop transcription and translation respectively (**Scheme 1.1**), hence “turning off” the gene. Hudson’s group has used molecular probes based on FRET extensively for use in monitoring DNA hybridization.

These molecular probes adopt a hairpin structure and consist of a fluorophore and quencher at opposing termini, a complimentary stem and a loop that is complimentary to its target (**Scheme 1.3**). Upon hybridization of the target to the loop region, the molecular probe stem unravels and the fluorophore is no longer quenched as quenching due to FRET is distance dependant; hybridization can therefore be tracked inside the cell by fluorescence microscopy using this technology.<sup>[10-11]</sup>



**Scheme 1.2:** Illustration of a positive response (fluorescence) of a base discriminating fluorophore (BDF) upon hybridization to its match versus its mismatch.<sup>[10]</sup>



**Scheme 1.3:** Illustration of FRET mechanism operation used in molecular beacon technology.<sup>[10]</sup>

Traditionally, in Hudson's group, the molecular probe strand consists of peptide nucleic acid (PNA) (**Figure 1.5**). PNA is an oligonucleotide analog that provides tight binding to complementary nucleic acid and is not susceptible to enzymatic degradation,



however it is not very water soluble.<sup>[1]</sup> PNA lack of solubility in water can be problematic for in-vivo studies in regards to the uptake of these molecular beacons into the cell.

This project was focused on the synthesis of various fluorophores and quenchers that can be incorporated into DNA oligomers, hence addressing the water solubility issue of their PNA predecessors, as well as their ability to be used in molecular beacon technology based on FRET mechanism.

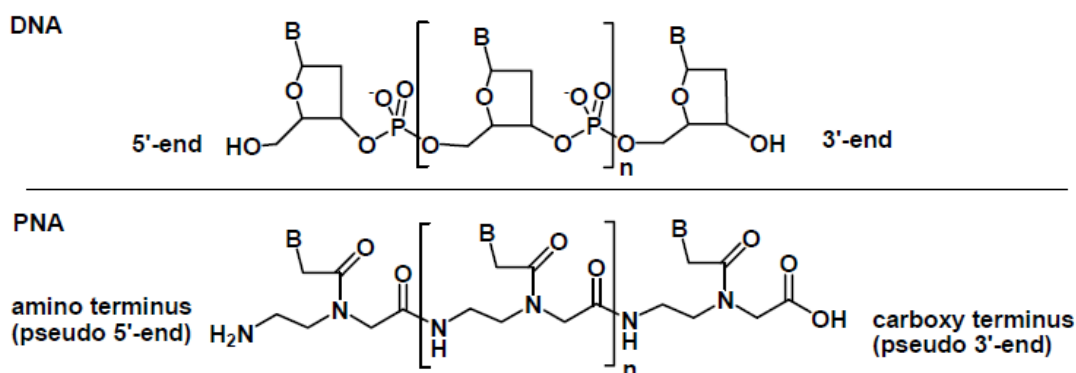


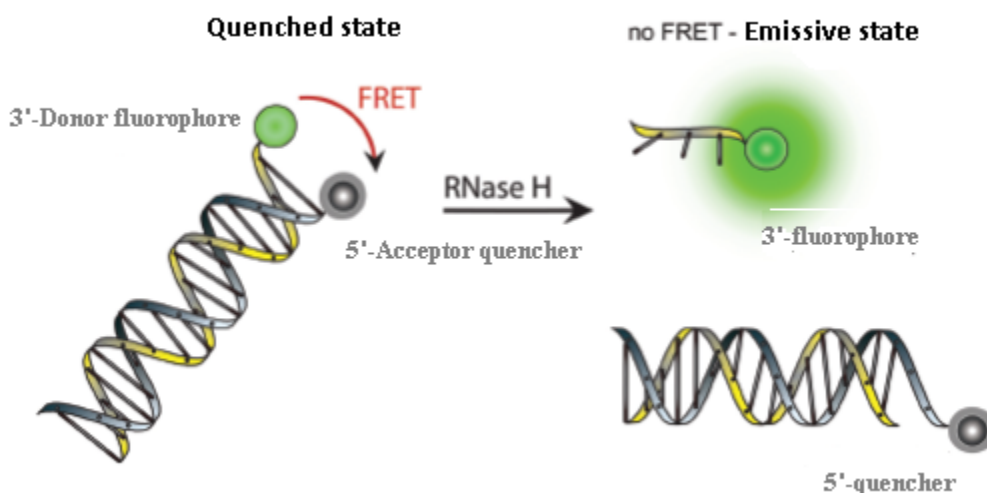
**Figure 1.5:** Comparison of the structures of DNA (top) and PNA (bottom).<sup>[1]</sup>

## 1.2 Nucleic acid analogues as molecular probes

In biological, medicinal research and diagnostics, molecular probes have applications such as: the detection of single nucleotide polymorphisms (SNP),<sup>[12]</sup> quantitative real-time PCR,<sup>[13]</sup> molecular beacon technology,<sup>[14]</sup> high-throughput semi automated sequencing and microarray development.<sup>[1, 15]</sup> In order for this technique to be successful, a molecular probe that can selectively bind to the sequence of interest over other similar sequences is essential. The molecular probes must also be able to respond to hybridization in the form of a change in conductance or a fluorimetric response, among others.<sup>[16]</sup>

In the Hudson group, hybridization of strands is monitored using fluorescence, which is a very powerful tool for detection due to its high sensitivity. In nucleic acid chemistry, fluorescent studies are most often done with luminescent tags such as rhodamine and fluorescein which are sometimes used in combination with a quencher

such as 4-(dimethylamino)azobenzene (DABCYL) (**Scheme 1.4**)<sup>[17]</sup>.<sup>[16b, 17]</sup> The ability of the fluorophore to be quenched by Förster Resonance Energy Transfer (FRET) is an important tool that is utilized to monitor hybridization. FRET is a nonradiative process that is distance dependant, in which the donor fluorophore transfers energy to the acceptor fluorophore and changes the fluorescence that is usually observed.<sup>[16b]</sup> This observed difference in fluorescence is due to the nonradiative transfer of energy from the donor to acceptor fluorophore. Luminescent tags such as fluorescein and rhodamine are disadvantageous, because they can perturb the system under investigation (due to their steric bulk) and their lack of polarity can disrupt the natural binding of the nucleobases.<sup>[17]</sup>



**Scheme 1.4:** Representation of a fluorescent RNase H assay using a dual label system employing a fluorophore and a quencher.<sup>[17]</sup>

Many luminescent modified nucleobases are derived from 7-substituted 7-deazapurines and 5-substituted pyrimidines (**Figure 1.6**). These positions are generally of interest, because they are useful sites of manipulation due to established chemistry. The substituent is generally well tolerated in a duplex, because it is directed into the major groove and allows for Watson-Crick base pairing.<sup>[1]</sup> Typically, the fluorophore is incorporated into the oligomer that is complementary to the target.<sup>[10]</sup>

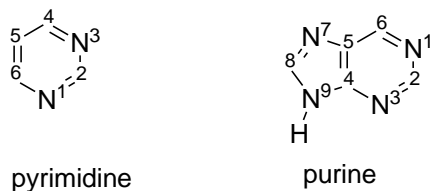


**Figure 1.6:** Structural example of the parent pyrimidine and purine showing the numbering system of the atoms.

According to a paper published in 2005 by the Hudson group, fluorescent nucleobases can be divided in three arbitrary classes (**Figure 1.7**): class I, II and III.<sup>[1]</sup> Class I as shown in **figure 1.7** comprises of a pendant fluorophore that is separated electronically and spatially from the base pairing competent nucleobase. The use of conventional fluorescent moieties attached to the nucleobase through a flexible linker, allows for free movement of the fluorophore. The fluorimetric response from these fluorophores may therefore not be indicative of the actual hybridization state of the oligomers.<sup>[1]</sup> These types of molecules are capable of base pairing with the natural nucleobases, however, there may be steric interactions associated with the pendant fluorophore upon hybridization. The second class of nucleobase is compact, autofluorescent and since modification involves the Watson-Crick base pairing face, are base-pairing incompetent.<sup>[1]</sup> The third type of fluorescent nucleobase is of particular interest, because they are autofluorescent, are base pairing competent and have the ability to report on their environment upon hybridization, whilst not drastically perturbing the nucleic acid structure.<sup>[1]</sup> The number of base analogs that fulfill the requirements of class III are limited.<sup>[1]</sup>

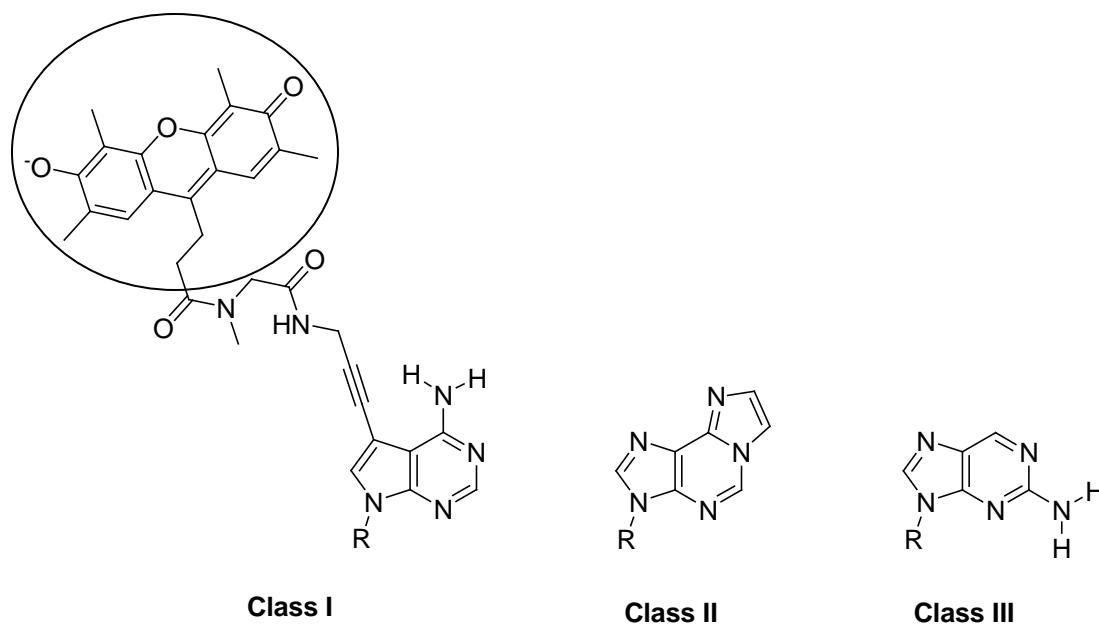


**Figure 1.7:** Illustrative examples of arbitrary classes of fluorescent nucleobases. Class I: pendant fluorophore (circled), class II: non base-pairing analogs; class III base-pairing capable analog.

### 1.3 Unnatural nucleic acid analogues

The design and synthesis of nucleic acid analogues is a major field in medicinal chemistry, with applications such as nucleic acid detection and antiviral chemotherapeutics.<sup>[7]</sup> Naturally occurring DNA provides an excellent scaffold for the introduction of polycyclic aromatic hydrocarbons to provide particular desired properties such as fluorescence. These modifications, while producing desirable properties, must not hinder the Watson-Crick base pairing face to allow for proper base pairing geometries.<sup>[18]</sup>

Of great interest in our group is the unnatural nucleobase pyrrolocytosine (pC), which can be achieved by the reaction of terminal alkynes to benzoyl protected 5-iodocytosine via Sonogashira coupling, followed by an intramolecular cyclization reaction.<sup>[18]</sup> The pyrrolocytosine moiety itself is fluorescent and the fluorescence properties can be tuned based upon the substituent at the 6-position (**Figure 1.8**). Another important feature of pyrrolocytosine is that the Watson-Crick face pairing is not disturbed and the hydrogen bonding donor and acceptor properties of cytosine are maintained (**Figure 1.8**).

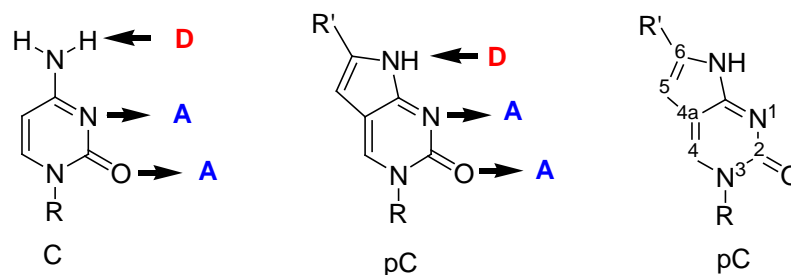
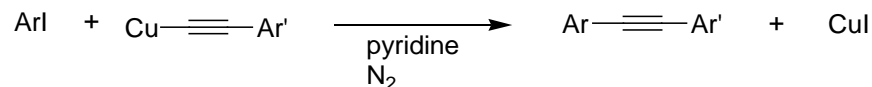


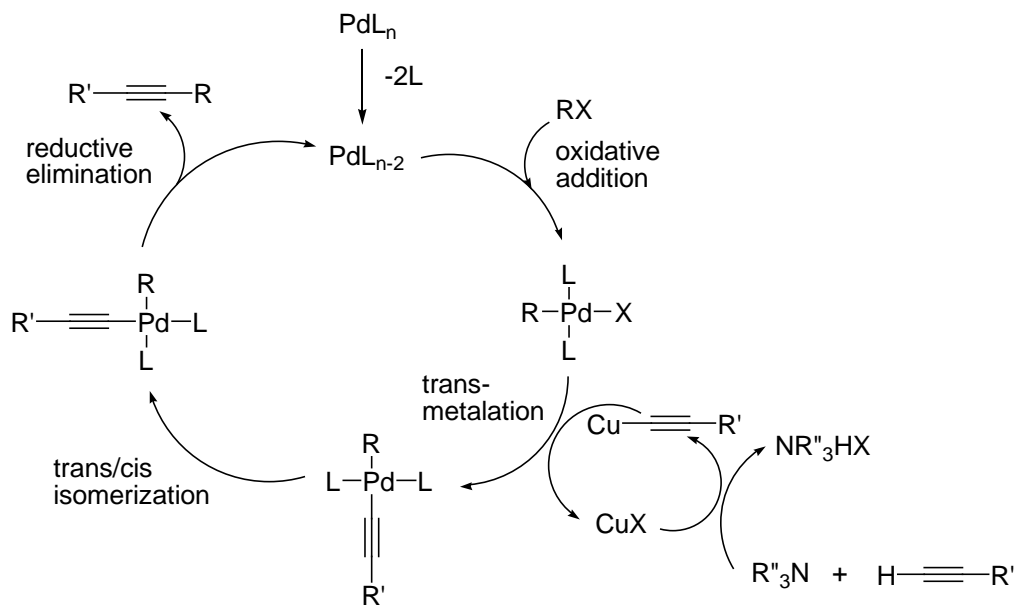
**Figure 1.8:** Illustration showing the H-bonding donor (D) and acceptor (A) properties of cytosine (C) and pyrrolocytidine (pC) analogs as well as the numbering system for pC.

## 1.4 Palladium/copper catalyzed reactions

The Sonogashira coupling<sup>[19]</sup> is an important and efficient carbon-carbon bond formation reaction, that was key for accessing the desired products reported in this thesis. It is a one pot catalytic variant of the Castro-Stephens<sup>[20]</sup> reaction (**Scheme 1.5**). Due to the mild reaction conditions and the number of products that makes use of aryl alkynes, the Sonogashira coupling has become a widely used reaction in synthetic organic chemistry. The reaction is thought to proceed with copper(I) iodide facilitating the deprotonation of the acetylene, generating the copper(I) acetylide in solution; the aryl undergoes oxidative addition to the palladium catalyst which is followed by a transmetalation regenerating the copper(I) iodide catalyst in solution. A trans/cis isomerization occurs, followed by the reductive elimination to the product, regenerating the palladium catalyst (**Scheme 1.6**).



**Scheme 1.5:** The Castro-Stephens reaction



**Scheme 1.6:** Catalytic cycle of the Pd/Cu Sonogashira reaction.

## 1.5 6-substituted pyrrolocytidines versus 5-substituted pyrrolocytidines

Our group has synthesized and studied the fluorescence properties of a number of 6-substituted pyrrolocytosine nucleobases, as well as examined their binding properties to complement nucleic acids once incorporated into oligomers.<sup>[15, 21]</sup> Although studies of 6-substituted pyrrolocytidines are still ongoing, it was decided to attempt the synthesis of a 5-substituted pyrrolocytidine DNA nucleobase in order to be able to compare the two regioisomers (**Figure 1.9**).

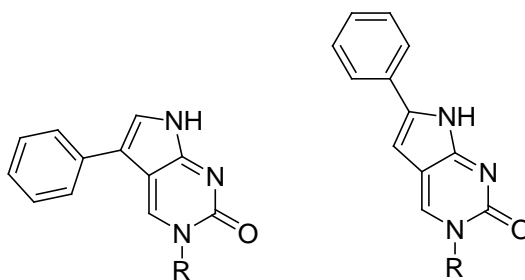


**Figure 1.9:** Illustration of a 5-substituted pC versus a 6-substituted pC.

## 1.6 Fluorescence quenching

Fluorescence is a form of luminescence which involves the emission of ultraviolet, visible or infrared photons from an electronically excited state (**Figure 1.10**).<sup>[22]</sup> When a singlet ground state molecule absorbs photons, it may be excited to higher energy levels. Once in these higher energy levels, the molecule can return to the ground state by several pathways including: emission by fluorescence, internal conversion (IC) and intersystem crossing (ISC) to the triplet state which is generally followed by phosphorescence. The energy dissipation back to the ground state can be radiative or nonradiative. Fluorescence and phosphorescence are both radiative processes, while the others are nonradiative.<sup>[23]</sup>

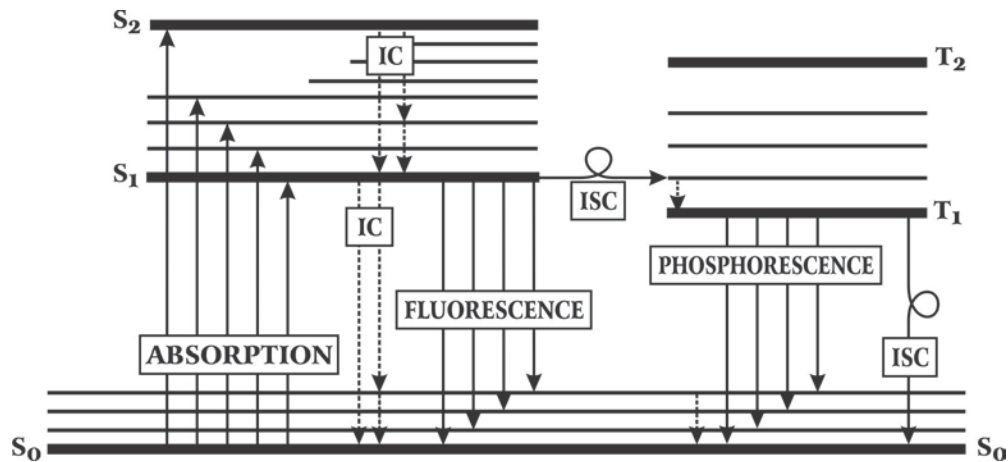


**Figure 1.10:** Jablonski diagram showing the radiative and nonradiative transition between electronic states.

The fluorescence emission occurs at lower energy compared to the absorbed energy. This phenomenon was first observed by George G. Stokes in 1852 at Cambridge and is now known as Stokes shift<sup>[22]</sup> (**Figure 1.11**).

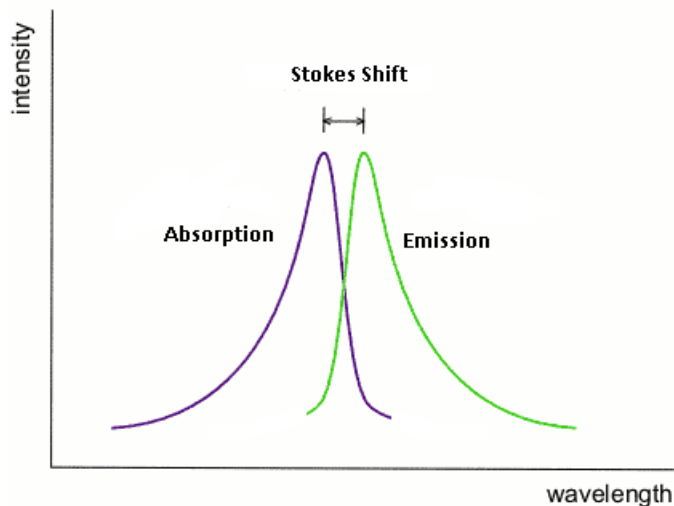


**Figure 1.11:** Diagram showing the Stokes shift resulting from the difference between the absorption and emission spectra.

The fluorescent emission resulting from the relaxation to the ground state is the basis for Förster Resonance Energy Transfer (FRET).<sup>[24]</sup> This excitation energy from the donor fluorophore can be transferred to a nearby acceptor fluorophore or quencher in a nonradiative manner. A quencher is a molecule with the capability to absorb the fluorescent signal from the donor fluorophore and not re-emit it as light. This relationship can be shown using a Stern-Volmer plot.

There are three different types of mechanisms for quenching: static, dynamic/collisional and apparent quenching.<sup>[25]</sup> In static quenching, a complex that is not fluorescent is formed between the quencher and fluorophore, whereas in dynamic quenching, the quencher has to diffuse towards the fluorophore while it is in its excited state and nonradiatively deactivate the excited state. Apparent quenching is not a true quenching process, but it may be due to absorption of emitted radiation by an excess concentration of fluorophore or by the presence of another absorbing species in the solution. This phenomenon is generally known as the “inner filter effect”.<sup>[25]</sup> For static or dynamic quenching to occur, there has to be interaction between the fluorophore and quencher.



## 1.7 Stern-Volmer plots

The Stern-Volmer relationship allows us to explore the variation in fluorescence of an intermolecular photophysical process for a compound in the presence of a quencher. Stern-Volmer plots are a ratio of the fluorescence intensity of the sample in the absence of the quencher to the fluorescence intensity for that sample in the presence of the quencher, versus the concentration of the quencher. This variation in fluorescence is denoted by the well-known Stern-Volmer equation 1.<sup>[26]</sup>

$$I_0/I = 1 + K_{sv} [Q] \quad (\text{equation 1})$$

Where:  $I_0$  = fluorescence intensity of the sample in the absence of the quencher

$I$  = fluorescence intensity of the sample when the quencher is present

$K_{sv}$  = Stern-Volmer constant

$[Q]$  = concentration of the quencher

In dynamic quenching, the Stern-Volmer rate constant ( $K_{sv}$ ) is equal to the product of the bimolecular quenching rate constant and the fluorescent lifetime of the excited state singlet of the fluorophore in the absence of the quencher. The Stern-Volmer rate constant is defined as:

$$K_{sv} = k_q \cdot \tau_0 \quad (\text{equation 2})$$

Equation 1 can then be written as:

$$I_0/I = 1 + k_q \cdot \tau_0 [Q] \quad (\text{equation 3})$$

The Stern-Volmer rate constant ( $K_{sv}$ ) can be determined directly from the slope of the plot from equation 1. The gradient can be used to determine how effective the quencher is at quenching the fluorescence of the fluorophore.

For the photophysical experiments reported in this thesis, the  $K_{sv}$  values were used to compare the efficiency of the quenchers.

## 1.8 Overview

The research in the following chapters of this master's thesis focuses on the synthesis of modified DNA nucleobases. Chapter II describes the attempted synthesis of 5-phenylpyrrolocytidine nucleoside, as well as the motivation for the synthesis.

Chapter III describes the synthesis of five 6-substituted pyrrolocytidines, as well as two aromatic alkynes: 1-ethynyl-4-nitrobenzene and a terminal alkyne that mimics the universal quencher DABCYL, which shall be incorporated in the synthesis of these pyrrolocytosines nucleobases.

Chapter IV focuses on the quenching studies of various quenchers: one 6-substituted DABCYL mimic pyrrolocytidine, a 6-(4-nitrophenyl)pyrrolocytosine ethyl ester and a 5-ethynyl cytosine ethyl ester. Their efficiencies as FRET pairs shall be tested, prior incorporation into oligomers.

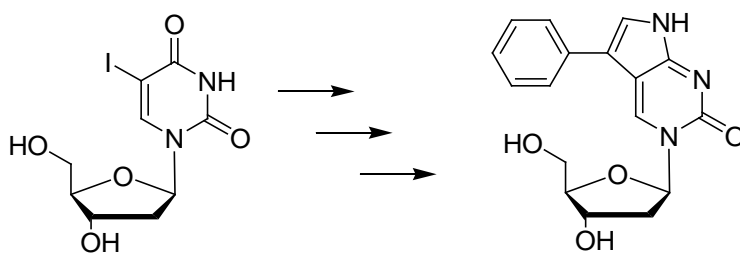
## Chapter 2

### 2 Towards 5-phenylpyrrolocytidine

#### 2.1 Chapter Introduction

To our knowledge, there has not been work reported on 5-substituted pyrrolocytidine nucleobases. The synthesis of a 5-phenylpyrrolocytidine nucleobase starting from 5-iodo-2'-deoxyuridine nucleobase (**Scheme 2.1**) was undertaken.

The 6-aromatic substituted pyrrolocytidine was found to be very fluorescent and well tolerated when used as a molecular beacon. Upon incorporation into a duplex, it was found to have a stabilizing effect.<sup>[15, 17]</sup> Based on our group's experience with 6-substituted aromatic pyrrolocytidine nucleobases, questions regarding the fluorescent and stabilizing/destabilizing effect of the 5-substituted aromatic pyrrolocytidine nucleobase arose. The goal of this particular project was to determine which position on the pyrrolocytosine framework is most suitable for substituted aromatic groups and to study the stabilizing/destabilizing effects the 5-phenylpyrrolocytidine has in the duplex formation, if any.



**Scheme 2.1:** Illustration of the starting material and the 5-phenylpyrrolocytidine nucleoside.

## 2.2 Results and Discussion

For the synthesis of the 5-phenylpyrrolocytidine, 2'-deoxyuridine was chosen as the starting nucleobase of choice, as it is a less expensive starting material than 2'-deoxycytidine and the use of protecting group chemistry was minimized.

A shortcoming of uracil when used to make the fluorophore is its inability to form three hydrogen bonds with the complementary purine to cytosine (C) (**Figure 2.1**). In order to overcome this shortcoming of the furanouridine nucleobase, an atom exchange is required to replace the oxygen atom with a nitrogen atom.

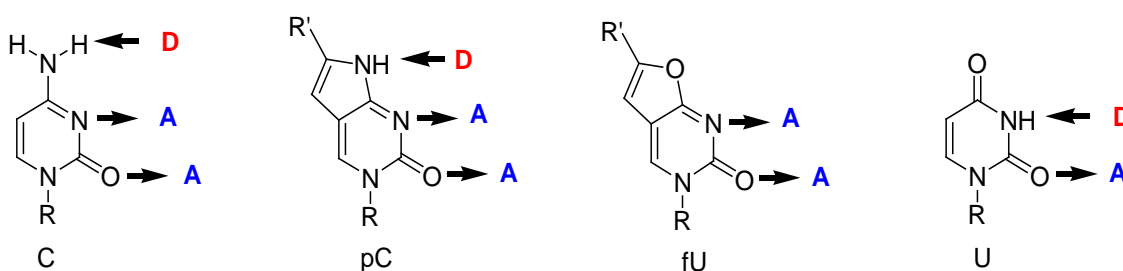
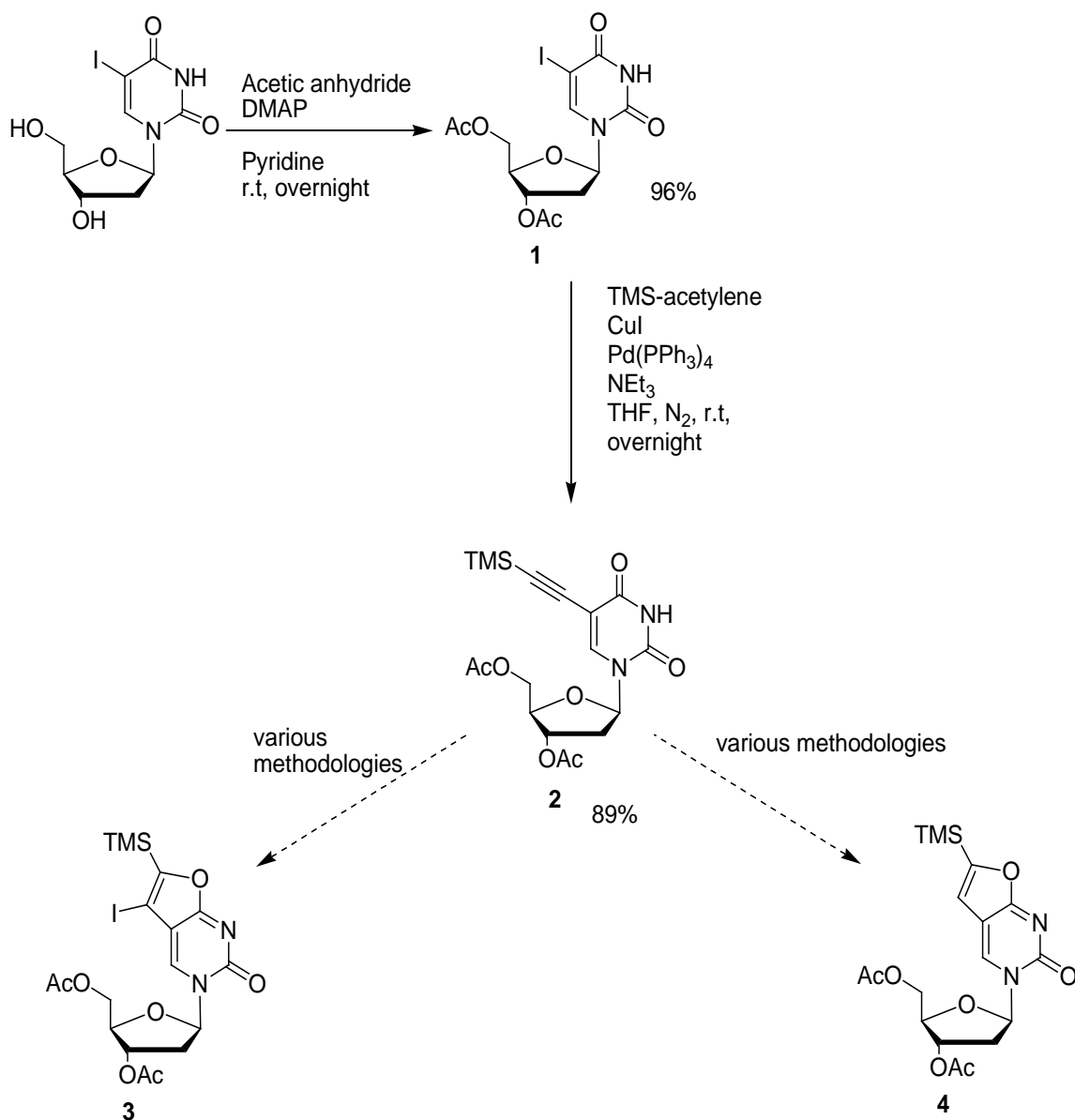


**Figure 2.1:** Structural representation of cytosine (C), pyrrolocytosine (pC), furanouracil (fU) and uracil (U) showing their hydrogen bonding donor (D) and acceptor (A) properties.

### 2.2.1 Synthesis of 5-(trimethylsilylethynyl)-3',5'-diacetyl-2'-deoxyuridine

The synthesis of this nucleoside starts with an acetylation of the sugar to impart solubility in organic solvents and for ease of purification by normal phase chromatography. The reaction was performed in pyridine and was catalyzed by DMAP and proceeded in excellent yield forming compound **1** (**Scheme 2.2**).<sup>[15]</sup>

The next step in this synthesis was a palladium and copper catalyzed reaction known as the Sonogashira coupling.<sup>[19]</sup> The reaction is sensitive to air, as the palladium(0) can be converted to palladium(II) oxide and becomes inactive as a catalyst. Therefore, it must be performed under deoxygenated conditions. Generally done in DMF, the reaction can be completed in THF as well, as it has a lower boiling point and is easier to remove after the reaction has gone to completion. The reaction was reproducible with good yields of 89% to produce compound **2** (**Scheme 2.2**).

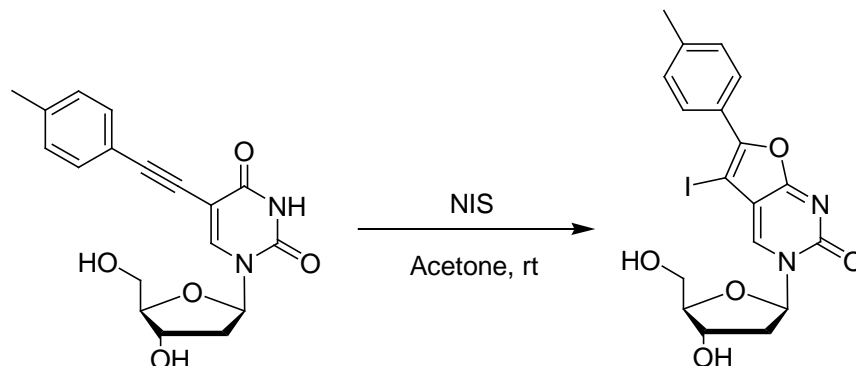


**Scheme 2.2:** Schematic illustration of the synthesis of 5-(trimethylsilylethynyl)-3',5'-diacetyl-2'-deoxyuridine. Also, the schematic for the attempted synthesis towards two substituted furanouridine nucleobases are shown.

Once compound **2** was synthesized, the next step was to perform the cyclization to the furanouridine nucleobase (**Scheme 2.2**, compound **3** or **4**). The synthesis of compound **3** was thought to be a critical and important step towards the synthesis of the 5-phenylpyrrolocytidine nucleoside. The ability to cyclize and simultaneously iodinate at the 5-position of the furanouridine nucleoside would provide a handle for a new carbon-

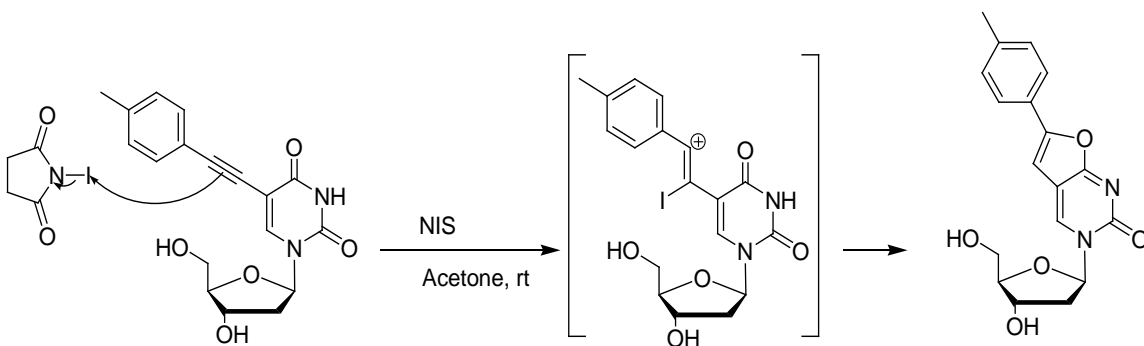
carbon bond towards the 5-phenylfuranouridine nucleoside via the Suzuki coupling.<sup>[27]</sup>

To that end, a 5-endo-dig electrophilic cyclization which has been reported by Dembinski<sup>[28]</sup> was attempted (**Scheme 2.3**). This method proved unsuccessful.



**Scheme 2.3:** Synthetic scheme of the 5-endo dig cyclization reported by Dembinski.

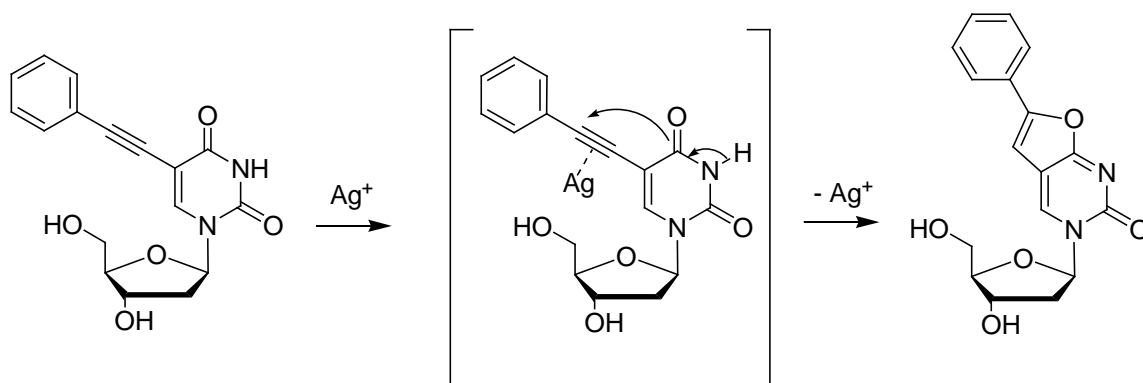
The reaction in **Scheme 2.3** proceeds mechanistically by a nucleophilic ‘attack’ of the alkyne towards the electrophilic source of iodine. This results in a secondary carbocation (**Scheme 2.4**) that is stabilized by the phenyl group. This is then followed by the 5-endo-dig cyclization to produce the product in **Scheme 2.3**.



**Scheme 2.4:** Illustration of the nucleophilic attack of the alkyne towards the electrophilic source of iodine.

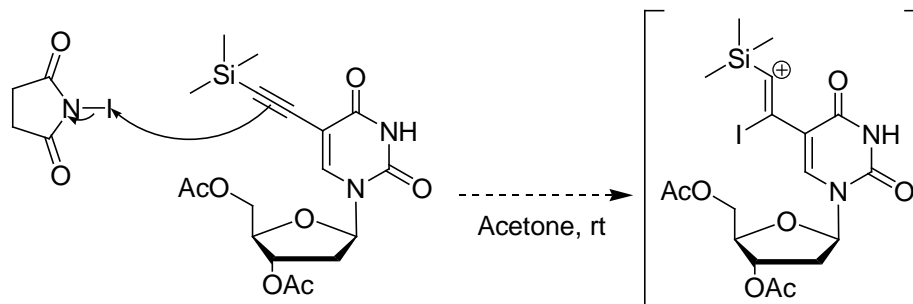
The cyclization of compound **2** to **4** was attempted using a modified version of a 5-endo-dig cyclization reported by Agrofoglio<sup>[29]</sup>. The reaction was run over a 48 hour period and for the first 24 hours the reaction was catalyzed by silver(I) nitrate ( $\text{AgNO}_3$ ). This was then followed by the addition of NIS in the hopes of achieving compound **3**. After 24 hours, there was no observable progress in the reaction when checked by TLC.

More NIS was added and the following day a yellow precipitate had formed. The yellow precipitate was analyzed and determined not to be the product by  $^1\text{H}$  NMR. Since the reaction reported by Agrofoglio is an electrophilic cyclization, it is thought the Lewis acid nature of  $\text{Ag}^+$  activates the triple bond for an intramolecular attack of the oxygen towards the carbon-carbon triple bond (**Scheme 2.5**).<sup>[29]</sup>



**Scheme 2.5:** Mechanism for the 5-endo-dig  $\text{Ag}^+$  catalyzed reaction proposed by Agrofoglio.<sup>[29]</sup>

The 5-endo-dig cyclization in **Scheme 2.3** and **Scheme 2.5** reported by Dembinski<sup>[28]</sup> and Agrofoglio<sup>[29]</sup> respectively, contains a phenyl group which can help stabilize the cation formed through resonance after the addition of an electrophile across the triple bond compared to the trimethylsilyl substituent used. Silicon is also less electronegative than carbon; hence the trimethylsilyl substituent would be expected to donate electron density to the carbon-carbon triple bond through induction, making it less electrophilic. Another factor that may be contributing to the phenyl group reaction being more facile is its planar structure compared to the trimethylsilyl group, which is tetrahedral in geometry. The geometry of the TMS group coupled with its decreased electronegativity may sterically and electronically hinder the 5-endo-dig cyclization. Therefore, progress to the intermediate species (**Scheme 2.6**) may not have been favourable. The reaction was also attempted at a higher temperature using  $\text{Et}_3\text{N}$  as the base with the same results as previously mentioned. The attempts towards the cyclization of compounds **3** and **4** are summarized in **table 2.1**.



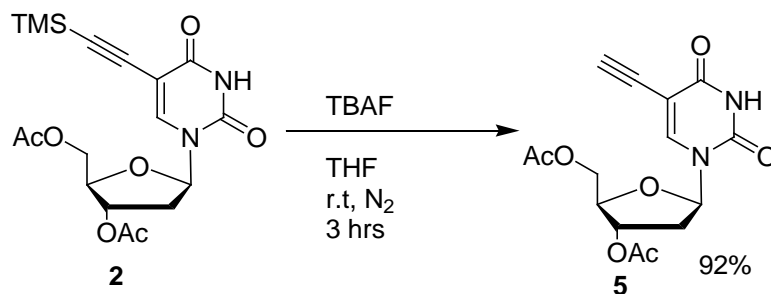
**Scheme 2.6:** Illustration of the cationic intermediate that would be formed during the 5-endo-dig cyclization product.



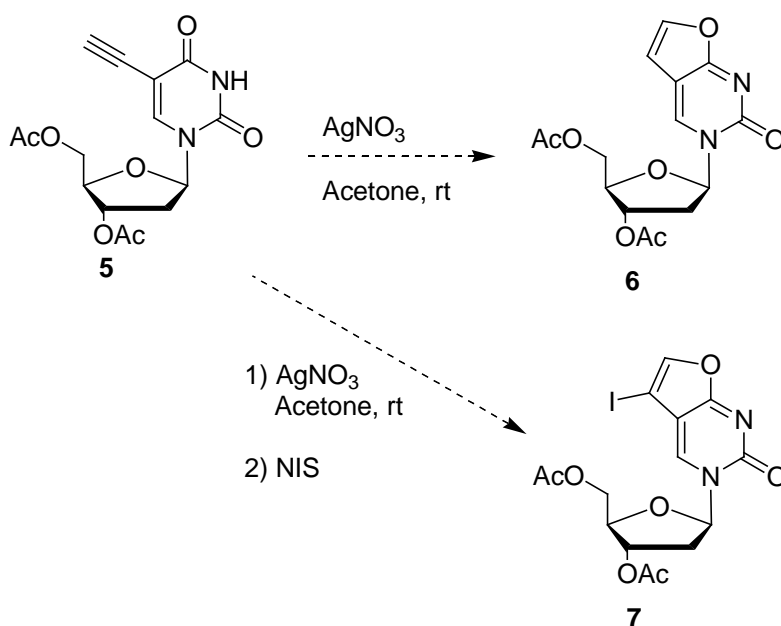
<b>Methodologies attempted for compound 3</b>	<b>Duration of reaction</b>	<b>Results</b>
NIS, Acetone	Overnight	Decomposition
AgNO <sub>3</sub> , Acetone/ then NIS	2 days	Decomposition (yellow precipitate)
NIS/AgNO <sub>3</sub> /THF/then NEt <sub>3</sub> / then I <sub>2</sub>	4 days	Decomposition
NIS/THF then added NEt <sub>3</sub> then heat to 40 °C	2 days	Decomposition
<b>Methodologies attempted for compound 4</b>	<b>Duration of reaction</b>	<b>Results</b>
AgNO <sub>3</sub> /Acetone	overnight	No reaction
AgNO <sub>3</sub> /Acetone	5 days	No reaction
AgNO <sub>3</sub> /Acetone/NEt <sub>3</sub> / 40 °C	2 days	Decomposition

**Table 2.1:** Summarized table of results for the attempted synthesis of the fU (compounds **3** and **4**) base.

The initial attempts towards the cyclization of the furanouridine were met with no success and lead to the investigation of alternative methodologies. Since we have postulated an electronic effect caused by the trimethylsilyl group preventing cyclization, the possibility of carrying out the cyclization in the absence of the TMS group was investigated. The removal of the TMS group was done by treatment of compound **2** with tetra-*n*-butylammonium fluoride (TBAF) in THF to yield compound **5** (**Scheme 2.7**). Once compound **5** was obtained, the cyclization methodology proposed by Agrofoglio to synthesize compound **6** or **7** was used with no success (**Scheme 2.8**).<sup>[29]</sup> Variations of Agrofoglio's methodology were attempted to simultaneously cyclize and iodinate at the 5-position of the furanouridine (**Table 2.2**).

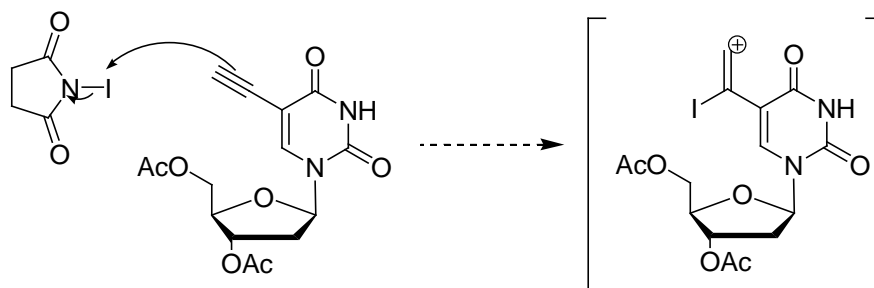


**Scheme 2.7:** Schematic of the desilylation reaction of compound **5**.



**Scheme 2.8:** Schematic of the attempted cyclization of compound **5** using Agrofoglio<sup>[29]</sup> methodology.

Compound **6** was not synthesized using Agrofoglio<sup>[29]</sup> methodology at room temperature as the energy barrier to form the product using  $Ag^+$  may have been too high to overcome. The cyclization to compound **7** was attempted using NIS, similar to the methodology published by Dembinski<sup>[28]</sup> without success (**Scheme 2.8**). In order for compound **7** to be formed via the 5-endo-dig electrophilic cyclization, it would have to first form an unfavourable carbocation (**Scheme 2.9**). Since the chances of this intermediate being formed in solution were not very likely, the tandem cyclization and iodination at the 5-position of the furanouridine was not suitable using this methodology.



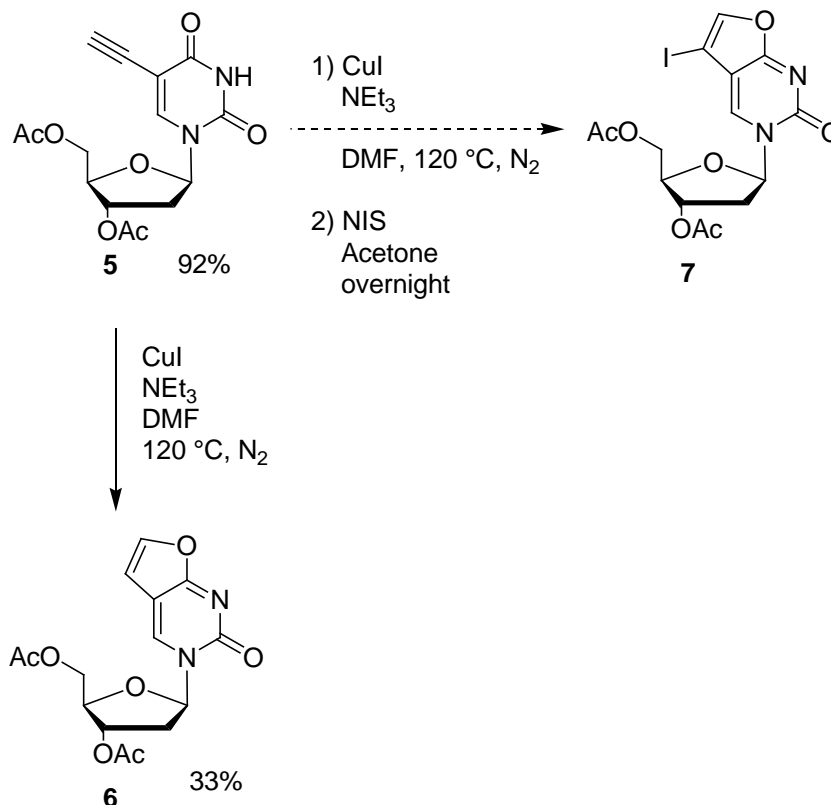
**Scheme 2.9:** Illustration of the unfavourable intermediate during the formation of compound **7**.

Methodologies	Duration	Results
1) AgNO <sub>3</sub> , Acetonitrile	overnight	No reaction
1) AgNO <sub>3</sub> , Acetone (5 days) 2) NIS (1 day)	6 days	After the first step the starting material was unreacted. The addition of NIS in the second step yielded an unknown yellow precipitate.

**Table 2.2:** Unsuccessful attempts towards the synthesis of compound **5** to **6**.

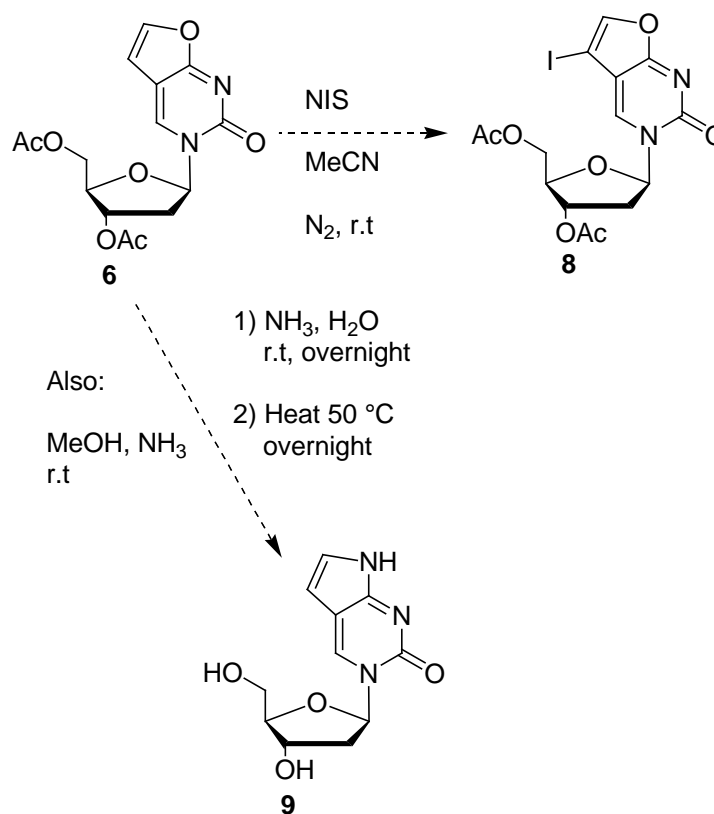
After a number of unsuccessful attempts to cyclize compounds **2** and **5** to the furanouridine, the methodology reported by Gamper's group in 1996, in which a cyclization to the furanouridine starting from the unprotected 5-ethynyluridine nucleobase **5** (**Scheme 2.10**) was attempted.<sup>[30]</sup> Gamper's methodology makes use of the copper(I) catalyst, which is well known to form a complex to the alkyne, making it more electrophilic. The first attempt to synthesize compound **7** using Gamper's methodology was monitored using TLC. Once there was no evidence of the starting material, a one-pot synthesis towards the 5-iodo-furanouridine nucleobase (compound **7**, **Scheme 2.8**) was attempted. The synthesis of compound **7** was unsuccessful and the reaction was done a second time and worked up after the disappearance of the starting material to yield compound **6** (**Scheme 2.10**) in low yields. The reaction of compound **5** to **6** was not

favourable at room temperature and was driven thermally at high temperature. The catalyst lowered the activation energy of the reaction, whilst the temperature increased the rate of the reaction, making it feasible.



**Scheme 2.10:** Schematic illustration for the synthesis of compound **6** from compound **5**.

Once compound **6** was obtained, the synthesis of compound **8** (**Scheme 2.11**) was the next step towards the furanouridine monomer. The reaction was attempted in acetonitrile using 1.5 equivalence of *N*-iodosuccinimide (NIS) and was left to run to completion overnight. The reaction was then monitored the following day by TLC and the starting material was still observed as a single spot, indicating no reaction. Due to the unresponsive nature of the nucleophile towards the electrophilic iodine source, it was attributed to the 5-position on the furanouridine being less nucleophilic than the 5-position on the pC. This reasoning was made on the basis that oxygen is more electronegative than nitrogen, making the 5-position less nucleophilic.



**Scheme 2.11:** Schematic of the attempted iodination and atom exchange on the fU nucleobase.

The furanouridine nucleobase resembles the benzofuran ring (**Figure 2.2**) and their reactivity was expected to be similar, because of their molecular similarities. A literature search for the iodination of the benzofuran ring at the 3-position and unsubstituted at the 2-position resulted in no published work. Iodination at the 3-position of the benzofuran ring resulted in no results, either because no one has been able to iodinate at that position due to the reasons mentioned above, or it has not been attempted, which seems less likely. However, the pC scaffold was expected to be more nucleophilic at the 5-position compared to the 3-position of the furanouridine nucleobase. Based on that hypothesis, the literature was searched for reactions that involved the iodination of the indole ring (**Figure 2.2**), because of its similarity to the pyrrolocytosine nucleobase. This search resulted in several literature procedures confirming the hypothesis of the difference in reactivity at the 3- and 5-position of the fU and pC nucleobase respectively (**Figure 2.2**). The paper published by Zolfigol<sup>[31]</sup> reported the iodination at the 3-position of the indole ring (**Scheme 2.12**).

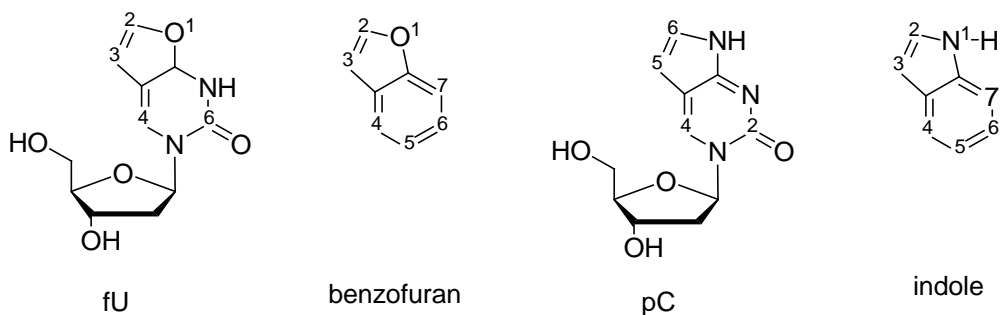
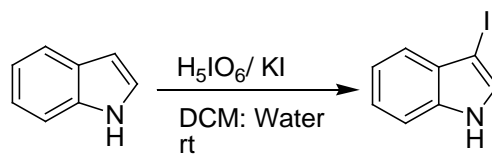


**Figure 2.2:** Illustration of the comparison between the fU and benzofuran as well as the pC and indole ring.



**Scheme 2.12:** Illustration of the iodination at the 3-position of the indole reaction reported by Zolfigol.<sup>[31]</sup>

Based on the inability to iodinate at the 3-position of the fU nucleobase and the knowledge that the best approach was to try iodinate the at the 5-position of the pC nucleobase, the synthesis of compound **9** (**Scheme 2.11**) was then attempted using a literature procedure that made use of aqueous ammonia at room temperature.<sup>[30]</sup> After 24 hours the reaction was stopped and the crude product was analysed by <sup>1</sup>H NMR, which indicated that there was a mixture of compound **9** and the deacetylated starting material **6** (**Scheme 2.11**). The crude product was then redissolved in the aqueous ammonia and the mixture was heated at 50 °C overnight. The crude product was then analysed, at which point the reaction mixture had gone to an intractable material.

The synthesis of compound **9** was attempted using another literature procedure, which involved concentrating a solution of methanol with ammonia (**Scheme 2.11**).<sup>[15]</sup> Based on the knowledge gained from the previous amination reaction, the reaction was monitored for the deacetylation of the nucleoside. Once all the acetylated starting material had disappeared, the unprotected furanouridine nucleobase disappearance was monitored for evidence that the reaction had gone to completion. After 28 hours, there was one fluorescent spot on the baseline of the TLC (eluent 90% CH<sub>2</sub>Cl<sub>2</sub>: 10% MeOH), that was believed to be the product. The analysis of the crude product by <sup>1</sup>H NMR after

drying looked promising. The NMR spectrum was complicated indicating a mixture, but the peaks corresponding to the pC nucleobase were observed. Attempted purification by column chromatography proved unsuccessful.

## 2.3 Conclusion

The synthesis towards the 5-phenylpyrrolocytidine nucleobase starting from the 5-iodo-2'-deoxyuridine was challenging and the final product was not attained. Once the Sonogashira coupled product was obtained, attempts to use methodologies reported by Dembinski, Agrofoglio, as well as variations of their procedures to the furanouridine nucleobase were unsuccessful.

The furanouridine, however, was attained in low yield by using the methodology reported by the Gamper group. Iodination at the 5-position of the furanouridine was unsuccessful using an electrophilic source of iodine. The amination of the furanouridine (**6**) to the pyrrolocytidine (**9**) looked promising when analyzed by  $^1\text{H}$  NMR. However, the crude material was not successfully purified.

## 2.4 Future Outlook

The ability to successfully synthesize the 5-phenylpyrrolocytidine would be an exciting step towards synthesizing a series of 5-substituted pyrrolocytidines. Although the final product was not attained, much was learned about the synthesis towards these 5-substituted pyrrolocytidines, such as: the difficulty associated with the cyclization in the presence of the TMS group and iodinating at the 5-position of the furanouridine ring, which has laid the groundwork for future endeavors.

## 2.5 Experimental

### General experimental procedures

All chemicals used were obtained from commercial sources, and used without further purification, except for pyridine which was purified by distillation using  $\text{CaH}_2$ . Thin layer chromatography was performed on Merck Kieselgel F-60 plates, and flash column chromatography was performed on Merck Kieselgel 60, 230-400 mesh. Proton

chemical shifts are reported in parts per million from tetramethylsilane (0 ppm), and are referenced to the residual proton in the deuterated solvents: DMSO-d<sub>6</sub> (2.50 ppm) and CDCl<sub>3</sub> (7.27 ppm) for <sup>1</sup>H NMR. Solution <sup>1</sup>H NMR was obtained using a Mercury 400 MHz spectrometer and an Inova 600 MHz at room temperature. <sup>13</sup>C NMR were recorded at 100 MHz. Peak multiplicities are described as; s (singlet), d (doublet), ddd (doublet of doublet of doublet), dt (doublet of triplet), t (triplet), q (quartet), m (multiplet) and br. s (broad singlet). Coupling constants (J) are reported in Hertz (Hz). High resolution mass spectra (HRMS) were obtained using electrospray ionization time of flight methods (ESI-TOF).

### 2.5.1 Synthesis of 3',5'-diacetyl-2'-deoxyfuranouridine

#### 5-iodo-3', 5'-diacetyl-2'-deoxyuridine (1)

5-iodo-2'-deoxyuridine (1.00 g, 2.82 mmol) was dissolved in 20 ml pyridine in a round bottom flask at room temperature. To this mixture was added acetic anhydride (1.33 ml, 14.1 mmol) and *N,N*-dimethyl-4-aminopyridine (DMAP) (catalytic). The reaction mixture was left to stir overnight under a nitrogen atmosphere. On completion, the solvent was removed in vacuo and an extraction was done with aqueous sodium bicarbonate and dichloromethane (CH<sub>2</sub>Cl<sub>2</sub>). The organic layer was then dried with sodium sulphate (Na<sub>2</sub>SO<sub>4</sub>) and then it was filtered and dried to yield 5-iodo-3',5'-diacetyl-2'-deoxyuridine (1.22 g, 2.78 mmol). Characterization of <sup>1</sup>H NMR was consistent with that reported for this known compound.<sup>[9]</sup> Yield: 98%

<sup>1</sup>H NMR (400 MHz, CDCl<sub>3</sub>) δ ppm 8.98 (s, 1 H) 6.30 (dd, *J*=8.4, 5.7 Hz, 1 H) 5.24 (dd, *J*=6.5, 2.3 Hz, 1 H) 4.27 - 4.46 (m, 3 H) 2.55 (ddd, *J*=14.3, 5.7, 2.0 Hz, 1 H) 2.09 - 2.25 (m, 7 H); TLC R<sub>f</sub>= 0.38 in DCM: MeOH; 95:5

#### 5-trimethylsilylethynyl-3',-5'-diacetyl-2'-deoxyuridine (2)

5-iodo-3',5'-diacetyl-2'-deoxyuridine (0.30 g, 0.685 mmol), copper(I) iodide (0.26 g, 0.137 mmol) and tetrakis(triphenylphosphine)palladium(0) were added to 12 ml of tetrahydrofuran (THF) in a round bottom flask and degassed at -78 °C (x3). To this mixture was added triethylamine (NEt<sub>3</sub>) (0.38 ml, 2.74 mmol) and trimethylsilylacetylene



(0.15 ml, 1.03 mmol); then the reaction mixture was degassed again (x3). The reaction was then stirred in the absence of light under a nitrogen atmosphere for 24 hours. After completion, the reaction was dried by rotary evaporation and then a liquid/liquid extraction was done with ethylenediamine tetraacetic acid (EDTA) in CH<sub>2</sub>Cl<sub>2</sub> (x3). The organic layer was then dried with Na<sub>2</sub>SO<sub>4</sub> and filtered off, then dried by rotary evaporation. The crude product was subjected to column chromatography. The eluent consisted of a mixture of CH<sub>2</sub>Cl<sub>2</sub>: methanol (MeOH), which was used as a gradient beginning with 0% MeOH, then moving up to 2% MeOH. The fractions of interest were dried in vacuo to yield 5-trimethylsilylethynyl-3',-5'-diacetyl-2'-deoxyuridine (0.25 g, 0.612 mmol). Characterization of <sup>1</sup>H NMR was consistent with that reported for this known compound. <sup>[9]</sup> Yield: 89%

<sup>1</sup>H NMR (400 MHz, CDCl<sub>3</sub>) δ ppm 8.82 (br. s., 1 H) 7.84 (s, 1 H) 6.33 (dd, *J*=7.8, 5.9 Hz, 1 H) 5.25 (dd, *J*=3.9, 2.3 Hz, 1 H) 4.33 - 4.41 (m, 2 H) 4.28 - 4.31 (m, 1 H) 2.53 (dd, *J*=14.4, 5.8, 2.2 Hz, 1 H) 2.16 - 2.25 (m, 4 H) 2.12 (s, 3 H) 0.22 (s, 8 H); R<sub>f</sub> = 0.59 in DCM: MeOH; 9:1

### **5-ethynyl-3', 5'-diacetyl-2'-deoxyuridine (5)**

To a round bottom flask was added 5-trimethylsilylethynyl-3',5'-diacetyl-2'-deoxyuridine (0.247 g, 0.605 mmol) and tetra-*n*-butylammonium fluoride (TBAF) (0.7 ml, 0.666 mmol). The mixture was dissolved in 5 ml of dry THF and left to stir in the absence of light for 3.5 hours. The solvent was dried in vacuo and then the crude product was subjected to flash column chromatography. The eluent consisted of a mixture of CH<sub>2</sub>Cl<sub>2</sub>: methanol (MeOH), which was used as a gradient beginning with 0.5 % MeOH, then moving up to 6% MeOH. The fractions containing the product were combined and removed in vacuo to yield 5-ethynyl-3', 5'-diacetyl-2'-deoxyuridine (0.187 g, 0.556 mmol). Characterization of <sup>1</sup>H NMR was consistent with that reported for this known compound. Yield: 92%

<sup>1</sup>H NMR (400 MHz, CDCl<sub>3</sub>) δ ppm 8.45 (br. s., 1 H) 7.92 (s, 1 H) 6.31 (dd, *J*=7.8, 5.9 Hz, 1 H) 5.22 - 5.27 (m, 1 H) 4.36 - 4.44 (m, 2 H) 4.29 - 4.35 (m, 1 H) 3.22 (s, 1 H) 2.57

(ddd,  $J=14.2, 5.8, 2.3$  Hz, 1 H) 2.19 - 2.26 (m, 1 H) 2.18 (s, 3 H) 2.13 (s, 3 H);  $R_f = 0.52$  in DCM: MeOH; 9: 1

### **3', 5'-diacetyl-2'-deoxy-furanouridine (6)**

To a two necked flask containing dry dimethylformamide (DMF) was added 5-ethynyl-3',5'-diacetyl-2'-deoxyuridine (0.42g, 1.25 mmol) and copper(I) iodide (0.0524 g, 0.275 mmol). The reaction was degassed at  $-78$  °C (x3). To this mixture was added triethylamine (1.57 ml, 11.25 mmol) and the reaction was heated under nitrogen at  $120$ °C for two hours adding copper(I) iodide (0.262 g, 0.138 mmol) every half hour. The reaction was stopped after two hours and the solvent was removed in vacuo. The crude product was re-dissolved in  $\text{CH}_2\text{Cl}_2$  and an extraction was done in water (x3). The organic layer was then collected and dried using  $\text{Na}_2\text{SO}_4$ , then it was filtered. The volume was reduced in vacuo and the product was precipitated out of hexane to yield 3', 5'-diacetyl-2'-deoxyfuranouridine (0.14 g, 0.416 mmol). Characterization of  $^1\text{H}$  NMR was consistent with that reported for this known compound.<sup>[10]</sup> Yield: 33%

$^1\text{H}$  NMR (400 MHz,  $\text{CDCl}_3$ )  $\delta$  ppm 8.40 (s, 1 H) 7.37 (d,  $J=2.3$  Hz, 1 H) 6.56 (d,  $J=2.3$  Hz, 1 H) 6.25 - 6.35 (m, 1 H) 5.22 (d,  $J=5.9$  Hz, 1 H) 4.41 (s, 3 H) 2.91 - 3.04 (m, 1 H) 2.07 - 2.14 (m, 5 H) 2.05 (s, 3 H);  $R_f = 0.47$  DCM: MeOH; 9: 1

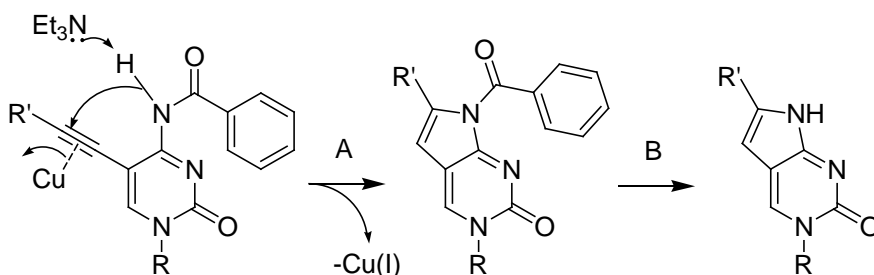
## Chapter 3

### 3 Synthesis of 6-substituted pyrrolocytidines

#### 3.1 Chapter Introduction

The 6-substituted pyrrolocytidines are intrinsically fluorescent nucleobases that falls into the class III base-pairing capable analogs (Chapter 1.1, **Figure 1.5**). The unsubstituted pyrrolocytidine nucleobase by itself is fluorescent, but it was found that greater fluorescence emission occurred when the substituent at the 6-position was aromatic.<sup>[15]</sup> This finding lead to the investigation of a 6-phenylpyrrolocytosine nucleobase in our group as a potential base discriminating probe.<sup>[15]</sup> The fluorescence of these 6-phenylpyrrolocytosine (PhpC) can be tuned electronically based on the substitutions on the phenyl ring to intensify, or quench the fluorescence.

The cyclization to the pyrrolocytosine fluorophore is achieved through a 5-endo-dig cyclization (**Scheme 3.1**). Our group has investigated a wide variety of 6-substituted pyrrolocytosines in regards to their synthesis and fluorescent studies. This research was meant to extend these studies by investigating the synthesis, as well as the photophysical properties of various 6-substituted pyrrolocytidine that were expected to have fluorescent and quenching properties to be incorporated into DNA oligomers for use as molecular probes. These pyrrolocytidines, once incorporated into DNA oligomers will be water soluble hence addressing the aqueous solubility of their pyrrolocytosine predecessors which contained different N<sup>3</sup>-position substituent.



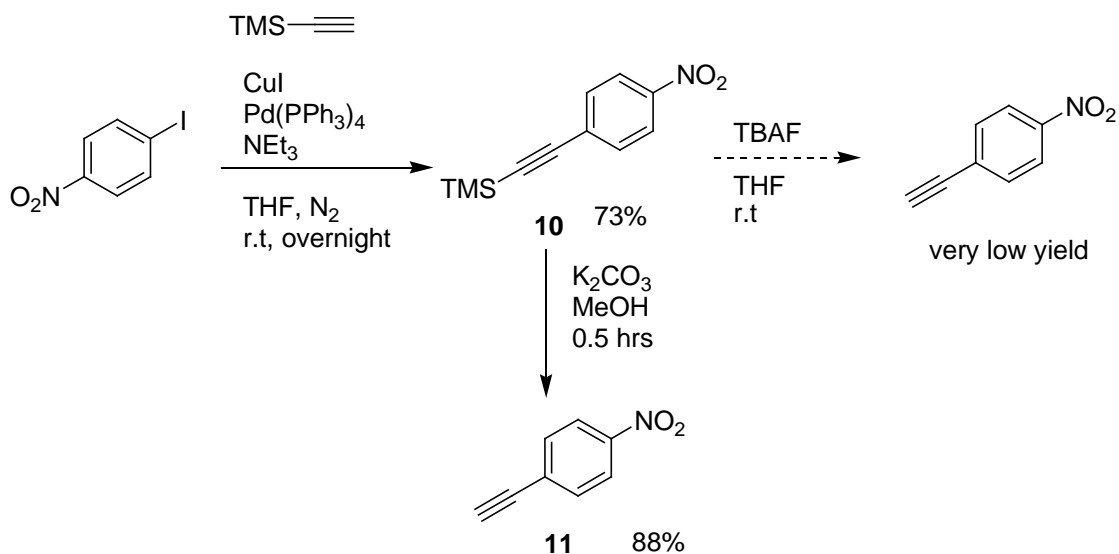
**Scheme 3.1:** Schematic representation of the 5-alkynylcytidine via the 5-endo-dig cyclization to the pyrrolocytidine nucleobase (A) and subsequent removal of the benzoyl group (B).

## 3.2 Results and Discussion

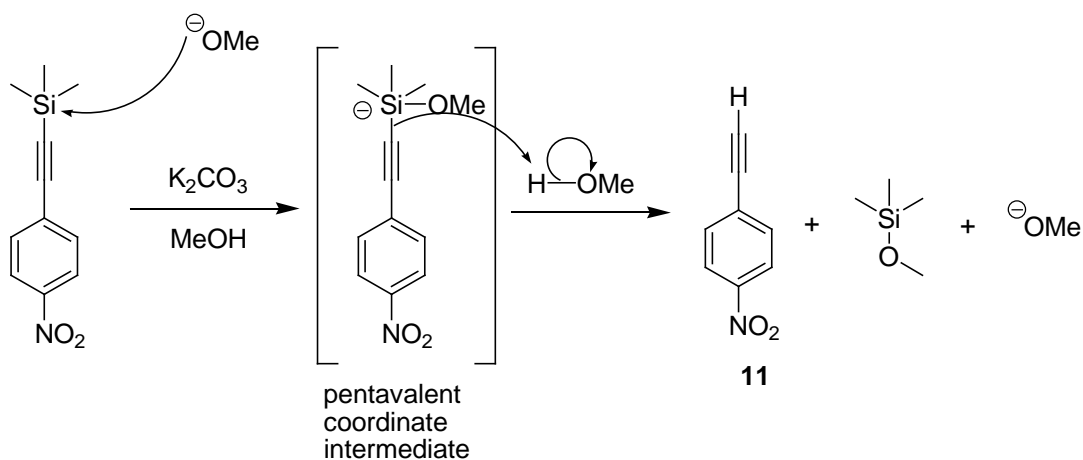
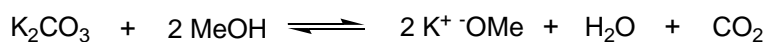
### 3.2.1 Synthesis of aromatic alkynes

One of the 6-substituted pyrrolocytidines of interest in the series to be synthesized and studied is the *para*-nitrobenzene. The nitro group is expected to quench the fluorescence of the pyrrolocytidine, making the 6-(4-nitrobenzene)pyrrolocytidine a quencher. The synthesis of compound **11** (**Scheme 3.2**) started with the commercially available 4-iodonitrobenzene, which was subjected to Sonogashira coupling conditions in tetrahydrofuran (THF) to yield compound **10** <sup>[19]</sup> in good yields. Once compound **10** was obtained, the next step was the removal of the trimethylsilyl group to form the desired alkyne. The deprotection was first done using TBAF in THF, which proceeded in very low yields, due to the quality of the TBAF. The crude, desired compound **11** was then obtained by reacting compound **10** with potassium carbonate (K<sub>2</sub>CO<sub>3</sub>) in methanol.

Silicon has an affinity for oxygen, because its two unpaired 3P orbitals are shared with the two 2P orbitals of oxygen, thus completing the 2P orbitals of oxygen. Due to this affinity, the deprotection of the trimethylsilyl group in methanol is thought to proceed by a nucleophilic attack of the methoxide forming the pentavalent coordinate intermediate (**Scheme 3.3**). This will then form the unprotected alkyne in the presence of a proton source. Due to the propensity of some alkynes to polymerize under acidic conditions, the purification of compound **11** using silica gel purification was done carefully using a short column.



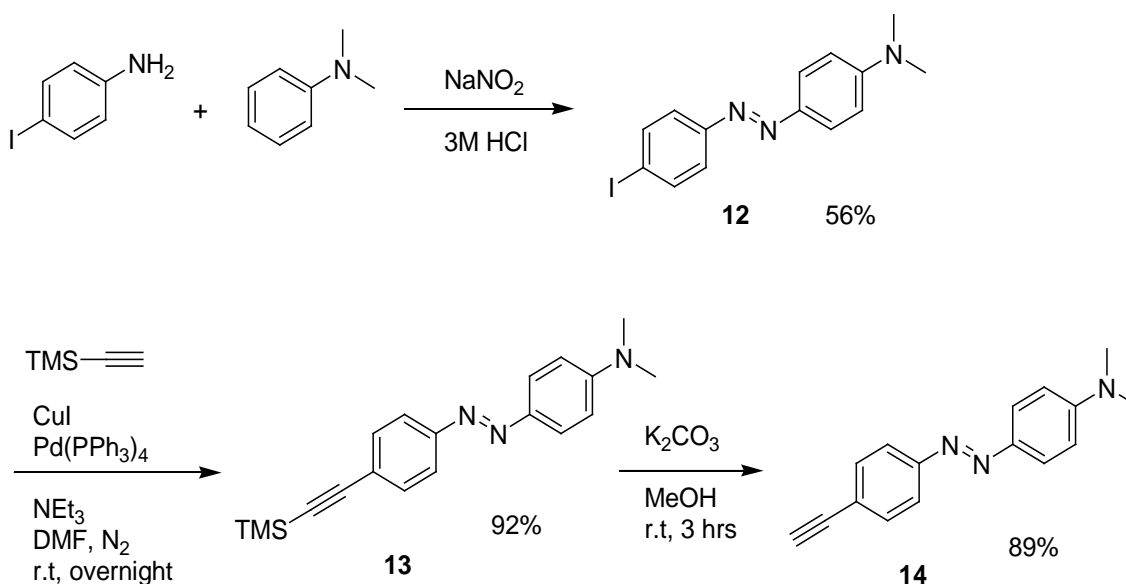
**Scheme 3.2:** Schematic of the synthetic methodology used to obtain compound **11**.



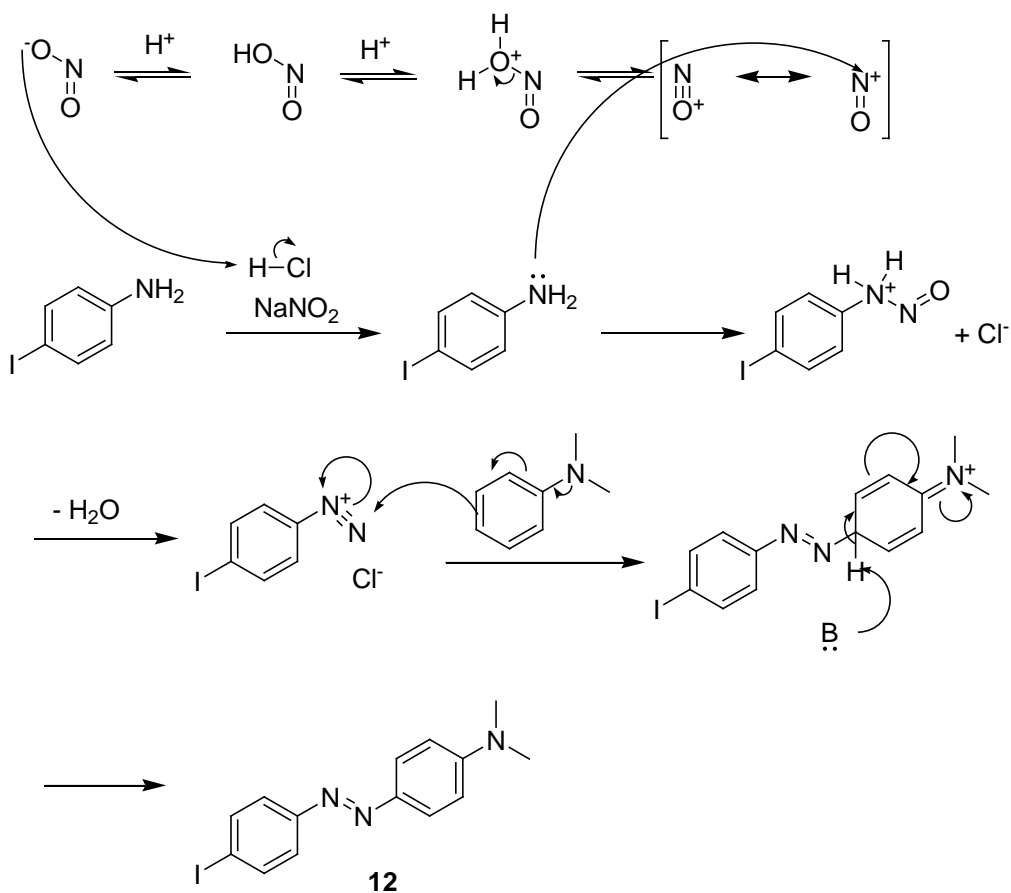
**Scheme 3.3:** Mechanism for the deprotection of trimethylsilyl in methanol with potassium carbonate.

Another alkyne of particular interest is the DABCYL mimic, (4-((*N,N*-dimethylamino)phenyl)azo)benzene)acetylene. DABCYL is known as the universal quencher<sup>[32]</sup> and it has found usage in molecular beacon technology.<sup>[33]</sup> The mimic, compound **14**, once incorporated into the pyrrolocytidine was expected to be an efficient azopyrrolocytidine based quencher.

The synthesis started with the diazonium coupling of the commercially available 4-iodoaniline and *N,N*-dimethylaniline (**Scheme 3.4**). The 4-iodoaniline was first dissolved in a 3 M solution of warm hydrochloric acid (HCl), due to its limited solubility at room temperature. The 4-iodoaniline was then converted to a diazonium salt using sodium nitrite ( $\text{NaNO}_2$ ). The solution was slowly added to a 1M HCl solution of *N,N*-dimethylaniline to form the desired product **12**, via an electrophilic aromatic substitution (**Scheme 3.5**). Initial attempts at isolating the product resulted in low yields, however the yield was improved to 56%, which is closer to the reported yield of 70%.<sup>[34]</sup> **Scheme 3.5** shows the proposed mechanism for the formation of compound **12**.



**Scheme 3.4:** Synthetic illustrations for the synthesis of the DABCYL mimic alkyne **14**.



**Scheme 3.5:** Proposed mechanism for the formation of compound **12** via the diazonium salt, where ‘B’ stands for base.

The synthesis towards compound **14** proceeded by subjecting compound **12** to Sonogashira coupling<sup>[19]</sup> conditions to form compound **13**. Compound **13** was obtained in moderate to high yields of 70% - 92%. Once compound **13** was purified by column chromatography, the compound was subjected to basic conditions in methanol using potassium carbonate for the deprotection of the TMS group, yielding the desired azo alkyne in 89%.

### 3.2.2 Synthesis of 6-substituted pyrrolocytidine nucleobases

The synthesis towards the various 6-substituted pyrrolocytidines started with the acetylation of the 2'-deoxycytidine nucleoside (**Scheme 3.6**). This was done in chloroform using glacial acetic acid and acetyl chloride. The reaction proceeded in very

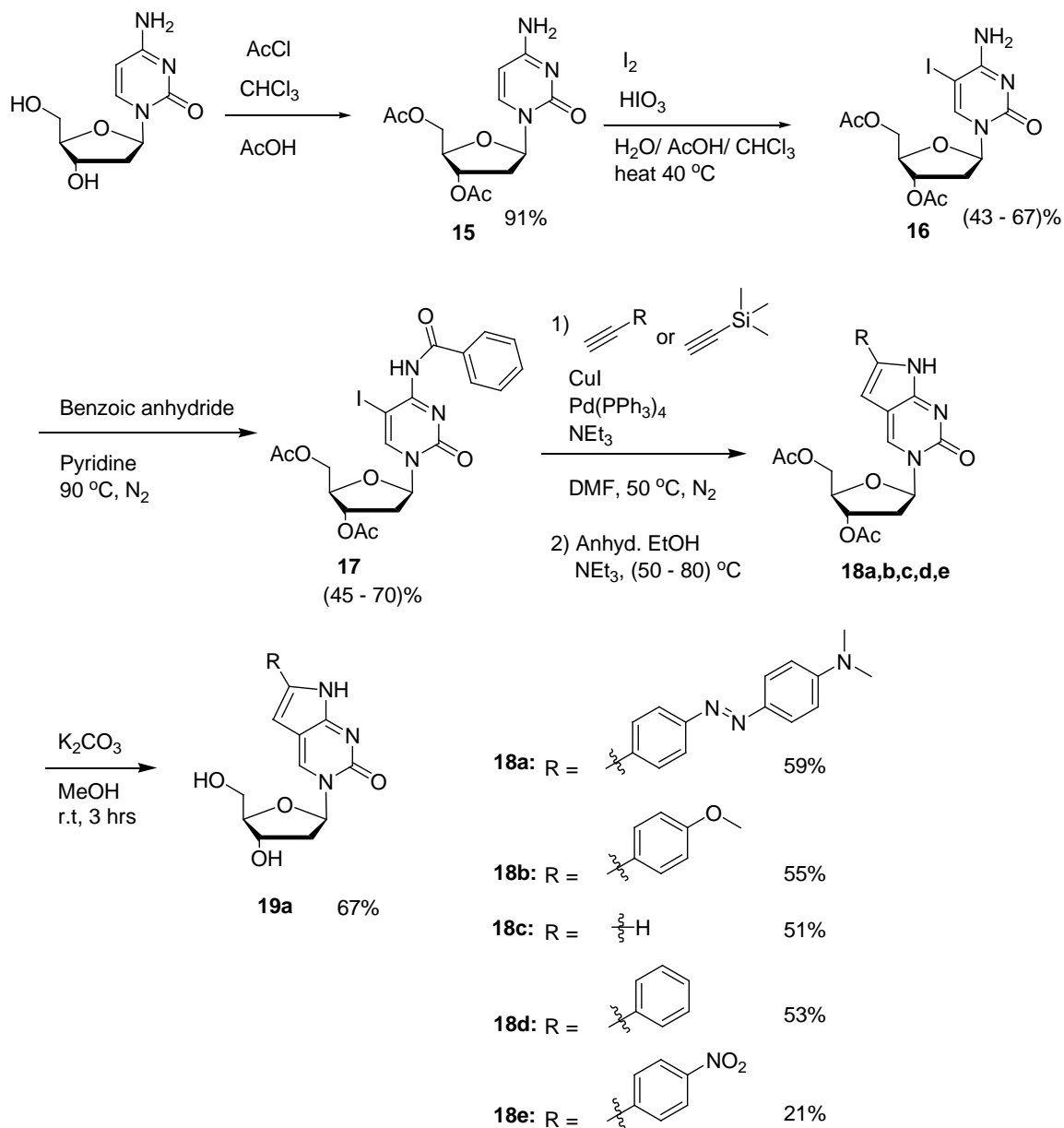
good yields and compound **15** was isolated in 91% yield after purification by column chromatography.

Iodination of the acylated 2'-deoxycytidine (compound **15**) was done in water using chloroform and glacial acetic acid. The purpose of this iodination reaction was to provide the nucleobase with a "handle" for the Sonogashira coupling reaction, which requires an aryl or vinyl halide.<sup>[19]</sup> The iodination was performed using 0.6 equivalence of iodine (I<sub>2</sub>) and 0.2 equivalence of iodic acid (HIO<sub>3</sub>). The I<sub>2</sub> was not used in stoichiometric amount in this reaction, because it was regenerated in-situ by HIO<sub>3</sub> as the reaction progressed. The reaction proceeded in low to moderate yields of up to 67% to obtain compound **16**.

Protection of the exocyclic amine of compound **16** to form compound **17** is a key step towards the synthesis of the pyrrolocytosine. In the Hudson group, while studying 5-iodonucleobases with terminal alkynes, it was noted that under mildly forcing conditions the adjacent heteroatoms underwent a cyclization with the 5-alkynyl substituents to yield furanouracils and pyrrolocytosines.<sup>[35]</sup> Mild basic conditions will deprotect the amide hydrogen and the coordination of copper(I) with the 5-alkynyl increases its electrophilicity, leading to the cyclization reaction. The synthesis of compound **17** was performed in anhydrous pyridine under a nitrogen atmosphere, since the benzoylation is sensitive to moisture, yielding the desired product in moderate yields.

The synthesis to the pyrrolocytidine from compound **17** is a one pot two step synthesis, which started with the Sonogashira coupling<sup>[19]</sup> between the terminal alkyne and the 5-iodocytidine nucleobase. At a temperature of 50 °C, 24 hours is generally enough for the tandem coupling and *ortho*-heteroatom to facilitate an attack towards the 5-substituted alkyne to form the pyrrolocytidine nucleobase. Once the cyclization to the pyrrolocytidine was completed, the removal of the benzoyl was done using anhydrous ethanol (Anhyd. EtOH) in triethylamine (Et<sub>3</sub>N) to yield compound **18a,b,c,d** and **e**.





**Scheme 3.6:** Synthetic scheme towards the various 6-substituted pyrrolocytidine nucleobases.

For the synthesis of compound **18c** trimethylsilylacetylene underwent the tandem coupling and cyclization with compound **17**. This reaction was done at  $80^\circ\text{C}$  and the trimethylsilyl group at the 6-position of the pyrrolocytidine was not stable under these reaction conditions. This was not surprising since the trimethylsilyl is removed under basic conditions (as proposed in **Scheme 3.3**) and mild basic conditions are used in the

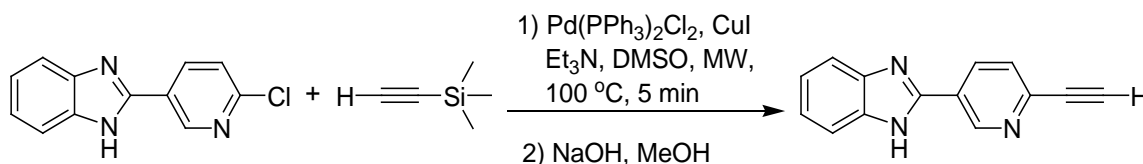
deprotection of the benzoyl group (**Scheme 3.1**, reaction **B**) to afford the unprotected pyrrolocytidine.

The incorporation of electron withdrawing aromatic alkynes into the pyrrolocytidine scaffold resulted in slower annulation in comparison to the electron donating aromatic alkynes, which may be due to the ability of the alkyne to donate electrons to the Lewis acid. The tandem coupling and cyclization of 1-ethynyl-4-nitrobenzene to compound **17** yielded the 6-(4-nitrobenzene)pyrrolocytidine in low yields following the conventional 48 hours reaction time. Due to the slower reaction time of the electron withdrawing aromatic alkyne, the reaction time was increased to seven days in order to improve the yield. The Hudson group had previously reported a minimum reaction time of six days for these electron withdrawing substituents, due to their decreased reaction times.<sup>[36]</sup> As reported in the literature, microwave-assisted Sonogashira coupling<sup>[37]</sup> was utilized as a non conventional energy source to reduce the reaction time. Raut and co-worker reported the microwave assisted Sonogashira coupling towards 2-[6-arylethynyl]pyridin-3-yl]-1H-benzimidazole using microwave technology (**Scheme 3.7**) in 87% yield.<sup>[37]</sup> They reported the successful Sonogashira coupling for trimethylsilylacetylene after 5 minutes at 100 °C,<sup>[37]</sup> therefore the coupling reaction was attempted at temperatures of 120 – 150 °C for 5 – 10 minutes, because of the electron withdrawing nature of the aromatic alkyne. The deprotection of the benzoyl group was attempted conventionally at 50 °C overnight in anhydrous ethanol. The reaction was not successful when done in the microwave under these reaction conditions.

The attempt to incorporate 4-ethynylbenzotrile into the pyrrolocytidine was unsuccessful. The cyclized product was not obtained after the reaction was worked-up and <sup>1</sup>H NMR analysis of the isolated fractions from column purification indicated no coupled product either. The starting material was not recovered since it was consumed based on the monitoring of the reaction by TLC.

The synthesis of compound **19a** was achieved by the deprotection of the 3'- and 5'-hydroxyl groups using K<sub>2</sub>CO<sub>3</sub> in MeOH. This step was done to obtain the unprotected

nucleobase to perform further studies. Compound **19a** was then purified via column chromatography using 10% MeOH in DCM.



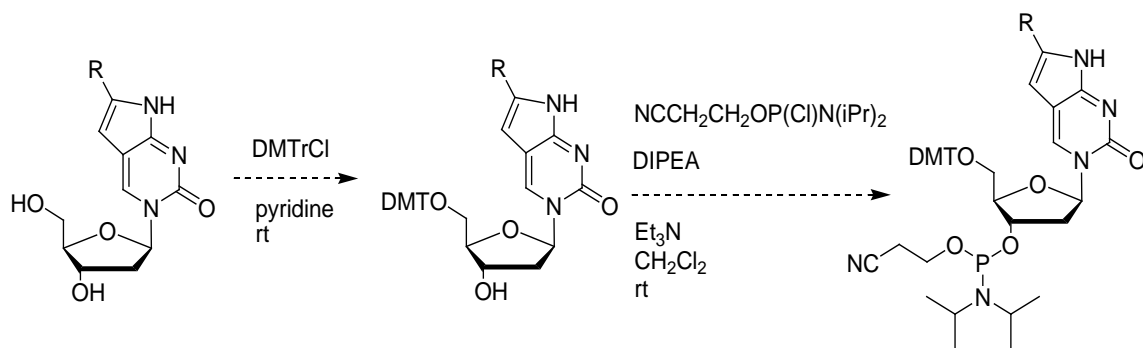
**Scheme 3.7:** Synthetic scheme of 2-[6-arylethynyl]pyridin-3-yl]-1H-benzimidazole using microwave technology reported by Raut.<sup>[37]</sup>

### 3.3 Conclusion

Two aromatic alkynes: **11** and **14** were synthesized using the Sonogashira coupling methodology to incorporate the trimethylsilylacetylene. This was then followed by the deprotection of the trimethylsilyl group. Compound **11** and **14** were then successfully incorporated into the pyrrolocytidine scaffold to afford compounds **18e** and **18a**, respectively. Three other 6-substituted pyrrolocytidines were synthesized: **18b**, **18c** and **18d**. The attempt to incorporate the 4-ethynylcyanobenzene electron withdrawing aromatic substituent was unsuccessful.

### 3.4 Future Outlook

Synthesis of the pyrrolocytidine nucleosides on a larger scale to be able to synthesis the phosphoramidite (**Scheme 3.8**), after which they can be incorporated into DNA oligomers to be used in molecular beacon technology. Further studies using microwave technology to perform the tandem coupling and cyclization to the pyrrolocytidine with electron withdrawing substituents would be an asset in order to reduce reaction time.



**Scheme 3.8:** Scheme of the synthesis from the pyrrolocytidine nucleoside to the phosphoramidite derivative.

## 3.5 Experimental

### 3.5.1 Synthesis of the *para*-nitrobenzene acetylene (**11**)

#### Trimethyl((4-nitrophenyl)ethynyl)silane (**10**)

To a 100 ml round bottom flask were added 4-iodonitrobenzene (8.03 mmol, 2.00 g) and 15 ml of tetrahydrofuran. The reaction was then degassed at -78 °C using an acetone and dry ice bath. To that were added copper(I) iodide (2.41 mmol, 0.4588 g) and tetrakis (triphenylphosphine) palladium(0) (0.803 mmol, 0.9279 g) and the reaction was then degassed again. Triethylamine (32.1 mmol, 4.48 ml) and trimethylsilylacetylene (16.1 mmol, 2.29 ml) were then added to the reaction and the mixture was left to run to completion overnight under a nitrogen atmosphere in the absence of light. The reaction was stopped the following day and the solvent was removed in vacuo. The crude product was then purified by column chromatography using a gradient of 2.5% - 5% ethyl acetate: hexane. The fractions containing the product were collected and dried to obtain compound **10** in 73% (5.84 mmol, 1.28 g).

<sup>1</sup>H NMR (400 MHz, CDCl<sub>3</sub>) δ ppm 8.18 (d, *J*=9.0 Hz, 2 H) 7.60 (d, *J*=9.0 Hz, 2 H) 0.28 (s, 10 H); <sup>13</sup>C NMR (101 MHz, CDCl<sub>3</sub>) δ ppm 147.4, 133.0, 130.3, 123.8, 103.0, 100.9, 77.6, 77.3, 0.2

### 1-ethynyl-4-nitrobenzene (**11**)

To a flask containing compound **10** (3.92 mmol, 0.86 g) were added 18 ml of methanol and potassium carbonate (0.784 mmol, 0.1084 g). The reaction was stirred for half an hour, after which it was stopped. The solvent was removed in vacuo and the crude product was run quickly through a short column using a 1:1 mixture of dichloromethane: ethyl acetate as the eluent. The fraction containing the product were collected and dried to obtain compound **11** (3.47 mmol, 0.51 g) in 88% yield.

$^1\text{H}$  NMR (400 MHz,  $\text{CDCl}_3$ )  $\delta$  ppm 8.20 (d, 2 H) 7.64 (d, 2 H) 3.37 (s, 1 H);  $^{13}\text{C}$  NMR (101 MHz,  $\text{CDCl}_3$ )  $\delta$  ppm 132.6, 128.6, 123.2, 122.0, 82.0, 81.3, 76.7, 76.4; HRMS (ESI) calculated for  $[\text{C}_8\text{H}_5\text{NO}_2]^+$ : 147.1308, Found 147.1310.

### 3.5.2 Syntheses of the DABCYL mimic alkyne (**14**)

4-iodoaniline (2.20 g, 10.0 mmol) was dissolved in a 3.5 M hydrochloric acid solution. The solution was then cooled rapidly to 0 °C to precipitate the anilinium hydrochloride as a microcrystalline solid. To this was added sodium hydrogen sulfite ( $\text{NaHSO}_3$ ) (0.0145 g, 0.139 mmol). An ice cold solution of sodium nitrite ( $\text{NaNO}_2$ ) (0.69 g, 10.0 mmol) in water (10 ml) was added drop wise to the stirred suspension. After 15 minutes, the resulting yellow solution of the diazonium species was added drop wise to a stirred solution of *N,N*-dimethylaniline (1.21 g, 10.0 mmol) in a 1 M HCl (11 ml) solution. The mixture was stirred for 30 minutes and the reaction was kept between 0 to 5 °C during the entire procedure. A saturated aqueous solution of  $\text{Na}_2\text{CO}_3$  was added until the evolution of  $\text{CO}_2$  stopped. To this mixture was added 50 ml of brine and the brown solid was isolated by filtration. The crude product was purified by silica column chromatography using chloroform as the eluent to afford compound **12** in 56% yield (1.97 g, 5.61 mmol).

$^1\text{H}$  NMR (400 MHz,  $\text{CDCl}_3$ )  $\delta$  ppm 7.88 (d,  $J=9.4$  Hz, 2 H) 7.81 (d,  $J=8.6$  Hz, 2 H) 7.59 (d,  $J=8.6$  Hz, 2 H) 6.76 (d,  $J=9.4$  Hz, 2 H) 3.10 (s, 6 H);  $^{13}\text{C}$  NMR (101 MHz,  $\text{CDCl}_3$ )  $\delta$  ppm 152.3, 152.2, 143.1, 137.7, 124.8, 123.6, 111.1, 94.9, 76.7, 76.4, 40.0; HRMS (ESI) calculated for  $[\text{C}_{14}\text{H}_{14}\text{IN}_3]^+$ : 351.1855, Found 351.1852.

**((4-((N,N-(dimethylamino)phenyl)azo)benzene)ethynyl)trimethylsilyl (13)**

To a 50 ml round bottom flask was added compound **12** (0.58 g, 1.65 mmol) and 12 ml of DMF. The mixture was then degassed at -78 °C and tetrakis (triphenylphosphine)palladium(0) (0.1907 g, 0.17 mmol) and copper(I) iodide (0.0628 g, 0.33 mmol) were added and the mixture was degassed again. Triethylamine (0.92 ml, 6.60 mmol) and trimethylsilyl acetylene (0.47 ml, 3.30 mmol) were then added to the reaction and the mixture was left to run to completion in the absence of light. Once the reaction was complete, an extraction was done using 2% aqueous disodium ethylenediamine tetraacetate in dichloromethane (CH<sub>2</sub>Cl<sub>2</sub>). The CH<sub>2</sub>Cl<sub>2</sub> layer was collected and dried using sodium sulfate (Na<sub>2</sub>SO<sub>4</sub>). The organic layer was then separated by filtration and the organic layer was dried to produce the crude product. The product was then isolated by using silica gel chromatography, eluent conditions 30% CH<sub>2</sub>Cl<sub>2</sub>: hexanes. The product was isolated in 92% to yield compound **13** (0.53 g, 1.65 mmol).

<sup>1</sup>H NMR (400 MHz, CDCl<sub>3</sub>) δ ppm 7.89 (d, *J*=9.0 Hz, 2 H) 7.80 (d, *J*=8.6 Hz, 2 H) 7.58 (d, *J*=8.6 Hz, 2 H) 6.76 (d, *J*=9.4 Hz, 2 H) 3.10 (s, 6 H) 0.29 (s, 8 H); <sup>13</sup>C NMR (101 MHz, CDCl<sub>3</sub>) δ ppm 152.6, 152.6, 143.6, 132.7, 125.2, 123.8, 122.1, 111.5, 105.1, 95.9, 77.3, 76.7, 40.3, 0.0; HRMS (ESI) calculated for [C<sub>19</sub>H<sub>23</sub>N<sub>3</sub>Si]<sup>+</sup> :321.1661, Found 321.1667.

**DABCYL mimic alkyne (14)**

To a 50 ml round bottom flask was added compound **13** (0.20 g, 0.622 mmol) and 12 ml of methanol. To that was added potassium carbonate (0.0172 g, 0.124 mmol) and the reaction was left to run to completion at room temperature. The reaction was left to run for three hours after which it was stopped and the solvent was removed in vacuo. The crude product was dissolved in hexane and filtered. The filtrate was collected and dried to produce the desired product **14** in 92% yield (0.16 g, 0.642 mmol).

<sup>1</sup>H NMR (400 MHz, CDCl<sub>3</sub>) δ ppm 7.89 (d, *J*=9.4 Hz, 2 H) 7.81 (d, *J*=8.6 Hz, 2 H) 7.61 (d, *J*=8.6 Hz, 2 H) 6.76 (d, *J*=9.4 Hz, 2 H) 3.20 (s, 1 H) 3.10 (s, 7 H); <sup>13</sup>C NMR (101

MHz, CDCl<sub>3</sub>)  $\delta$  ppm 152.9, 152.6, 143.6, 132.9, 125.2, 122.7, 122.1, 111.5, 83.7, 78.6, 77.3, 76.7, 40.3; HRMS (ESI) calculated for [C<sub>16</sub>H<sub>15</sub>N<sub>3</sub>]<sup>+</sup> : 249.3104, Found 249.3108.

### 3.5.3 Synthesis of 6-substituted pyrrolocytidines (**18**)

#### **3', 5'-diacetyl-2'-deoxycytidine (15)**

In a round bottom flask was added deoxycytidine (1.00 g, 3.79 mmol) and glacial acetic acid (CH<sub>3</sub>COOH) (10 ml). The mixture was heated at 35 °C until dissolution. The mixture was then brought to room temperature and a mixture of chloroform (CHCl<sub>3</sub>) (8 ml) and acetyl chloride (AcCl) (3 ml) were added. The reaction was then left to run to completion overnight at room temperature. The solvent was then removed in vacuo and the crude product was purified by flash column chromatography: eluent conditions, methanol: ethyl acetate (EtOAc) 2: 8. The fractions containing the product were combined and the solvent was removed in vacuo to yield 3', 5'-diacetyl-2'-deoxycytidine (1.45 g, 4.66 mmol). Characterization of <sup>1</sup>H NMR was consistent with that reported for this known compound. Yield: 92%

<sup>1</sup>H NMR (400 MHz, DMSO-*d*<sub>6</sub>)  $\delta$  ppm 9.94 (s, 1 H) 8.83 (br. s., 1 H) 7.98 (d, *J*=7.8 Hz, 1 H) 6.23 (d, *J*=7.8 Hz, 1 H) 6.08 (s, 1 H) 5.19 (d, *J*=3.1 Hz, 1 H) 4.20 - 4.28 (m, 3 H) 2.37 - 2.48 (m, 2 H) 2.06 (s, 3 H) 2.04 (s, 3 H); <sup>13</sup>C NMR (101 MHz, DMSO-*d*<sub>6</sub>)  $\delta$  ppm 170.6, 170.5, 160.3, 147.6, 144.6, 110.0, 94.8, 86.6, 82.4, 74.2, 64.0, 37.0, 21.2, 21.1; TLC R<sub>f</sub> = 0.22 in DCM: MeOH; 9: 1

#### **5-iodo-3', 5'-diacetyl-2'-deoxycytidine (16)**

3', 5'-diacetyl-2'-deoxycytidine (1.45 g, 4.66 mmol) was added to a round bottom flask containing water (7 ml), acetic acid (12 ml) and was stirred until the solid went into solution. To this was added chloroform (5 ml), resublimed iodine (I<sub>2</sub>) (0.473 g, 1.86 mmol) and iodic acid (HIO<sub>3</sub>) (0.164 g, 0.932 mmol). The reaction mixture was then stirred at 50 °C for 21 hours. The solvent was then removed in vacuo and then subjected to flash column chromatography. Eluent was a gradient of acetone: ethyl acetate 50:50 to acetone: ethyl acetate 75:25. The fractions corresponding to the product were collected and removed in vacuo to yield 5-iodo-3', 5'-diacetyl-2'-deoxycytidine (1.33 g, 3.04

mmol). Characterization of  $^1\text{H}$  NMR was consistent with that reported for this known compound. Yield: 65%

$^1\text{H}$  NMR (400 MHz,  $\text{DMSO}-d_6$ )  $\delta$  ppm 8.09 (s, 1 H) 6.09 (t,  $J=6.8$  Hz, 1 H) 5.14 - 5.22 (m, 1 H) 4.19 - 4.33 (m, 3 H) 2.43 (d,  $J=7.4$  Hz, 2 H) 2.08 - 2.13 (m, 4 H) 2.06 (s, 3 H); TLC  $R_f$  value = 0.52 in  $\text{CH}_2\text{Cl}_2$ : MeOH; 9: 1

#### **$N^4$ -benzoyl-5-iodo-3', 5'-diacetyl-2'-deoxycytidine (17)**

In a round bottom flask was added 5-iodo-3',5'-diacetyl-2'-deoxycytidine (1.12 g, 2.56 mmol) and benzoic anhydride (0.869 g, 3.84 mmol). To this mixture was added pyridine (10 ml) and the reaction was heated at 90 °C for five hours under a nitrogen atmosphere. On completion, the solvent was removed in vacuo and the crude product was extracted in  $\text{CH}_2\text{Cl}_2$ . The organic layer was dried with sodium sulphate and filtered. The solvent was removed in vacuo and the crude product was subjected to flash column chromatography: eluent condition was  $\text{CH}_2\text{Cl}_2$ : methanol; 0 -10% methanol. The fractions corresponding to the product were collected and dried via rotary evaporation to yield  $N^4$ -benzoyl-5-iodo-3', 5'-diacetyl-2'-deoxycytidine (0.64 g, 1.18 mmol). Characterization of  $^1\text{H}$  NMR was consistent with that reported for this known compound. Yield: 48%

$^1\text{H}$  NMR (400 MHz,  $\text{CDCl}_3$ )  $\delta$  ppm 8.37 (d,  $J=7.4$  Hz, 2 H) 8.10 (s, 1 H) 7.55 (d,  $J=7.0$  Hz, 1 H) 7.43 - 7.49 (m, 2 H) 6.30 (d,  $J=2.7$  Hz, 1 H) 5.24 (d,  $J=6.6$  Hz, 1 H) 4.31 - 4.46 (m, 3 H) 2.23 (s, 3 H) 2.19 (s, 1 H) 2.12 (s, 3 H);  $^{13}\text{C}$  NMR (101 MHz,  $\text{CDCl}_3$ )  $\delta$  ppm 179.5, 170.0, 169.8, 156.1, 146.9, 144.3, 136.1, 132.7, 129.9, 127.9, 85.6, 82.5, 76.7, 76.4, 73.8, 63.4, 38.2, 20.8, 20.5; TLC  $R_f$  value = 0.41 MeOH: EtOAc; 1: 9

#### **General procedure for the synthesis of the pyrrolocytidine compounds (18b, 18c, 18d and 18e)**

To a round bottom flask was added compound **17** (0.050 g, 0.092 mmol) and 3 ml of *N,N*-dimethylformamide. The reaction mixture was then degassed at -78 °C using an acetone bath. To this mixture was added copper(I) iodide (0.002 g, 0.009 mmol) and



tetrakis(triphenylphosphine)palladium(0) (0.011 g, 0.009 mmol) and the reaction was degassed again. Triethylamine (0.051 ml, 0.368 mmol) and the appropriate terminal alkyne [1-ethynyl-4-nitrobenzene (0.027 g, 0.184 mmol); 4-((*N,N*-dimethylamino)phenyl)azo)benzene)acetylene (0.276 g, 1.11 mmol); 4-ethynylanisole (0.14 ml, 1.11 mmol); 4-ethynylbenzonitrile (0.023 g, 0.184 mmol); trimethylsilylacetylene (0.026 ml, 0.184 mmol); phenylacetylene (0.020 ml, 0.184 mmol)] were added to the reaction mixture and degassed again. The reactions were then stirred overnight at a range of 50 °C to 80 °C under a nitrogen atmosphere. The following day, 1 ml of anhydrous ethanol and 0.5 ml of triethylamine were added to the reaction and it was continued to be heated at 50 °C overnight. The reaction was stopped the following day and an extraction was done with CH<sub>2</sub>Cl<sub>2</sub> and 2% aqueous disodium ethylenediamine tetraacetate. The organic layer was then collected and dried using Na<sub>2</sub>SO<sub>4</sub> and the solvent was dried by rotary evaporation. The crude product was subjected to column chromatography using a gradient of CH<sub>2</sub>Cl<sub>2</sub>: methanol as the mobile phase starting from 0 - 2% MeOH: CH<sub>2</sub>Cl<sub>2</sub>. The fractions corresponding to the product were collected and removed in vacuo to yield the pyrrolocytidines in various yields.

### Procedure for the synthesis of 18a

To a round bottom flask was added compound **17** (0.20 g, 0.369 mmol) and 5 ml of *N, N*-dimethylformamide. The reaction mixture was then degassed at -78 °C using an acetone bath. To this mixture was added copper(I) iodide (0.014 g, 0.074 mmol) and tetrakis(triphenylphosphine)palladium(0) (0.043 g, 0.037 mmol) and the reaction was degassed again. Triethylamine (0.21 ml, 1.48 mmol) and 4-((*N,N*-dimethylamino)phenyl)azo)benzene)acetylene (0.276 g, 1.11 mmol) were added to the reaction mixture and degassed again. The reactions were then stirred overnight at 50 °C under a nitrogen atmosphere. The following day, 2 ml of anhydrous ethanol and 1 ml of triethylamine were added to the reaction and it was continued to be heated at 50 °C overnight. The reaction was stopped the following day and an extraction was done with CH<sub>2</sub>Cl<sub>2</sub> and 2% aqueous disodium ethylenediamine tetraacetate. The organic layer was then collected and dried using Na<sub>2</sub>SO<sub>4</sub> and the solvent was dried by rotary evaporation. The crude product was subjected to column chromatography using a gradient of CH<sub>2</sub>Cl<sub>2</sub>:

methanol as the mobile phase starting from 0 - 2% MeOH: CH<sub>2</sub>Cl<sub>2</sub>. The fractions corresponding to the product were collected and removed in vacuo to yield the pyrrolocytidines in various yields.

**Compounds 18a:**

Yield: (0.122 g, 0.218 mmol) 59%

<sup>1</sup>H NMR (400 MHz, CDCl<sub>3</sub>) δ ppm 11.98 (br. s., 1 H) 8.18 (s, 1 H) 7.98 (d, *J*=8.6 Hz, 2 H) 7.83 - 7.90 (m, 4 H) 6.74 (d, *J*=9.4 Hz, 2 H) 6.51 (s, 1 H) 4.36 (s, 2 H) 3.08 (s, 7 H) 2.10 (s, 3 H) 2.04 (s, 3 H); <sup>13</sup>C NMR (101 MHz, CDCl<sub>3</sub>) δ ppm 170.5, 170.4, 154.4, 152.8, 152.4, 143.7, 140.9, 133.9, 131.0, 126.2, 125.1, 122.8, 111.5, 97.0, 88.1, 83.0, 77.4, 77.0, 76.7, 74.5, 63.8, 40.3, 39.3, 20.9; HRMS (ESI) calculated for [C<sub>29</sub>H<sub>30</sub>N<sub>6</sub>O<sub>6</sub>]<sup>+</sup>: 558.5851, Found 558.5849.

**Compounds 18b:**

Yield: (0.022 g, 0.051 mmol) 55%

<sup>1</sup>H NMR (400 MHz, CDCl<sub>3</sub>) δ ppm 12.01 (br. S., 1 H) 8.09 (br. s., 1 H) 7.75 (d, *J*=8.2 Hz, 2 H) 6.84 (d, *J*=8.6 Hz, 2 H) 6.25 (s, 1 H) 6.29 (s, 1 H) 5.12 - 5.21 (m, 1 H) 4.26 - 4.42 (m, 3 H) 3.74 (s, 3 H) 1.89 - 2.15 (m, 7 H); <sup>13</sup>C NMR (101 MHz, CDCl<sub>3</sub>) δ ppm 169.9, 169.9, 159.3, 141.0, 132.5, 126.5, 122.4, 113.7, 93.9, 87.5, 82.2, 76.7, 76.4, 73.8, 63.3, 54.7, 38.6, 29.1, 20.3, 20.3

**Compound 18c:**

Yield: (0.016 g, 0.047 mmol) 51%

<sup>1</sup>H NMR (400 MHz, CDCl<sub>3</sub>) δ ppm 8.37 (s, 1 H) 7.13 (d, *J*=3.9 Hz, 1 H) 6.41 (d, *J*=7.0 Hz, 1 H) 6.25 (d, *J*=3.9 Hz, 1 H) 5.25 (d, *J*=6.3 Hz, 1 H) 4.33 - 4.53 (m, 4 H) 2.12 - 2.16 (m, 4 H) 2.08 (s, 3 H); TLC R<sub>f</sub> value = 0.14 in DCM: acetone; 8: 2

**Compound 18d:**

Yield: (0.020 g, 0.049 mmol) 53%

$^1\text{H}$  NMR (400 MHz,  $\text{CHCl}_3$ )  $\delta$  ppm 11.55 (br. s., 1 H) 7.84 (d,  $J=7.0$  Hz, 2 H) 7.45 (t,  $J=7.2$  Hz, 2 H) 7.36 (d,  $J=7.0$  Hz, 1 H) 5.26 (d,  $J=5.9$  Hz, 1 H) 4.39 - 4.50 (m, 3 H) 2.16 (br. s., 1 H) 2.14 (s, 3 H) 2.09 (s, 3 H)

**Compound 18e:**

Yield: (0.009 g, 0.019 mmol) 21%

$^1\text{H}$  NMR (400 MHz,  $\text{DMSO}-d_6$ )  $\delta$  ppm 12.10 (br. s., 1 H) 8.61 (s, 1 H) 8.29 (d,  $J=9.0$  Hz, 2 H) 8.10 (d,  $J=9.0$  Hz, 2 H) 7.11 (s, 1 H) 6.28 (s, 1 H) 4.26 - 4.42 (m, 4 H) 2.09 (s, 3 H) 2.06 (s, 3 H);  $^{13}\text{C}$  NMR (101 MHz,  $\text{CDCl}_3$ )  $\delta$  ppm 179.9, 170.3, 170.1, 156.4, 147.3, 144.6, 136.4, 133.0, 130.3, 128.3, 86.0, 82.9, 77.4, 77.0, 76.7, 74.1, 63.8, 38.5, 21.2, 20.9

**De-acetylation pyrrolocytidine nucleobase (19a)**

To a round bottom flask was added compound **18a** (0.071 g, 0.127 mmol) and 3 ml of methanol. To that mixture was added potassium carbonate (0.004 g, 0.025 mmol) and the mixture was stirred at room temperature for 3 hours. The reaction was monitored by TLC and once completed, the solvent was removed in vacuo and the crude product was purified by silica gel column chromatography using 10% methanol in dichloromethane as the eluent to provide compound **19a**.

**Compound 19a:**

Yield: (0.040 g, 0.084 mmol) 67 %

$^1\text{H}$  NMR (400 MHz,  $\text{DMSO}-d_6$ )  $\delta$  ppm 11.89 (br. s., 1 H) 8.77 (s, 1 H) 7.98 (d,  $J=8.6$  Hz, 2 H) 7.81 (t,  $J=9.4$  Hz, 4 H) 6.79 - 6.89 (m, 3 H) 6.27 (s, 1 H) 5.32 (br. s., 1 H) 3.92 (d,  $J=3.1$  Hz, 1 H) 3.06 (s, 6 H); HRMS (ESI) calculated for  $[\text{C}_{25}\text{H}_{26}\text{N}_6\text{O}_4]^+$ : 474.5117, Found 474.5113

## Chapter 4

### 4 Photophysical Quenching Studies

#### 4.1 Chapter Introduction

UV-visible spectroscopy refers to absorption spectroscopy in the ultraviolet-visible spectral region, which causes molecules to undergo electronic transitions and concomitant vibrational excitation. The Jablonski diagram shown in **Figure 1.7** represents the possible photophysical processes upon absorption of photons. UV-visible spectroscopy is complementary to luminescence, in that absorption measures the transition from the ground state to the excited state, while luminescence measures the energy dissipation from the excited state to the ground state.<sup>[22]</sup>

In the last two decades the detection of DNA hybridization has attracted much attention, due to its potential application in the treatment and diagnostics of diseases. One methodology for the detection of hybridization is the molecular beacon technology, which is one of the most widely used techniques.<sup>[38]</sup> This is achieved by the labeling of DNA probes with fluorescent dyes and non fluorescent quenchers. The technology is based on the ability of the quencher to decrease the intensity of the fluorophore when they are in close proximity to each other via the FRET mechanism<sup>[24]</sup> (**Figure 4.1**).

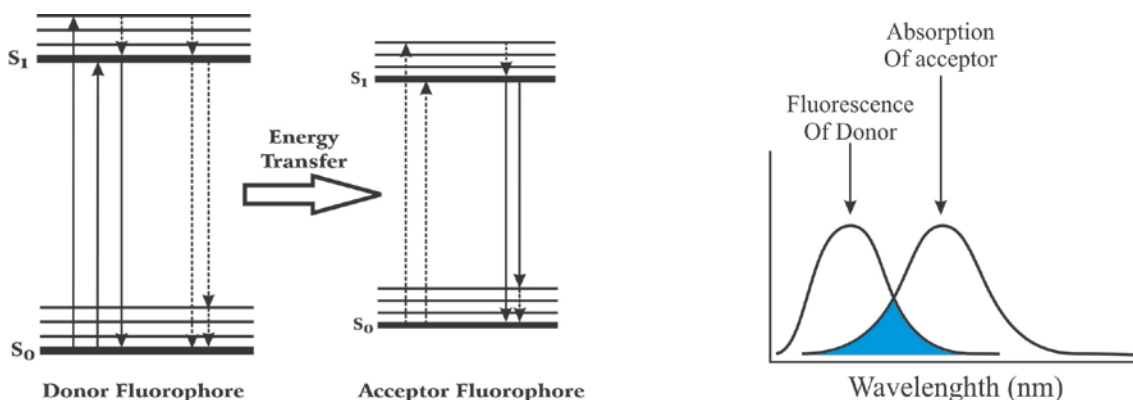


**Figure 4.1:** Jablonski diagram showing resonance energy transfer between donor and acceptor fluorophore, as well as the spectral overlap for donor emission and absorption spectra of fluorophores.

## 4.2 Results and Discussion

The photophysical experiments discussed in this chapter for the various fluorophores and quenchers were performed in order to determine viable FRET pairs for use in molecular probes for the detection of nucleic acids function. In the following experiments, the three quenchers used were labeled: **18a**, **Qb** and **Qc** (**Figure 4.2**). The fluorophores chosen were pyrene (**Fa**), and a phenylpyrrolocytosine acid moiety (**Fb**) (**Figure 4.2**). Compound **18a** was chosen as a quencher, because azo compounds are known to be efficient quenchers and compound **Qb** and **Qc** were found to have quenching properties. The two fluorophores (compound **Fa** and **Fb**) were chosen, because they emit in a region of the UV-visible spectrum which overlaps with the absorption of the three quenchers, which is a requirement for quenching by FRET mechanism.

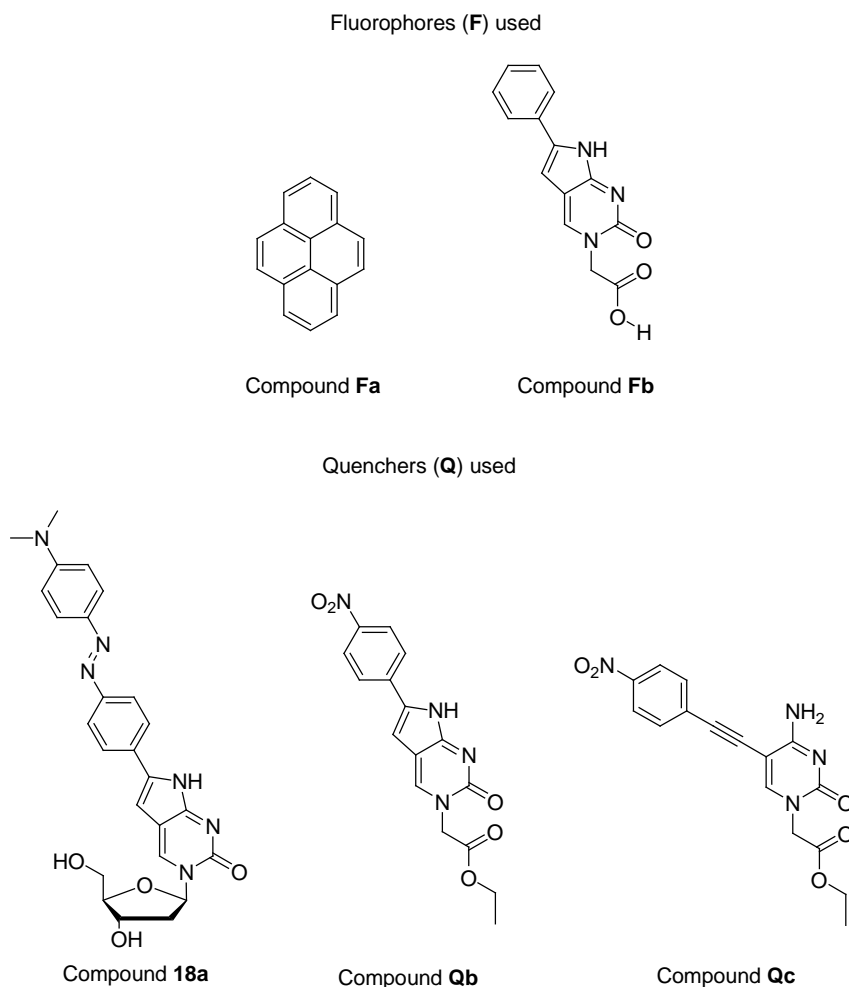


**Figure 4.2:** Illustration showing structural components of fluorophores and quenchers used in quenching studies.

The fluorophores were chosen based on their excitation and emission wavelengths, which are red-shifted from the absorption of natural nucleic acids. For optimal performance of fluorescence quenching, delicate matching of the fluorophore and quencher is important. The quenchers: **18a**, **Qb**, and **Qc** absorption are also red-shifted from natural nucleic acids. Their  $\lambda_{\text{max}}$  absorptions are 445 nm, 400 nm and 397 nm, respectively (**Figure 4.3**).

The fluorescent emission spectra of the two fluorophores: **Fa** and **Fb** were observed in the range of 350-650 nm and the fluorophores were excited in the range of 319 to 334 nm. The wavelength at which the fluorophores were irradiated was based on

the observed UV-visible absorbance of a 5  $\mu$ M solution of the quenchers: **18a**, **Qb** and **Qc** (Figure 4.3).

For each fluorophore, 1 ml of the solution was added to a cuvette and the sample was irradiated in the absence of the quencher. The quencher was then added in microliter volume increments and the fluorescent intensity of the solution was measured after each addition. The intensity of the fluorescence was measured in the units of counts per seconds (1/s).

The UV-visible spectra for each of the fluorophores was observed before the samples were irradiated and after each addition of the quencher. The purpose of this was to determine whether the quenching observed was indeed true quenching or direct absorption of the light by the quencher upon irradiation. Also, any inner filter effect due to the concentration of the fluorophores was constant, because the concentration of the fluorophore was not changed during these experiments.

A linear Stern-Volmer equation in the form of  $y = mx + b$  (y-intercept equal to one), was generated for each viable FRET pair. The Stern-Volmer rate constant ( $K_{sv}$ ) for the fluorescent quenching was determined from the slope of the line, using the Stern-Volmer equation:  $I_0/I = 1 + K_{sv} [Q]$ .

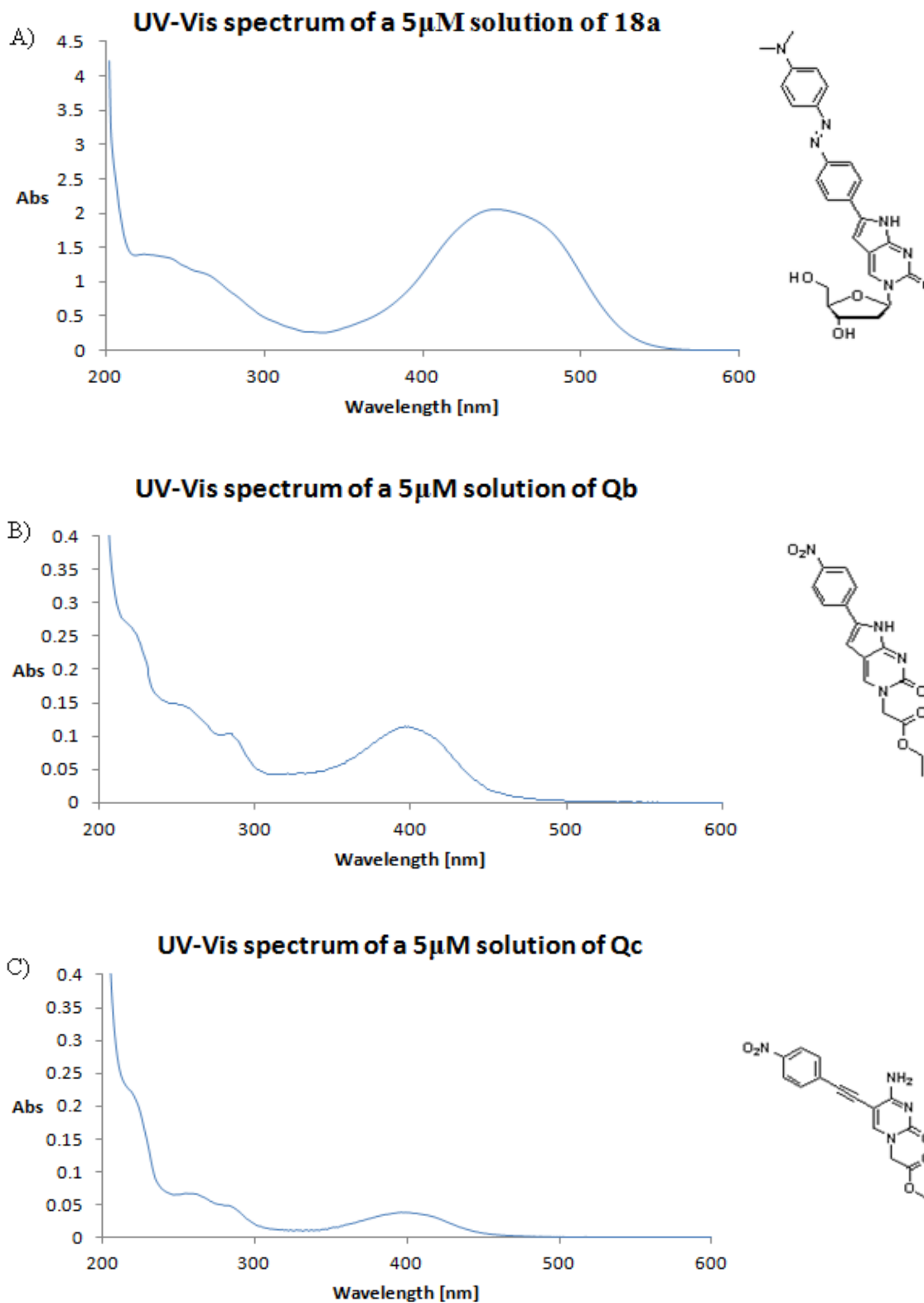


**Figure 4.3:** UV-visible spectra of a 5  $\mu$ M solution of 18a (A), Qb (B) and Qc (C).



#### 4.2.1 Quenching of 1 $\mu\text{M}$ pyrene (**Fa**) fluorophore with 1 mM of the quencher **18a**

The UV-visible spectrum in **Figure 4.4** with the lowest absorbance at 445 nm represents the intensity of the pyrene solution at zero concentration of the 1 mM quencher **18a** (**Figure 4.4**). The emission spectrum of **Fa** overlaps with the absorbance spectrum of **18a**, which was required for quenching via FRET mechanism as shown in **Figure 4.1**.

In this quenching experiment, the sample was irradiated at 334 nm and the UV-visible spectrum was taken after each addition of the quencher. This was done to observe whether there was an increase in the absorbance at the wavelength at which the sample was being irradiated with each addition of the quencher. A steady increase at the wavelength the sample was being irradiated (with each addition of the quencher) would indicate that the quencher was also absorbing the radiation directly. Since this was not the case for this fluorophore and quencher, the possibility of them being used as a FRET pair was promising. As the concentration of the quencher increased with each addition, there was a steady decrease in the fluorescence intensity of the pyrene fluorophore due to quenching and an increase in the UV-visible absorbance at approximately 450 nm. The increase in the UV-visible absorbance at the  $\lambda_{\text{max}}$  of **18a**, as well as the lack of absorbance of **18a** at the irradiated wavelength of 334 nm, was indicative of quenching by FRET mechanism. This was very important and crucial to confirm any quenching by FRET mechanism, hence the quenching observed was “true” quenching by FRET and not direct absorption of the light by the quencher upon irradiation.

Stern-Volmer analysis allowed explanation of the kinetics of a photophysical intermolecular deactivation process. This relationship resulted in a straight line with an  $R^2$  value of 0.9215 for **Fa** and **18a** which was consistent with the Stern-Volmer plot for the mechanism of dynamic quenching. The calculated slope was determined as being  $11,900 \text{ L}\cdot\text{mol}^{-1}$ , which was the Stern-Volmer rate constant for dynamic quenching. The inverse of the Stern-Volmer rate constant ( $K_{\text{sv}}^{-1}$ ), was the concentration of the quencher at which 50% of the intensity of the fluorophore was quenched. Therefore,  $8.43 \times 10^{-5} \text{ mol}\cdot\text{L}^{-1}$  of **18a** would be required to quench 50% of the pyrene (**Fa**) fluorophore. A  $K_{\text{sv}}$  of  $11,900 \text{ L/mol}$  is the product of the bimolecular quenching rate constant ( $k_q$ ) and the

fluorescence lifetime ( $\tau_0$ ) of the excited singlet state of the fluorophore in the absence of the quencher. Once the fluorescence lifetime ( $\tau_0$ ) of the fluorophore is known, the quenching rate constant ( $k_q$ ) can be calculated from the slope. In the case of pyrene, the fluorescence lifetime ( $\tau_0$ ) in ethanol at 293 K was reported as  $410 \times 10^{-9}$  seconds,<sup>[23]</sup> hence the bimolecular quenching rate constant  $k_q$  for the process was,  $2.89 \times 10^{10} \text{ L.mol}^{-1}.\text{s}^{-1}$ . This was significant in understanding the interaction between the two molecules, the larger the magnitude of the slope, the greater the interaction between the pyrene (**Fa**) fluorophore and the quencher **18a**.

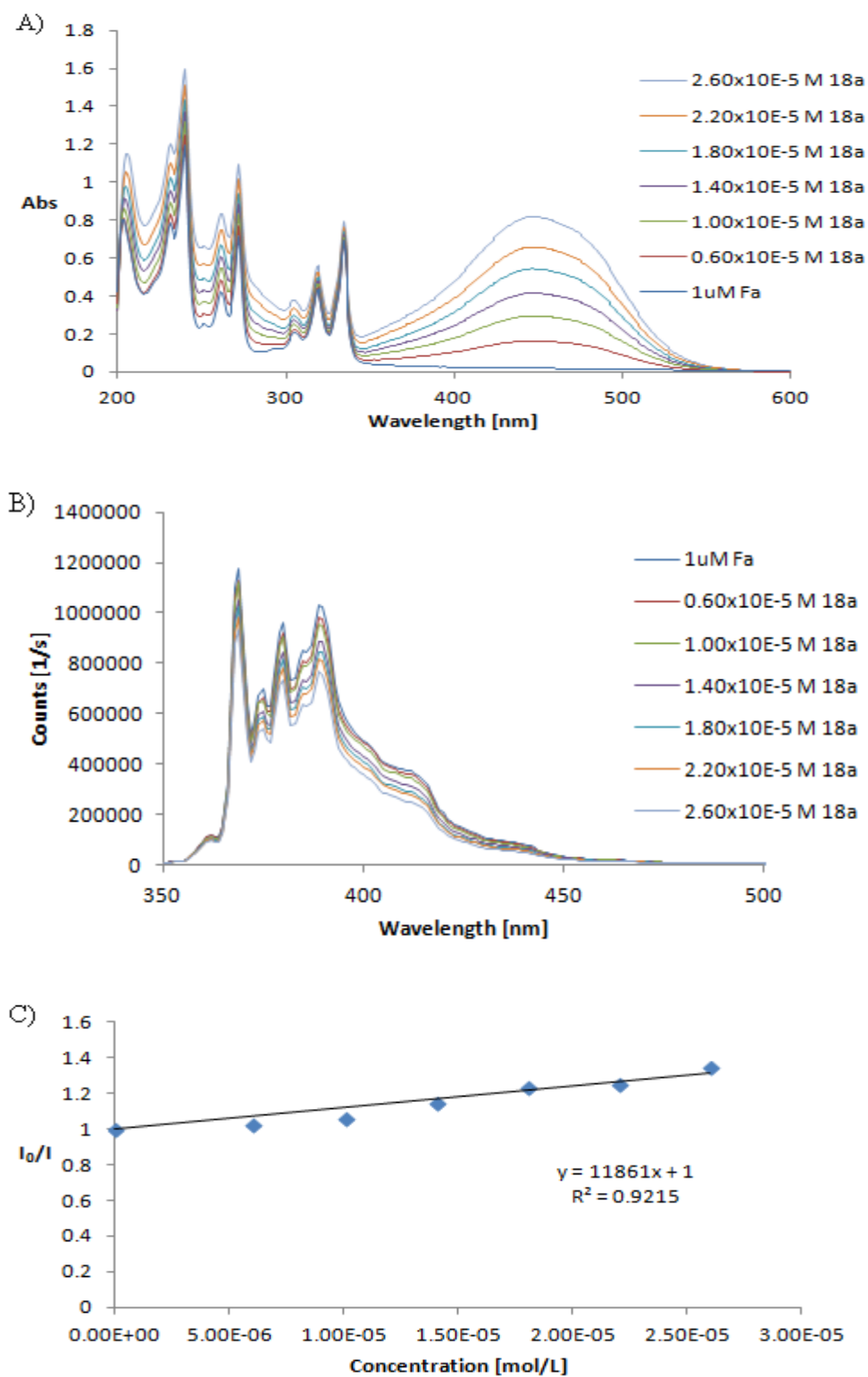


**Figure 4.4:** UV-Visible spectra (A), quenching spectra ( $\lambda_{\text{ex}} = 334 \text{ nm}$ ) (B) and Stern-Volmer plot (C) for 1  $\mu\text{M}$  pyrene and 18a.

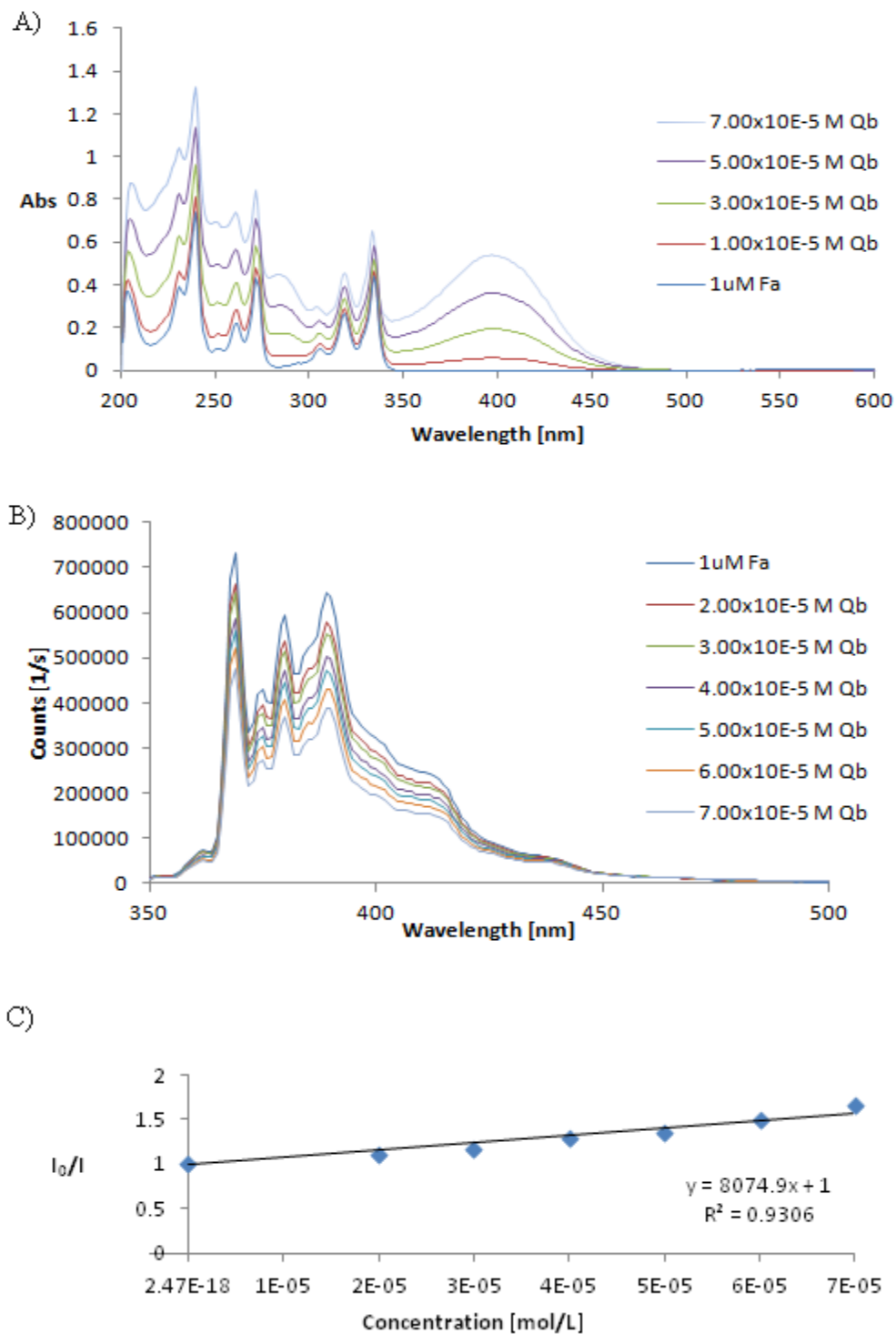
#### 4.2.2 Quenching of 1 $\mu$ M pyrene (Fa) fluorophore with 10 mM *p*-nitrophenylpC moiety (Qb)

In a second quenching experiment using the pyrene fluorophore, 10 mM of another quencher 6-(4-nitrophenyl)pyrrolocytidine ethyl ester moiety (**Qb**) was used. This sample was irradiated at 319 nm and the UV-visible spectra (**Figure 4.5**) were taken before and after the addition of the quencher with each successive addition. The UV-visible spectra indicated that the majority of the light absorbed upon irradiation was being absorbed directly by the fluorophore and not the quencher. This coupled with the results obtained in **Figure 4.5**, which shows the decrease in the fluorescence intensity of the pyrene fluorophore (**Fa**) as the concentration of the quencher in the solution was increased, was an indication of quenching by the mechanism of FRET. Also important for the quenching mechanism by FRET is the overlap of the emission spectrum of the fluorophore and the absorption spectrum of the quencher, which was the case in this experiment.

A Stern-Volmer linear analysis plot was used to determine the relationship between the quenching mechanism of the fluorophore and quencher. A plot of the ratio of the fluorescence intensity versus the concentration of the quencher resulted in a straight line, which was consistent with the mechanism of dynamic quenching using the Stern-Volmer plot. The slope was calculated as being 8,100 L.mol<sup>-1</sup> from the equation  $I_0/I = 1 + K_{sv} [Q]$  and had an R<sup>2</sup> value of 0.9306. From the slope, the  $K_{sv}^{-1}$  (which is the concentration of the quencher that is required to quench 50% of the fluorophore) was determined as being 1.24 x 10<sup>-4</sup> mol.L<sup>-1</sup>. The bimolecular quenching rate constant ( $k_q$ ) can also be calculated from the slope once the lifetime ( $\tau_o$ ) was known. The lifetime of pyrene was reported as 410 x 10<sup>-9</sup> seconds in ethanol at 293 K.<sup>[23]</sup> The bimolecular quenching rate constant was determined as being 1.97 x 10<sup>10</sup> L.mol<sup>-1</sup>.s<sup>-1</sup> for the pyrene fluorophore (**Fa**) and **Qb**.

Based on the results obtained from the first two quenchers (**18a** and **Qb**) used to quench the fluorescence of pyrene, they were able to quench the fluorescence by FRET mechanism. The quencher **18a** was proven to be more effective at quenching the fluorescence of pyrene based on the results obtained. Their  $K_{sv}^{-1}$  value calculated from

the slope of their Stern-Volmer plot resulted in a lower concentration of the quencher **18a** which was required to quench 50% of the pyrene fluorescence. This was an indication that **18a** was more effective at quenching the fluorescence of the pyrene, since a lower concentration was required to have the same effect.



### 4.2.3 Quenching of 5 $\mu$ M pyrene (Fa) fluorophore with 10 mM 5-((4-nitrophenyl)ethynyl) cytosine moiety (Qc)

In this experiment, a third quencher: 5-((4-nitrophenyl)ethynyl)cytosine ethylester moiety (**Qc**), (**Figure 4.2**) was used to compare its effectiveness as a quencher compared to the first two pyrrolocytosines based quenchers: **18a** and **Qb**. The UV-visible spectra (**Figure 4.6**), which were taken before and after each successive addition of the quencher to the pyrene fluorophore did not show any evidence that the quencher absorbed the light directly upon irradiation at 334 nm. This was crucial, in order to prove that the observed decrease in the fluorescence intensity of the pyrene was due to quenching by FRET mechanism and not direct absorption of the light by the quencher at the wavelength of excitation.

A Stern-Volmer plot relating the ratio of the fluorescence intensity to the concentration of the quencher was used to better understand the observed quenching. A plot of  $I_0/I = 1 + K_{sv} [Q]$  resulted in a Stern-Volmer rate constant of  $2,100 \text{ L}\cdot\text{mol}^{-1}$ , with an  $R^2$  value of 0.9617. The inverse of the Stern-Volmer rate constant ( $K_{sv}^{-1}$ ) was calculated as being  $4.83 \times 10^{-4} \text{ mol}\cdot\text{L}^{-1}$ , which was the concentration of the **Qc** quencher required to quench 50% of the pyrene fluorophore. The bimolecular quenching rate constant ( $k_q$ ) for the quenching process was determined as being  $5.05 \times 10^9 \text{ L}\cdot\text{mol}^{-1}\cdot\text{s}^{-1}$ .

Of the three quenchers used in the quenching of pyrene, the quencher **Qc** was the least efficient at quenching the fluorescence. This was determined from the Stern-Volmer rate constants and the  $K_{sv}^{-1}$  values for each one. The mechanism of quenching for the three quenchers with the pyrene fluorophore was due to dynamic quenching. This was based on the UV-visible absorbance of each mixture, which is one method for distinguishing static from dynamic quenching. This was also supported by the bimolecular quenching rate constant  $k_q$ , since diffusion-controlled values can result in a  $k_q$  value close to  $1 \times 10^{10} \text{ L}\cdot\text{mol}^{-1}\cdot\text{s}^{-1}$ .<sup>[39]</sup>

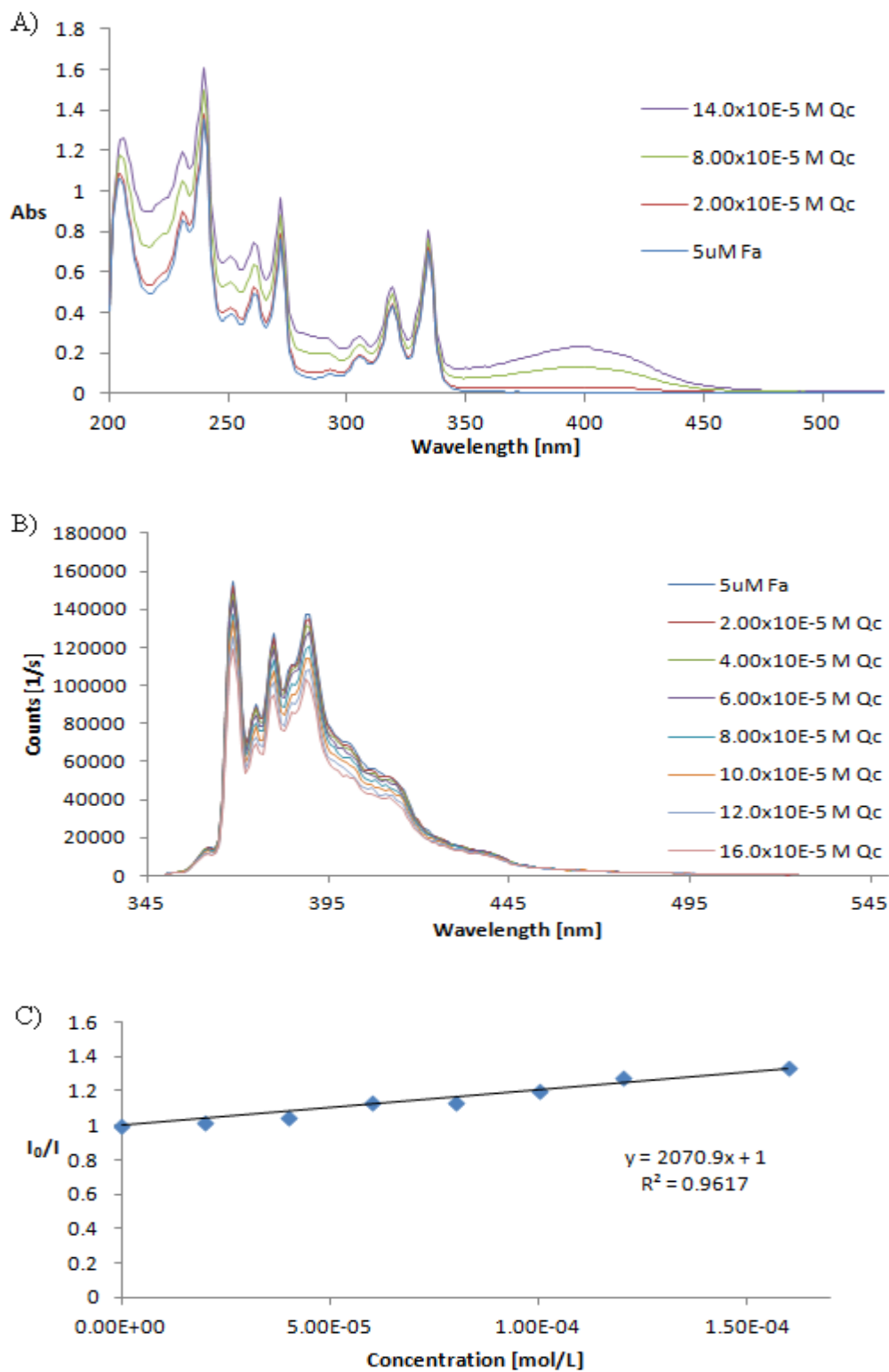


**Figure 4.6:** UV-visible spectra (A), quenching spectra ( $\lambda_{\text{ex}} = 334 \text{ nm}$ ) (B) and Stern-Volmer analysis plot (C) for 5  $\mu\text{M}$  pyrene and Qc.



#### 4.2.4 Quenching of 1 $\mu$ M Fb fluorophore with 1 mM DABCYL mimic (18a)

In this photophysical experiment, another fluorophore was used with the 1 mM **18a** quencher to determine their viability to be used as a FRET pair. The 1  $\mu$ M solution of **Fb** (**Figure 4.2**), was analyzed by UV-visible absorbance before the quencher was added to the solution and after each successive addition of the quencher. The results of these absorbance spectra can be seen in **figure 4.7**. The fluorophore was irradiated at 320 nm and at that wavelength the quencher appeared to have absorbed some of the radiation directly (**Figure 4.7**), this is thought to have been attributed to static and dynamic quenching competing with each other. The ability of the quencher to absorb the radiation at that wavelength does not appear to be very significant; hence, the observed decrease in the fluorescence intensity was probably mainly due to the quenching (**Figure 4.7**) by FRET mechanism.

The Stern-Volmer analysis plot (**Figure 4.7**), based on the equation  $I_0/I = 1 + K_{sv}$  was used to understand further the mechanism of quenching. Based on the UV-visible spectra, it was suspected that the quenching may have been due to a combined static and dynamic quenching. In that case, the Stern-Volmer plot was expected to curve upwards towards the y-axis.<sup>[39]</sup> The plot yielded a straight line which was consistent with dynamic quenching with a Stern-Volmer rate constant of 16,800 L.mol<sup>-1</sup> and an R<sup>2</sup> value of 0.9543. The  $K_{sv}^{-1}$  for the quencher was calculated as being 5.95 x 10<sup>-5</sup> mol.L<sup>-1</sup>. This quencher was slightly more effective at quenching the pyrene fluorophore over the **Fb** fluorophore based on their  $K_{sv}^{-1}$  value obtained from their slopes. This may be due to better overlap of the emission spectrum of pyrene and the absorption spectrum of **18a** for quenching by FRET mechanism. The emission of the **Fb** fluorophore was more red-shifted than the pyrene fluorophore (**Fa**), so a quencher that absorbs closer to the red region in comparison to **18a** may be more effective at the quenching of the **Fb** fluorophore.

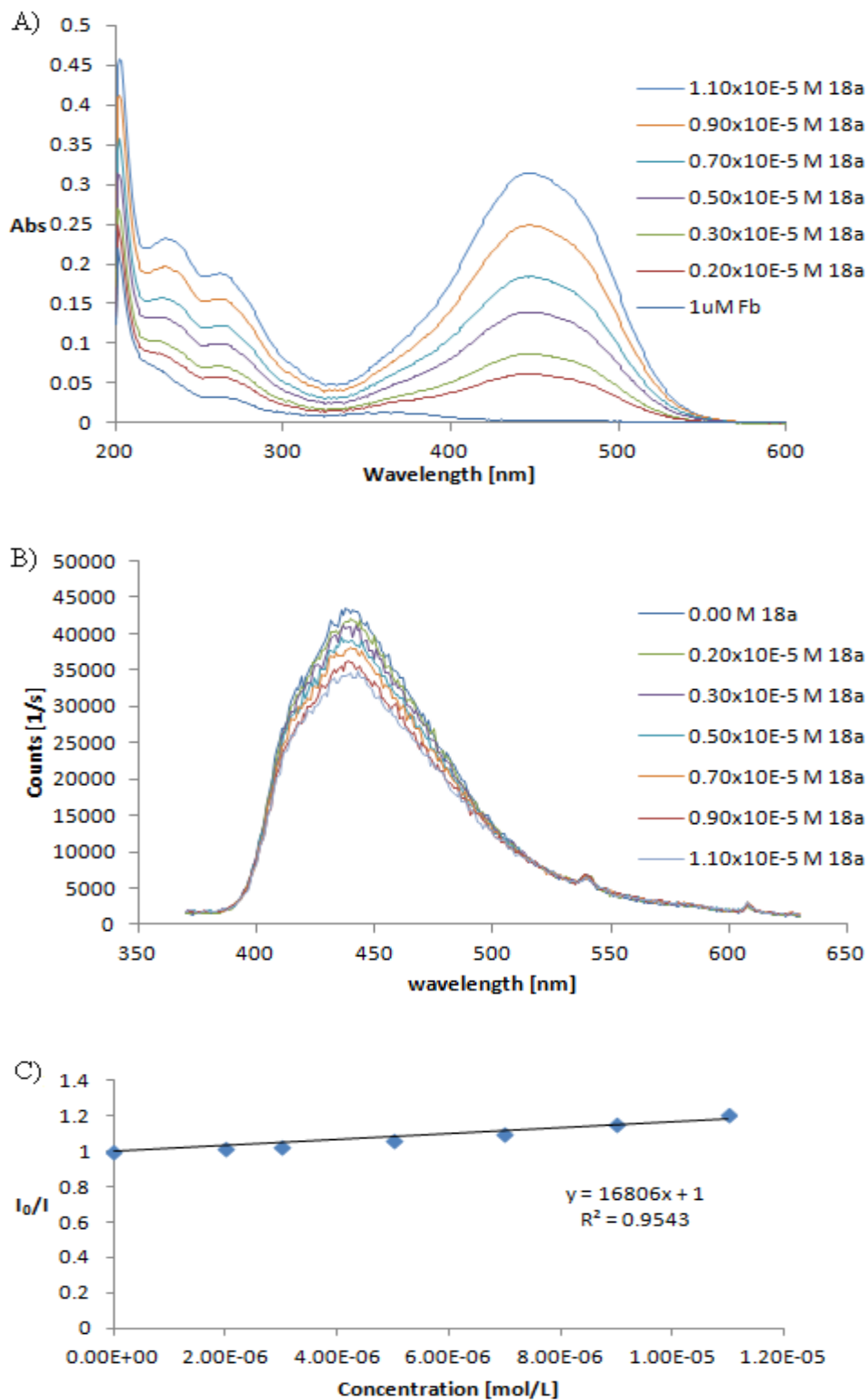


**Figure 4.7:** UV-visible spectra (A), quenching spectra ( $\lambda_{\text{ex}} = 320$  nm) (B) and Stern-Volmer analysis plot (C) for 1  $\mu\text{M}$  phenylpC acid and **18a**.

#### 4.2.5 Quenching of 1 $\mu$ M Fb fluorophore with 10 mM 6-(4-nitrophenyl)pC ethylester moiety (Qb)

The quencher **Qb** ability to be used as a possible FRET pair with another fluorophore (**Fb**) was determined photophysically. In this experiment, a 1  $\mu$ M solution of **Fb** was used and the UV-visible spectrum was taken. The sample was then irradiated at 320 nm, after which the quencher **Qb** was added to the sample and the UV-visible spectrum was taken again. The UV-visible spectra obtained from the experiment after each successive addition of the quencher indicated that the quencher absorbed the light directly upon irradiation (**Figure 4.8**), or that a ground state complex was being formed which perturbed the absorption spectrum of the fluorophore. The sample was irradiated at different wavelengths but the result did not change.

A Stern-Volmer plot was then used to better understand the mechanism of the observed quenching. A Stern-Volmer plot of the fluorescence ratio versus the concentration of the quencher was expected to produce a straight line for dynamic or static quenching, but the line was expected to be second order in relation to the concentration of the quencher **Qb** and curve upwards towards the y-axis in the case of a combined static and dynamic quenching happening simultaneously. The Stern-Volmer plot yielded a straight line with slope 5600 L.mol<sup>-1</sup> and an R<sup>2</sup> value of 0.9913. Based on the photophysical data obtained, dynamic quenching was eliminated as a possible mechanism of quenching due to the perturbation of the UV-visible spectra. The Stern-Volmer plot indicated that there was not a combined static and dynamic quenching happening, because the plot was not second order in relation to the quencher **Qb**.

The quenching observed may be due to static quenching, but this was difficult to confirm without the fluorescence lifetime ( $\tau_0$ ) of the fluorophore **Fb**. For static quenching  $\tau_0/\tau = 1$ .<sup>[39]</sup> Another reason for the observed quenching may be due to direct absorption of the light upon irradiation by the quencher **Qb**. The fluorescence lifetime is required to confirm the exact mechanism of quenching, but the photophysical data collected has eliminated collisional/dynamic quenching. Based on these experimental results, the fluorophore **Fb** and the quencher **Qb** do not appear to be a good FRET pair.

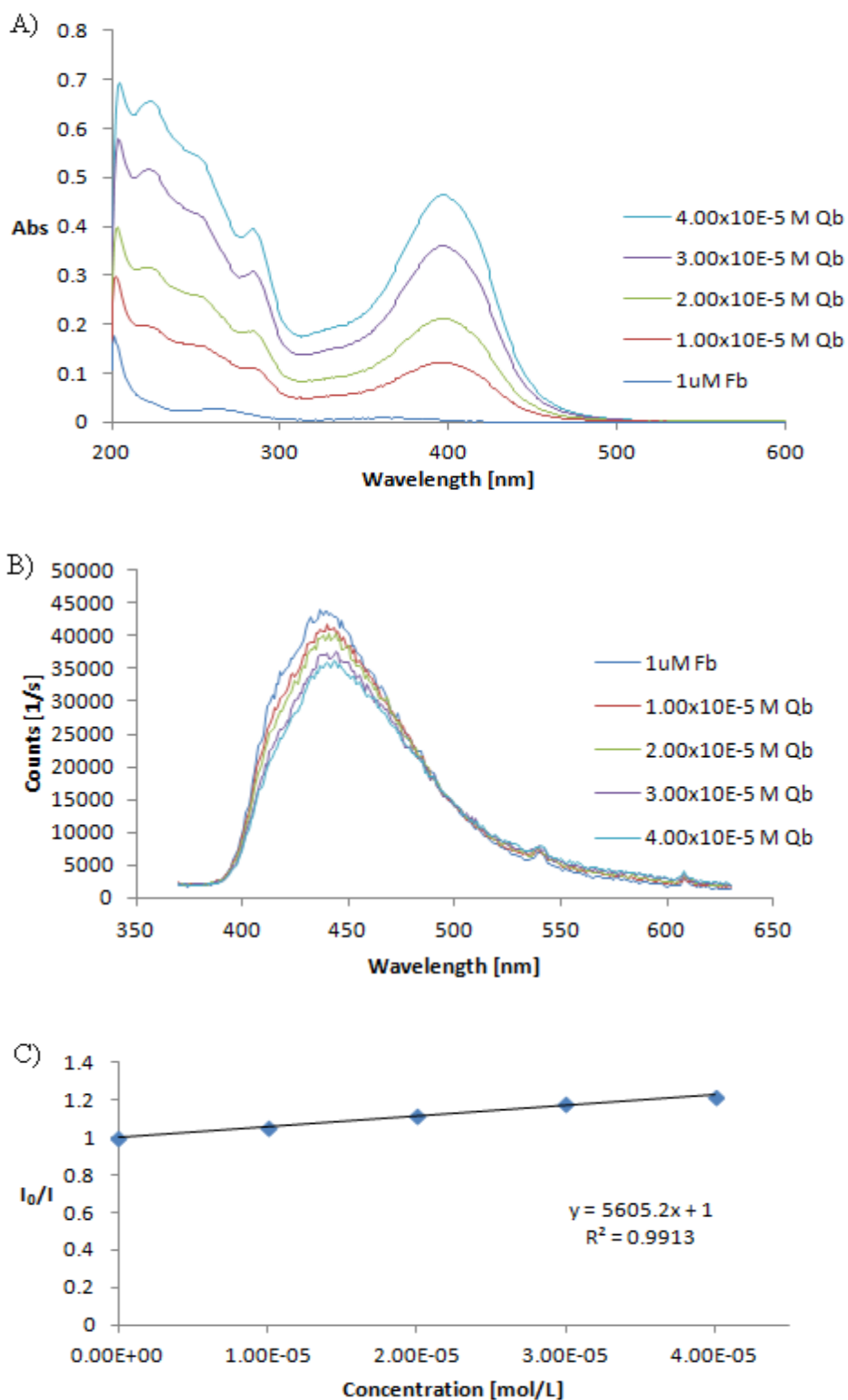
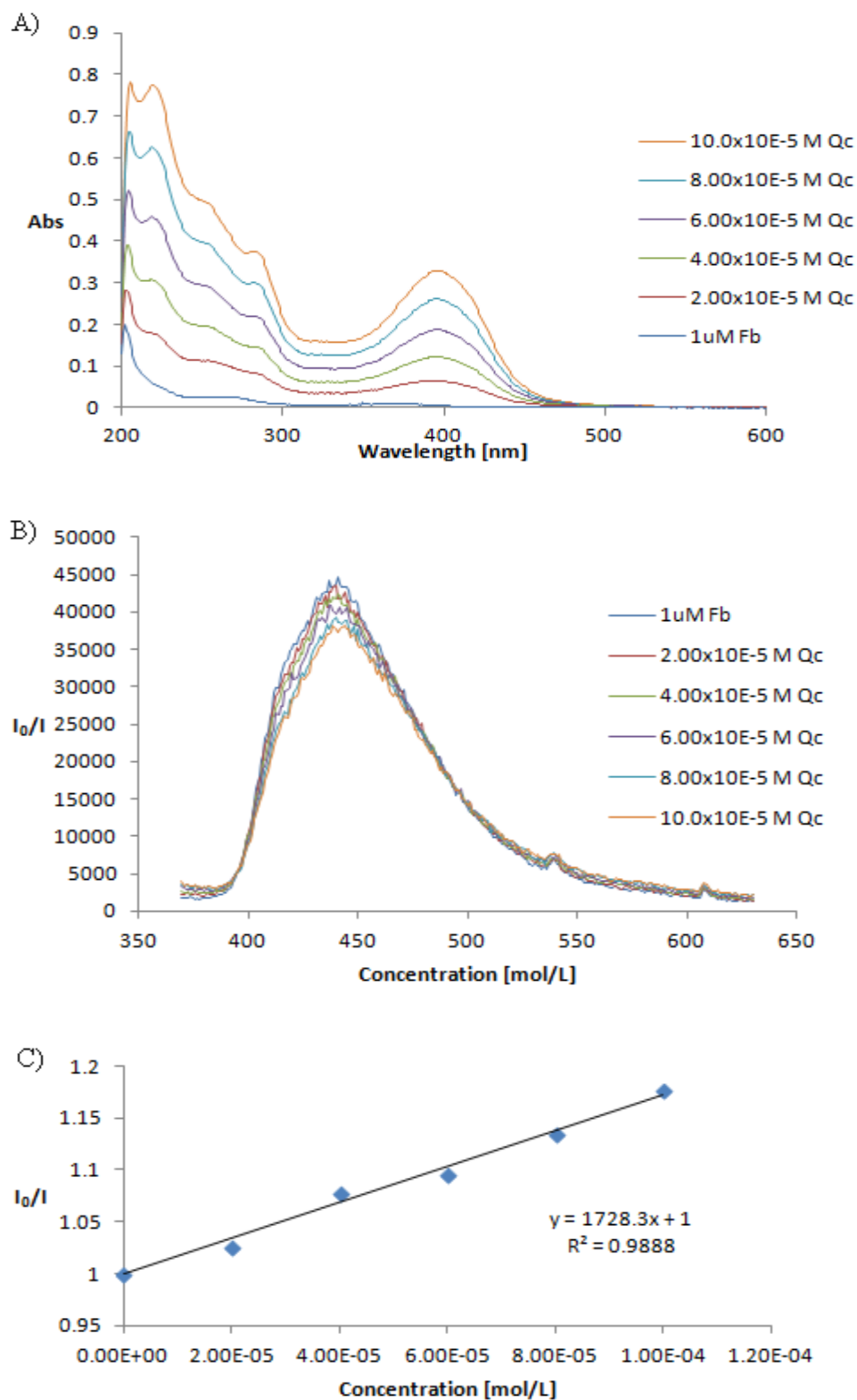


**Figure 4.8:** UV-Visible spectra (A), quenching spectra ( $\lambda_{\text{ex}} = 320$  nm) (B) and Stern-Volmer plot (C) for 1  $\mu$ M phenylpC acid moiety and Qb.

#### 4.2.6 Quenching of 1 $\mu$ M Fb fluorophore with 10 mM 5-((4-nitrophenyl)ethynyl) cytosine ethylester moiety (Qc)

In this quenching experiment, a 1  $\mu$ M solution of the fluorophore **Fb** and 10 mM solution of the quencher **Qc** were used. The sample was irradiated at 320 nm before and after each successive addition of the quencher and the results obtained from the UV-visible absorbance (**Figure 4.9**) indicated that it was perturbed. The attempt to irradiate at different wavelengths gave the same results. Based on these results, the mechanism of dynamic quenching was eliminated as the possible reason for the decrease in the fluorescence intensity of the **Fb** fluorophore.

A Stern-Volmer plot which related the ratio of the fluorescence intensity versus the concentration of the quencher **Qc** was plotted to better understand the mechanism of the observed quenching. The Stern-Volmer plot was linear with a  $K_{sv}$  value of 1700  $L \cdot mol^{-1}$  and an  $R^2$  value of 0.9888. A combined quenching of static and dynamic occurring simultaneously was eliminated, because the slope was not second order in relation to the quencher. Based on these results obtained, the quenching observed may have been due to static quenching, but this cannot be confirmed without the fluorescence lifetime of the fluorophore. Another possible reason for the observed quenching was direct absorption of the light by the quencher **Qc** at the wavelength the sample was being irradiated. Based on these photophysical quenching experiments, the fluorophore **Fb** and **Qc** are not a good FRET pair.



#### 4.2.7 Isomerization test for the quencher 18a

This experiment was designed to mimic the conditions that the quencher (**18a**) was subjected to upon irradiation to determine if there was any geometric isomerization of the azopyrrolocytidine quencher (**18a**) during the quenching experiments. The trans isomer is planar and the pi electrons are delocalized throughout the azopyrrolocytidine quencher **18a**, making it more thermodynamically stable compared to the cis isomer where there is steric clash between the two phenyl rings, causing them to have a skewed conformation. Based on previous photoisomerization studies done in the Hudson group with azobenzene, the cis form was expected to have an absorbance spectrum with a peak that was more red-shifted than the trans form, as well as a decrease in the absorbance at the  $\lambda_{\text{max}}$  of the trans form (**Figure 4.11**).<sup>[40]</sup> The azopyrrolocytidine quencher (**18a**) was expected to be more red-shifted than azobenzene, due to the conjugation between the azobenzene moiety and the pyrrolocytosine chromophore, as well as the auxochromic  $\text{NH}_2$  group attach to the chromophore. This bathochromic shift can be observed by the difference in absorbance of the  $\lambda_{\text{max}}$  of the two trans isomers (**Figure 4.10** and **Figure 4.11**).

The isomerization test was performed by the irradiation of a 1  $\mu\text{M}$  sample of **18a** at 443 nm for 68 seconds in order to be consistent with the integration time per nm with the quenching experiments. This was done fifteen times and then the UV-visible spectrum of the sample was taken afterwards to observe if there was any change in the absorbance. It should be noted that the cumulative irradiation that the **18a** sample was subjected to during this isomerization experiment was longer than the excitation time of the quenching studies. After the sample was irradiated, there was a decrease in the absorbance spectrum (**Figure 4.10**), which may have been due to the formation of the cis product. However, there was no new noticeable peak observed at longer wavelength as seen in **Figure 4.11** for the azobenzene. Although this was not the result obtained, the decrease in the absorbance after the first few irradiations may have been due to a small percentage of the cis product in equilibrium with the trans isomer. Therefore, the equilibrium for this isomerization was to the left (**Scheme 4.1**) when the azopyrrolocytidine was irradiated at 443 nm. Based on the work done by the Hudson

group, the azobenzene isomerizes to the cis product when excited under UV light between 300 – 400 nm and returns to the trans product when excited thermally or at wavelength greater than 400 nm.<sup>[40]</sup> **Scheme 4.2** shows the two proposed mechanisms for the trans to cis isomerization of azobenzene.<sup>[41]</sup>

Based on the UV-visible spectra obtained after the sample was irradiated, it was reasonable to say that the quenching observed by the addition of **18a** was due mainly to the trans form of the quencher, since the absorbance of the spectrum is directly proportional to the concentration of the solution.

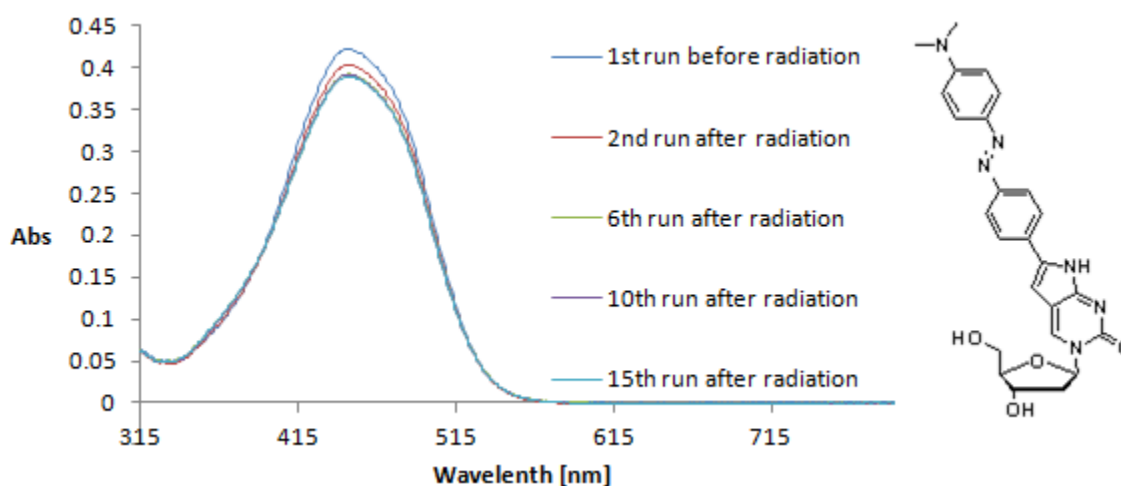


**Figure 4.10:** Spectra of a 1 μM irradiated sample of **18a**.



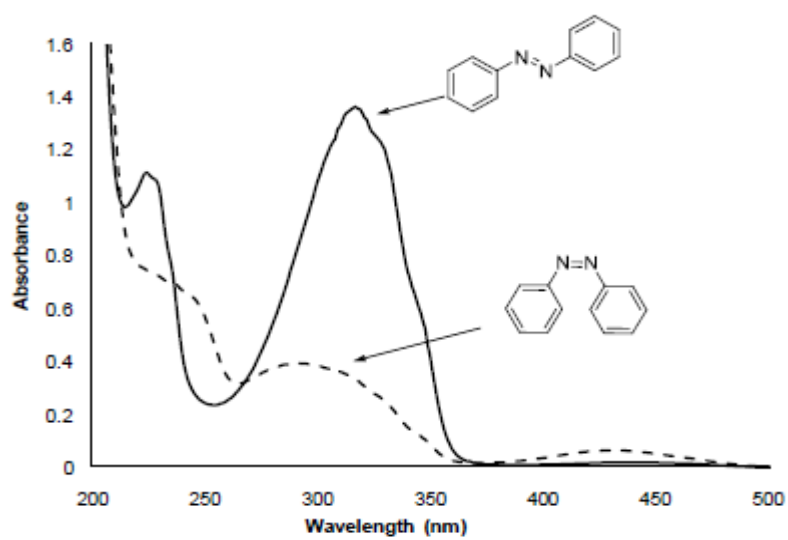
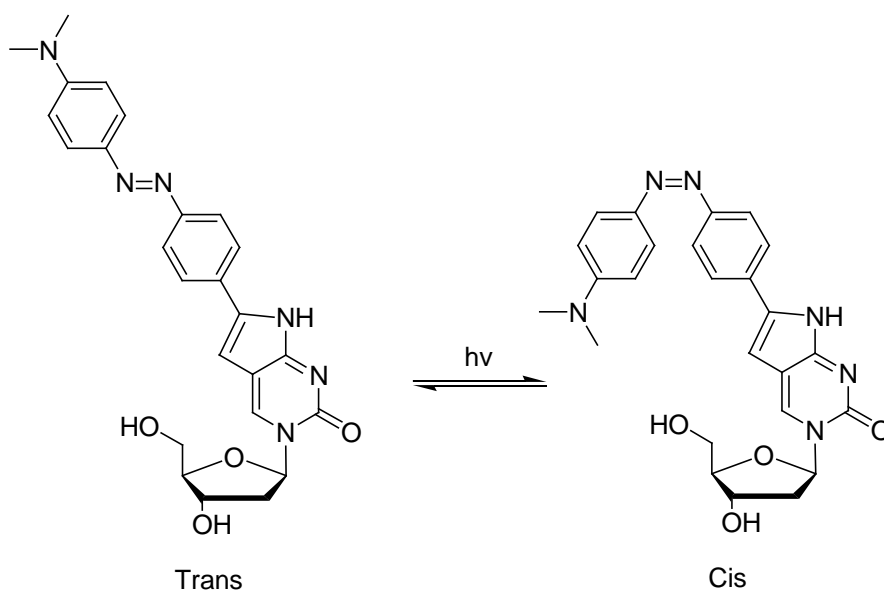
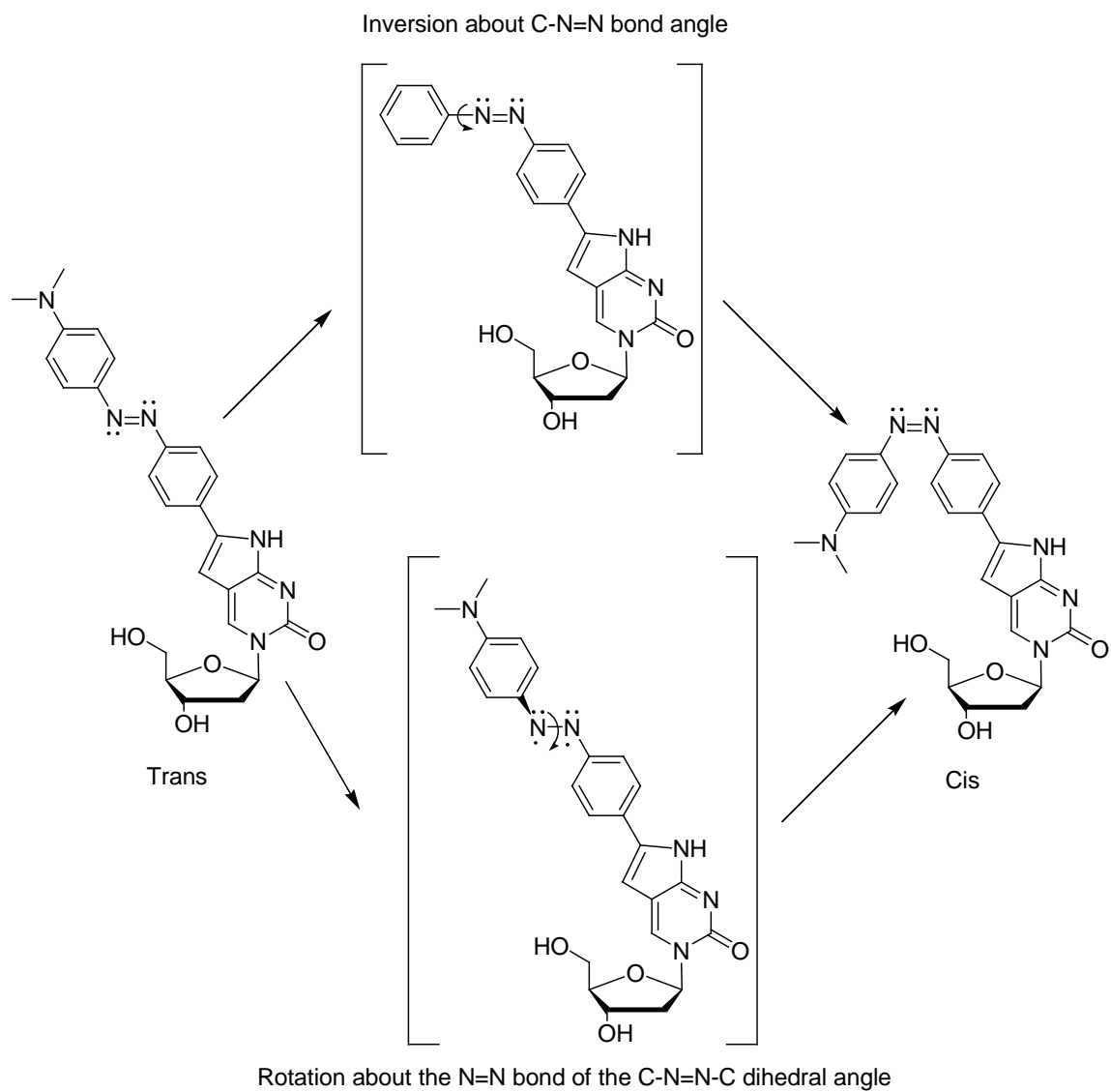


**Figure 4.11:** UV-visible spectrum of the trans and cis isomer of azobenzene in ethanol at room temperature.<sup>[40]</sup>



**Scheme 4.1:** Trans (left) to cis (right) equilibrium for the isomerization of the azopyrrolocytidine quencher.



**Scheme 4.2:** Proposed mechanisms for the isomerization of the azopyrrolocytidine quencher (**18a**) from the trans-cis isomer.

#### 4.2.8 Determination of the quencher **18a** molar absorptivity

In this experiment, the molar absorptivity of the quencher **18a** was determined from a plot of the absorbance versus concentration at various wavelengths, according to the Beer-Lambert law:  $A = \epsilon bc$  where:

$A$  = Absorbance

$\epsilon$  = molar absorptivity ( $\text{L}\cdot\text{mol}^{-1}\text{cm}^{-1}$ )

$b$  = path length (cm)

$c$  = concentration (mol/L)

The molar absorptivity was determined at two wavelengths: 260 and 445 nm, because the pyrrolocytosines possess a relatively strong absorbance in the region of 260 nm<sup>[1]</sup> and at approximately 445 nm, the quencher **18a** possess another strong absorbance (**Figure 4.3**). The molar absorptivity at 260 and 445 nm was found to be 44,300 and 47,600  $\text{L}\cdot\text{mol}^{-1}\cdot\text{cm}^{-1}$ , respectively (**Figure 4.12**) in ethanol. The accepted molar absorptivity for DABCYL, SE was found as being 32800  $\text{L}\cdot\text{mol}^{-1}\text{cm}^{-1}$  at 453 nm in methanol<sup>[42]</sup> (**Figure 4.13**).

The molar absorptivity for compound **Qb** was determined by the Hudson group as being 9,000  $\text{L}\cdot\text{mol}^{-1}\text{cm}^{-1}$  at 436 nm in dichloromethane.<sup>[1]</sup> The molar absorptivity for compound **Qc** was also determined by the Hudson group and was determined to be 2,800  $\text{L}\cdot\text{mol}^{-1}\text{cm}^{-1}$  in dichloromethane.<sup>[1]</sup> Compounds **Qb** differ from **Qc** only in the pyrrole ring, yet its molar absorptivity was three times that of **Qc**. The increase in the molar absorptivity from the DABCYL, SE quencher was a measure of how strongly **18a** absorbs light in comparison to the universal DABCYL quencher. This was attributed to the intrinsic property of the pyrrolocytosine scaffold which increased the electron complexity of the quencher. This has the effect of broadening its absorption spectrum which can increase its quenching efficiency; the absorbance ( $A$ ) of the sample was dependant on the path length ( $b$ ) and the concentration ( $c$ ) via the Beer-Lambert law. Based on the calculated molar absorptivity, the universal DABCYL quencher was made

more effective electronically at absorbing light by coupling it to the pyrrolocytosine scaffold. This was not surprising, since a similar observation was made by the Crisalli group when they increased the electronic complexity of the DABCYL quencher, broadening its absorption spectrum, which increased its quenching efficiency and versatility.<sup>[43]</sup>

The two reference compounds used to compare the values of **18a**, **Qb** and **Qc** were **reference compounds 1** and **2** (**Figure 4.13**). The cytosine-1-acetic acid nucleobase (**reference compound 2**) had a molar absorptivity of  $700 \text{ L}\cdot\text{mol}^{-1}\text{cm}^{-1}$  at 344 nm in methanol.<sup>[1]</sup>

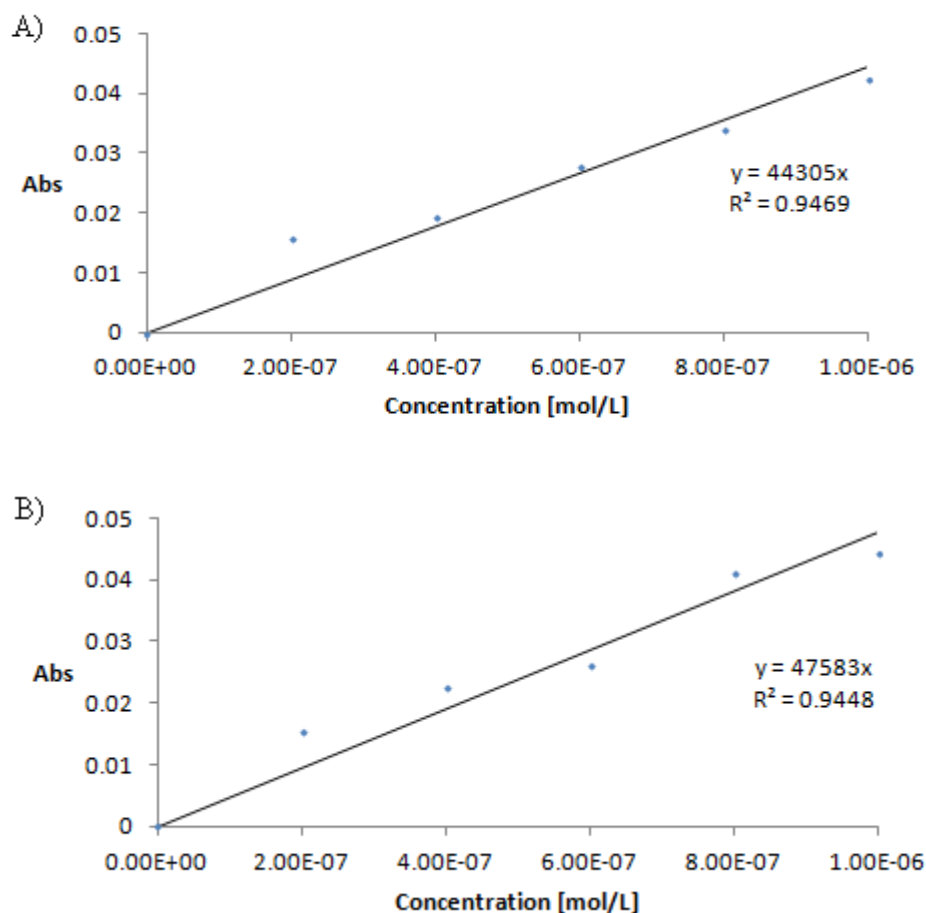
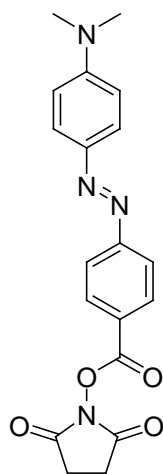
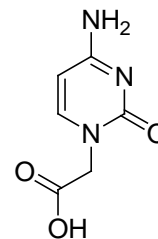


**Figure 4.12:** Plots of absorbance versus concentration to determine the molar absorptivity at 260 nm (A) and 445 nm (B) for **18a**.



4-((4-(dimethylamino)phenyl)azo)benzoic acid, succinimidyl ester (DABCYL, SE)

**Reference compound 1**



Cytosine-1-acetic acid

**Reference compound 2**

**Figure 4.13:** Structural representation of DABCYL, SE and cytosine-1-acetic acid reference compounds.

### 4.3 Conclusion

In conclusion, the Stern-Volmer rate constants ( $K_{sv}$ ),  $K_{sv}^{-1}$  and the bimolecular quenching rate constant ( $k_q$ ) were calculated for the FRET pairs (**Fa** with **18a**, **Qb** and **Qc**) where dynamic quenching was observed. The  $K_{sv}$  and  $K_{sv}^{-1}$  were also calculated for **Fb** and **18a**, but their  $k_q$  was not determined, because the lifetime of **Fb** was not known. The quenching experiments of **Fb** using **Qb** and **Qc** determined that dynamic quenching did not occur. For the three quenchers: **18a**, **Qb** and **Qc**, the azopyrrolocytidine (**18a**) had the highest  $K_{sv}$  and a lower concentration was required to quench 50% of the fluorophores fluorescence ( $K_{sv}^{-1}$ ), making it the best quencher of the three.

Upon subjection to UV-visible irradiation, the azopyrrolocytidine quencher (**18a**) underwent isomerization to the cis product. It was also determined that the equilibrium was to the left, based on the UV-visible spectrum of the trans isomer.

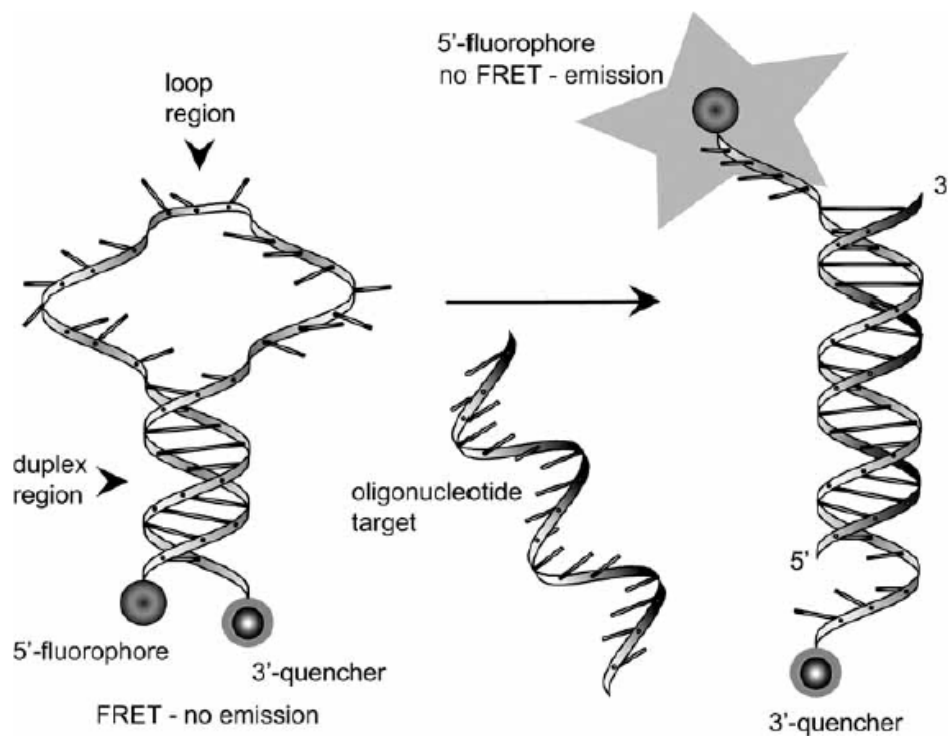
The molar absorptivity was also determined for the azopyrrolocytidine quencher (**18a**) at 260 and 445 nm and was found to be 44,300 and 47,600  $L \cdot mol^{-1} \cdot cm^{-1}$ , respectively. This data indicated that the new azopyrrolocytidine quencher (**18a**) was

more efficient at absorbing light than the universal DABCYL, SE quencher based on the Beer-Lambert law.

Overall, the azopyrrolocytidine based on the universal DABCYL quencher was found to be a very efficient quencher and the pyrrolocytosine scaffold was found to electronically improve the intrinsic property of the DABCYL quencher, hence increasing its molar absorptivity.

## 4.4 Future Outlook

Based on the results obtained from the quenching experiments, the quenchers: **18a**, **Qb** and **Qc**, were all capable of effectively quenching the pyrene (**Fa**) fluorophore via FRET mechanism. The next step is to synthesize them on a larger scale in order to incorporate them into oligomers to be used as molecular beacon technology<sup>[14]</sup>, based on the FRET mechanism (**Scheme 4.1**)<sup>[10]</sup>.



**Scheme 4.3:** Illustration of FRET mechanism operation used in molecular beacon technology.<sup>[10]</sup>

## 4.5 Experimental

The excitation wavelength, at which the pyrene and 6-phenylpyrrolocytidine were excited, was determined experimentally using UV-visible spectroscopy. The fluorescence emission spectra were recorded in the range of 350-650 nm for the pyrene and the 6-phenylpyrrolocytidine fluorophore, by exciting in the range of 319 to 334 nm. This was done using a PTI 6000 fluorescence spectrometer. The fluorescence intensity was measured in the arbitrary unit of counts per second (1/s).

The isomerization experiment of the azopyrrolocytidine was done by irradiating the quencher at 443 nm and the UV-visible spectra were observed in the range of 800 – 315 nm. This was performed on a Cary 300 Bio UV-visible spectrometer.

### 4.5.1 Preparation of the 5 $\mu$ M pyrene (Fa) solution

A 5  $\mu$ M solution of the pyrene fluorophore was prepared by weighing out 0.0106  $\pm$  0.0001 g of the fluorophore. It was then dissolved in 10 ml of anhydrous ethanol to produce the stock solution. From that stock solution, 0.01 ml was taken and diluted to 10 ml in anhydrous ethanol to give the desired concentration of solution.

### 4.5.2 Preparation of the 1 $\mu$ M pyrene (Fa) solution

A 1  $\mu$ M solution of the pyrene solution was prepared by taking 1 ml of a 5  $\mu$ M stock solution and diluting it to 5 ml in a volumetric flask.

### 4.5.3 Preparation of the 1 $\mu$ M phenyl pC acid (Fb) solution

A 5  $\mu$ M solution of the 6-phenylpyrrolocytidine acid moiety fluorophore was prepared by weighing out 0.0011  $\pm$  0.0001 g of the material and it was dissolved in 10 ml of anhydrous ethanol. From that stock solution, 2 ml was then taken and diluted to 10 ml in a volumetric flask; producing the desired concentration of the 1  $\mu$ M solution of **18a**.

#### 4.5.4 Preparation of the 1 mM azopyrrolocytidine (18a) solution

A 1 mM solution of the DABCYL mimic quencher (azopyrrolocytidine) was made by weighing out 0.0047 +/- 0.0001 g of the starting material and it was dissolved in 10 ml of anhydrous ethanol to give the desired concentration of solution.

#### 4.5.5 Preparation of the 10 mM 6-(4-nitrophenyl) pC moiety (Qb) solution

A 10 mM solution of the 6-(4-nitrophenyl)pyrrolocytidine moiety was prepared by weighing out 0.0034 +/- 0.0001 g of the material and it was then dissolved in 1 ml of anhydrous ethanol to give the desired concentration of solution.

#### 4.5.6 Preparation of the 10 mM 5-((4-nitrophenyl)ethynyl)cytosine moiety (Qc) solution

A 10 mM solution of the 5-((4-nitrophenyl)ethynyl)cytosine moiety was prepared by weighing out 0.0034 +/- 0.0001 g of the material and it was then dissolved in 1 ml of anhydrous ethanol to give the desired concentration of solution.

#### 4.5.7 Quenching studies

1 ml of the respective fluorophores (**Fa** and **Fb**) dissolved in anhydrous ethanol were added to a cuvette and the excitation wavelength were determined using UV-visible absorption. The excitation wavelength for the solution of **Fa** and **Fb** were in the range of 319 – 334 nm. Their emission spectrum was first run in the absence of the quencher and then  $\mu\text{L}$  volumes of the various quenchers were added to the fluorophore and their emission spectrum was run to determine the level of quenching. The UV-visible spectrum of each sample was run before and after the addition of the quencher. The total concentration of the quencher after each addition was determined and a Stern-Volmer analysis plots was used in the analysis of the possible FRET pairs.



#### 4.5.8 Isomerization test for the 18a quencher

1 ml of a 1  $\mu\text{M}$  solution of **18a** was added to a quartz cuvette and the sample was scanned by UV-visible absorbance from 800 – 315 nm. The sample was then irradiated at 443 nm for 68 seconds on a pti 6000 fluorometer. After the sample was irradiated, the UV-visible absorbance was observed again for any visible changes in the spectrum. The radiation and UV-visible absorbance step was repeated fifteen times.

#### 4.5.9 Determination of the molar absorptivity of 18a

Using a 100  $\mu\text{L}$  Hamiltonian syringe, 1, 2, 3, 4 and 5  $\mu\text{L}$  volumes of the 1 mM quencher **18a**, was diluted to 5 ml in a volumetric flask to obtain concentrations of 0.2, 0.4, 0.6, 0.8 and 1  $\mu\text{M}$  respectively. The UV-visible absorbance of a 1 ml volume for each concentration was determined and the absorbance at 260 and 445 nm for each concentration was noted. The molar absorptivity was then determined from a plot of absorbance versus concentration.

## Chapter 5

### 5 Conclusion and Outlook

This thesis reports work that was done in the field of nucleic acid chemistry with emphasis on the synthesis of modified pyrrolocytidines. The synthesis of these modified pyrrolocytidines started with the synthesis towards the 5-phenylpyrrolocytidine, which was unsuccessful. The target compound was not attained due to the inability to iodinate at the 5-position of the furanouridine. Various methodologies, including Dembinski bicyclic halofuranopyrimidine were used with no success. The 5-aromatic substituted pyrrolocytidines are still of great interest in our group; their successful synthesis would allow determination of the best position for substitution on the pyrrolocytidine scaffold in regards to fluorescent properties, as well as allow insight into its ability to form duplexes when incorporated into oligomers. It is proposed that for future work, synthesis should begin with the unsubstituted pyrrolocytosine nucleobase.

The successful synthesis of five 6-substituted pyrrolocytidine monomers was completed, namely the pyrrolocytidine, 6-(4-methoxyphenyl)pyrrolocytidine and the 6-phenylpyrrolocytidine fluorophore, as well as the 6-(4-nitrophenyl)pyrrolocytidine and 6-(4-((*N,N*-(dimethylamino)phenyl)azo)benzene)pyrrolocytidine quencher. These pyrrolocytidine quenchers will be added to our group's archive of fluorescent quenchers. In molecular beacon technology, delicate matching of the fluorophore and quencher is required, therefore having quenchers that absorb in the violet to near-infrared region of the spectrum (which has broad absorption spectrum) is important.

The 6-(4-((*N,N*-(dimethylamino)phenyl)azo)benzene)pyrrolocytidine monomer (**19a**), was used in fluorescence quenching studies to determine if quenching occurred via FRET mechanism with a solution of pyrene and 6-phenylpyrrolocytosine fluorophore. Two other quenchers (**Qb** and **Qc**) were also used to observe their ability to quench the selected fluorophores by FRET. Dynamic quenching was observed for the pyrene fluorophore with the three quenchers (**18a**, **Qb** and **Qc**), but when paired with the 6-phenylpyrrolocytosine based fluorophore, the quenching observed was not dynamic

quenching. The chromophores, for which FRET was observed, can now be incorporated into oligomers after synthesis on a larger scale and subsequent synthesis to the phosphoramidite to be used in molecular beacon technology.

The quencher **18a** underwent isomerization to the cis product upon irradiation at 443 nm for 68 seconds intervals. Based on the decrease in the absorbance of the trans form due to isomerization, it was determined that the equilibrium reached between the trans-cis isomer was to the left. This was based on the Beer-Lambert law where the absorbance is directly proportional to the concentration of the species in solution.

The molar absorptivity was determined for the quencher **18a** at 260 and 445 nm and was determined as being 44,300 and 47,600 L.mol<sup>-1</sup>.cm<sup>-1</sup>, respectively. The calculated molar absorptivity of the azopyrrolocytidine (**18a**) indicated that the new quencher was more effective at absorbing light than the universal quencher DABCYL. The azopyrrolocytidine (**18a**) was more effective at quenching the two fluorophores compared to the other two quenchers used. This is significant, because it may be a good substitute for quenchers **Qb** and **Qc** in molecular beacon technology, due to its improved quenching ability and broader absorption spectrum.

Linear Stern-Volmer analysis plots were used to determine the Stern-Volmer constant and concentration of the quencher required to quench 50% of the fluorescence for the various FRET pairs. The Stern-Volmer bimolecular quenching rate constant ( $k_q$ ) were calculated for the pyrene fluorophore and the quenchers **18a**, **Qb** and **Qc**; the  $k_q$  values obtained were:  $2.89 \times 10^{10}$ ,  $1.97 \times 10^{10}$  and  $5.05 \times 10^9$  L.mol<sup>-1</sup>.cm<sup>-1</sup>, respectively which confirmed the mechanism of quenching to be dynamic.

In conclusion, the description of the attempted synthesis towards the 5-phenylpyrrolocytidine laid the ground work for future endeavors in this area. The synthesis and photophysical studies of fluorophores and quenchers that can be used as FRET pairs, increases the accessibility to FRET pairs that can be used in molecular beacon technology for studies in the field of genetics and medical diagnostics.

## References

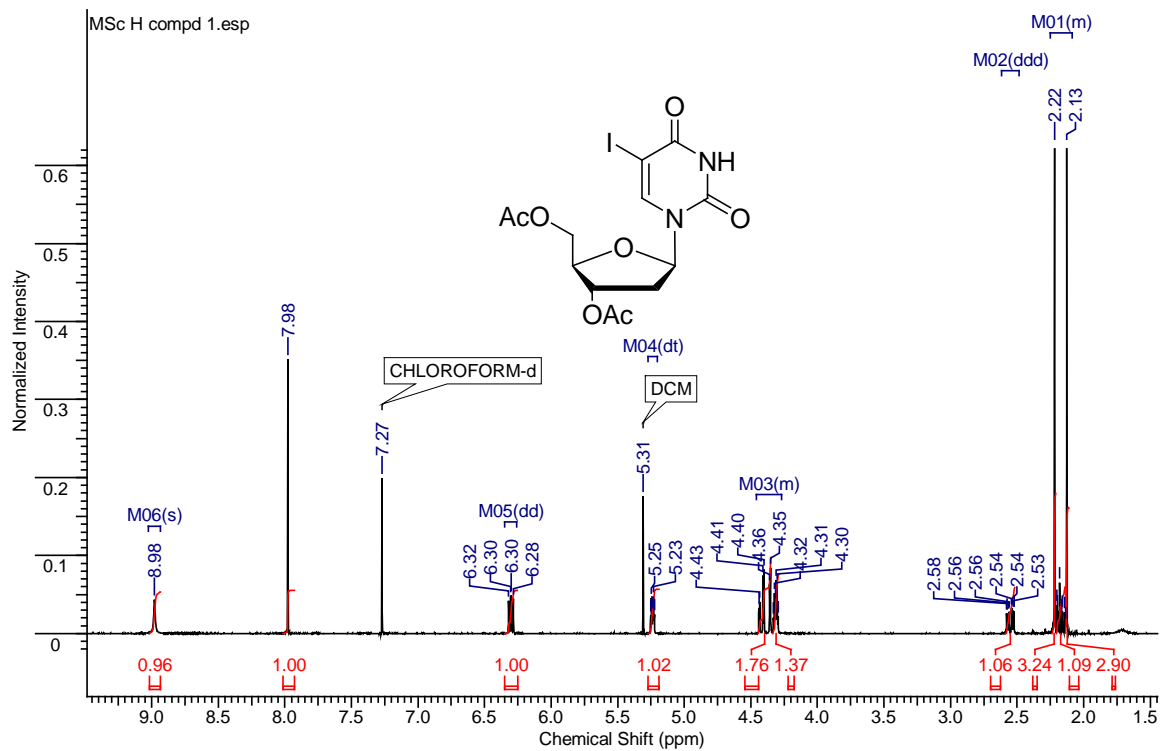
- [1] R. H. E. Hudson, A. K. Dambeniaks, J. M. Moszynski, *Proc. SPIE* **2005**, 5969, 59690J-59690J-59610.
- [2] F. H. Portugal, J. S. Cohen, *A century of DNA: a history of the discovery of the structure and function of the genetic substance*, MIT Press, Cambridge, Mass., **1977**.
- [3] O. T. Avery, C. M. MacLeod, M. McCarty, *J. Exp. Med.* **1944**, 79, 137-158.
- [4] J. D. Watson, F. H. C. Crick, *Cold Spring Harbor Symp. Quant. Biol.* **1953**, 18, 123-131.
- [5] J. C. Venter, *Science* **2001**, 291, 1304-1351.
- [6] E. M. Boon, J. K. Barton, *Bioconj. Chem.* **2003**, 14, 1140-1147.
- [7] J. L. Velasquez, S. M. Lipkin, *Curr Oncol Rep* **2005**, 7, 475-479.
- [8] <http://www.dnabaser.com/articles/SNP/SNP-single-nucleotide-polymorphism.html> (accessed Jan 20 2013).
- [9] <http://www.ncbi.nlm.nih.gov/About/primer/snps.html> (accessed Jan 20 2013).
- [10] D. W. Dodd, R. H. E. Hudson, *Mini-Reviews in Org. Chem.* **2009**, 6, 378-391.
- [11] J. Hu, D. W. Dodd, R. H. E. Hudson, D. R. Corey, *Bioorg. Med. Chem. Lett.* **2009**, 19, 6181-6184.
- [12] Y. Saito, Y. Miyauchi, A. Okamoto, I. Saito, *Tetrahedron Lett.* **2004**, 45, 7827-7831.
- [13] P. M. Holland, R. D. Abramson, R. Watson, D. H. Gelfand, *Proc. Natl. Acad. Sci. U. S. A.* **1991**, 88, 7276-7280.
- [14] S. Tyagi, F. R. Kramer, *Nat. Biotechnol.* **1996**, 14, 303-308.
- [15] R. H. E. Hudson, A. Ghorbani-Choghamarani, *Synlett* **2007**, 870-873.
- [16] a) Z. Li, B. Rajendran, T. I. Kamins, X. Li, Y. Chen, R. S. Williams, *Appl. Phys. A: Mater. Sci. Process.* **2005**, 80, 1257-1263; b) K. L. Robertson, L. Yu, B. A. Armitage, A. J. Lopez, L. A. Peteanu, *Biochemistry* **2006**, 45, 6066-6074.
- [17] A. S. Wahba, A. Esmaeili, M. J. Damha, R. H. E. Hudson, *Nucleic Acids Res.* **2010**, 38, 1048-1056.

- [18] D. W. Dodd, K. N. Swanick, J. T. Price, A. L. Brazeau, M. J. Ferguson, N. D. Jones, R. H. E. Hudson, *Org. Biomol. Chem.* **2010**, *8*, 663-666.
- [19] K. Sonogashira, Y. Tohda, N. Hagihara, *Tetrahedron Lett.* **1975**, 4467-4470.
- [20] R. D. Stephens, *J. Org. Chem.* **1963**, *28*, 3313-3315.
- [21] R. H. E. Hudson, A. G. Choghamarani, *Nucleoside, Nucleotides Nucleic Acids* **2007**, *26*, 533-537.
- [22] J. R. Lakowicz, *Principles of Fluorescence Spectroscopy, Vol. 1*, New York: Plenum Publishing Corp., **1983**.
- [23] B. Valeur, *Molecular Fluorescence: Principles and Applications*, Wiley-VCH **2001**.
- [24] S. J. Morris, T. C. Sudhof, D. H. Haynes, *Biochim. Biophys. Acta* **1982**, *693*, 425-436.
- [25] T. D. Gauthier, E. C. Shane, W. F. Guerin, W. R. Seitz, C. L. Grant, *Environ. Sci. Technol.* **1986**, *20*, 1162-1166.
- [26] S. H. Lee, J. Kumar, S. K. Tripathy, *Langmuir* **2000**, *16*, 10482-10489.
- [27] D. Sierra, C. Zuniga, G. E. Buono-Core, F. Godoy, A. Hugo Klahn, *Inorg. Chem. Commun.* **2011**, *14*, 961-963.
- [28] M. S. Rao, N. Esho, C. Sergeant, R. Dembinski, *J. Org. Chem.* **2003**, *68*, 6788-6790.
- [29] V. Aucagne, F. Amblard, L. A. Agrofoglio, *Synlett* **2004**, 2406-2408.
- [30] J. S. Woo, R. B. Meyer, H. B. Gamper, *Nucleic Acids Res.* **1996**, *24*, 2470-2475.
- [31] M. A. Zolfigol, A. Khazaei, E. Kolvari, N. Koukabi, H. Soltani, M. Behjunia, *Helv Chim Acta.* **2010**, *93*, 587-594.
- [32] M. E. Moustafa, R. H. E. Hudson, *Nucleoside, Nucleotides Nucleic Acids* **2011**, *30*, 740-751.
- [33] S. Yarasi, C. McConachie, G. R. Loppnow, *Photochem. Photobiol.* **2005**, *81*, 467-473.
- [34] U. Siemeling, C. Bruhn, M. Meier, C. Schirmacher, *Z. Naturforsch., B: J. Chem. Sci.* **2008**, *63*, 1395-1401.
- [35] R. H. E. Hudson, A. K. Dambeniaks, R. D. Viirre, *Nucleoside, Nucleotides Nucleic Acids* **2005**, *24*, 581-584.

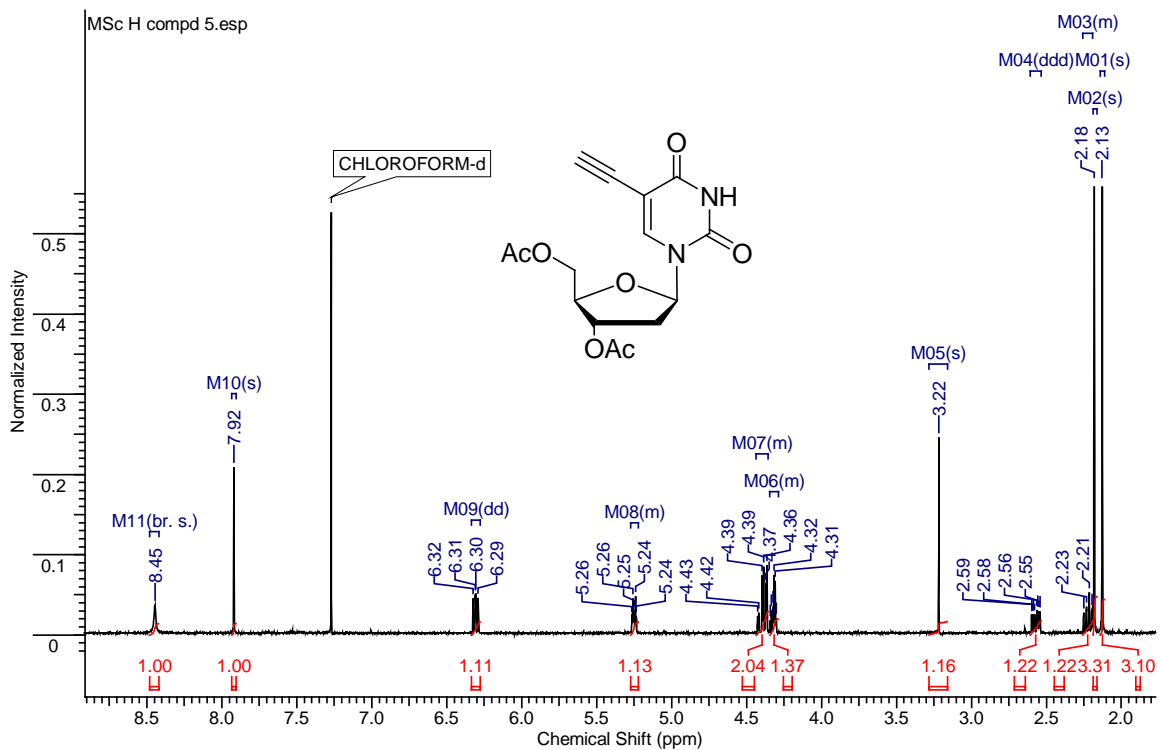
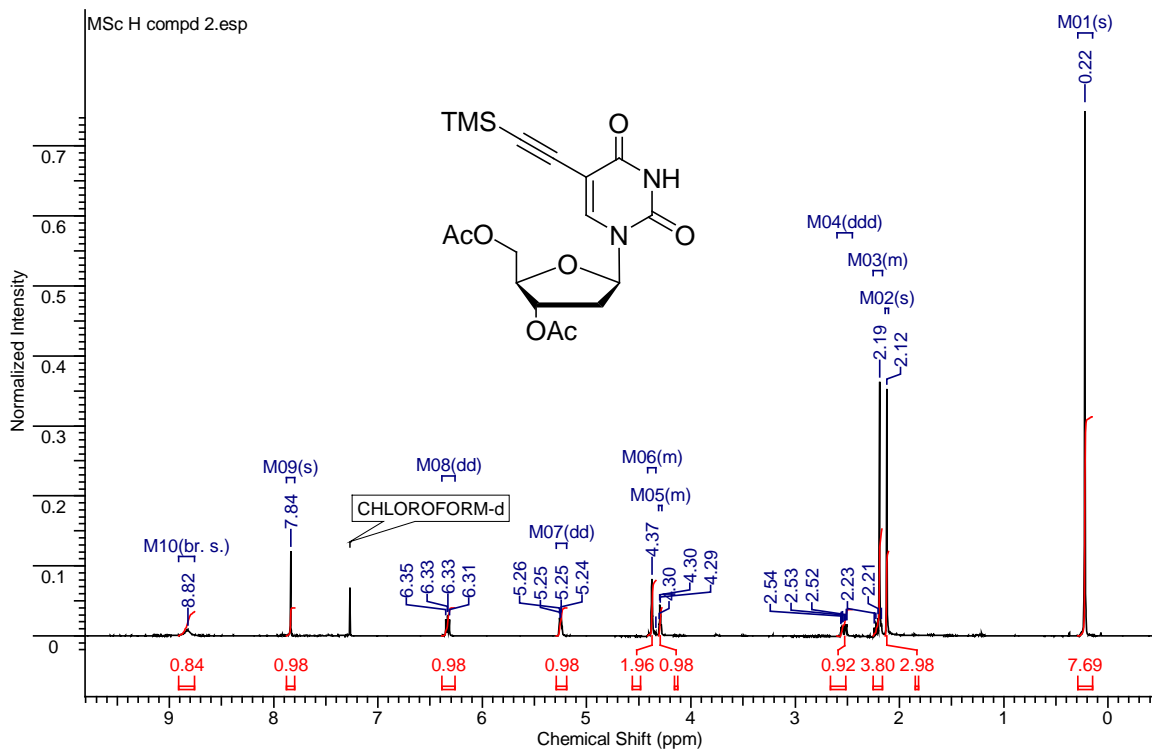
- [36] R. H. E. Hudson, J. M. Moszynski, *Synlett* **2006**, 2997-3000.
- [37] C. N. Raut, R. B. Mane, S. M. Bagul, R. A. Janrao, P. P. Mahulikar, *Arkivoc* **2009**, 105-114.
- [38] Y. Kim, D. Sohn, W. Tan, *Int. J. Clin. Exp. Pathol.* **2008**, *1*, 105-116.
- [39] J. R. Lakowicz, *Principles of Fluorescence Spectroscopy, Vol. 3*, Springer-Verlag New York, LLC, **2006**.
- [40] M. E. Moustafa, Monograph thesis, The University of Western Ontario (London Ontario), **2011**.
- [41] G. Olbrich, *Chem. Phys.* **1978**, *27*, 117-125.
- [42] Molecular probes Inc.  
[https://www.tools.invitrogen.com/content/sfs/COAPDFs/2012/1100201\\_D2245.pdf](https://www.tools.invitrogen.com/content/sfs/COAPDFs/2012/1100201_D2245.pdf) (accessed Oct 10 2012).
- [43] P. Crisalli, E. T. Kool, *Bioconj. Chem.* **2011**, *22*, 2345-2354.

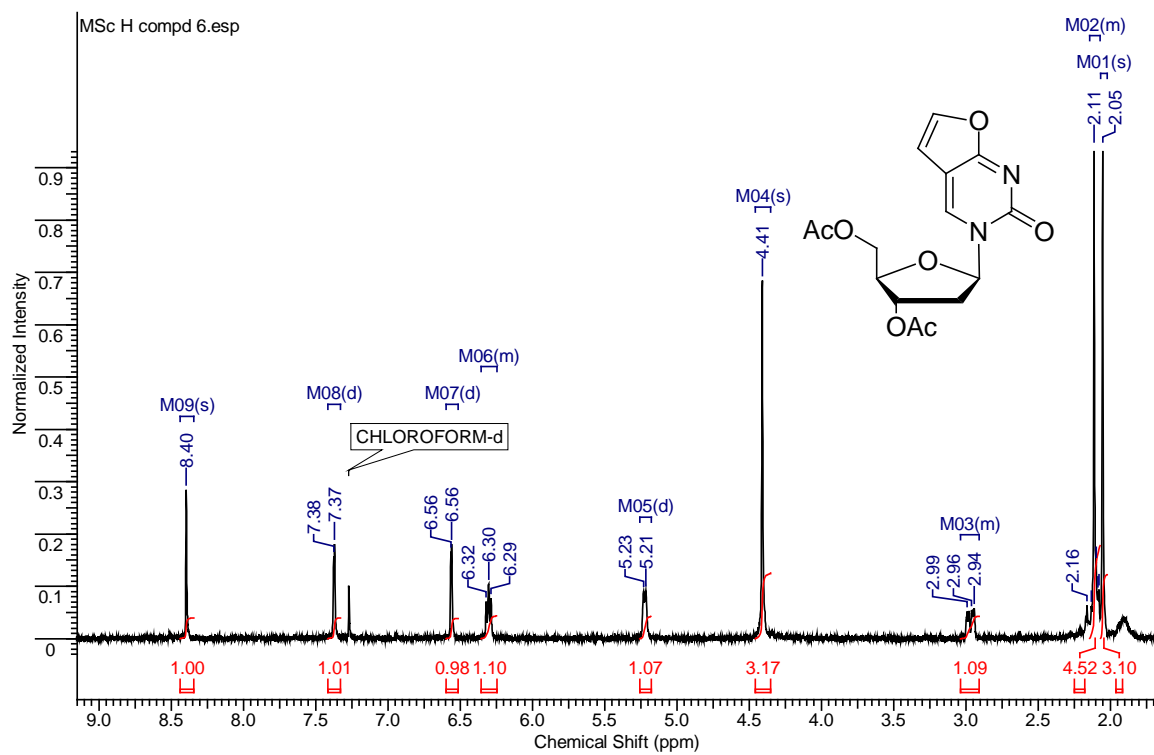
## Appendices

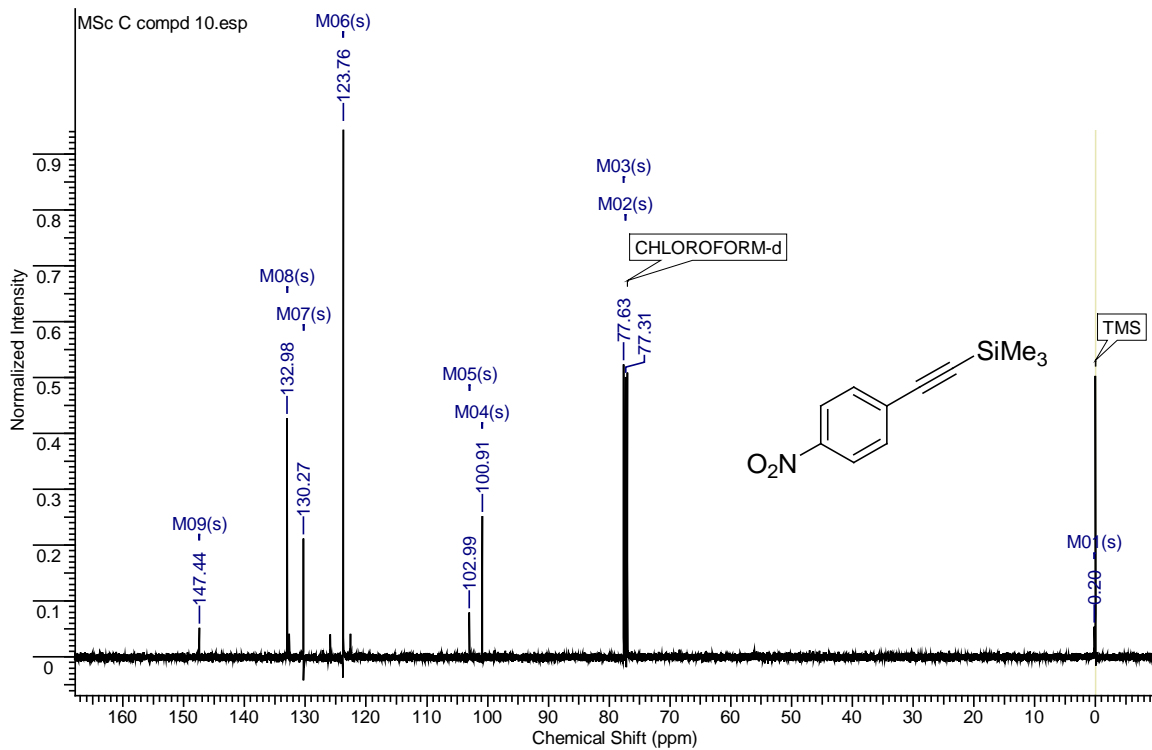
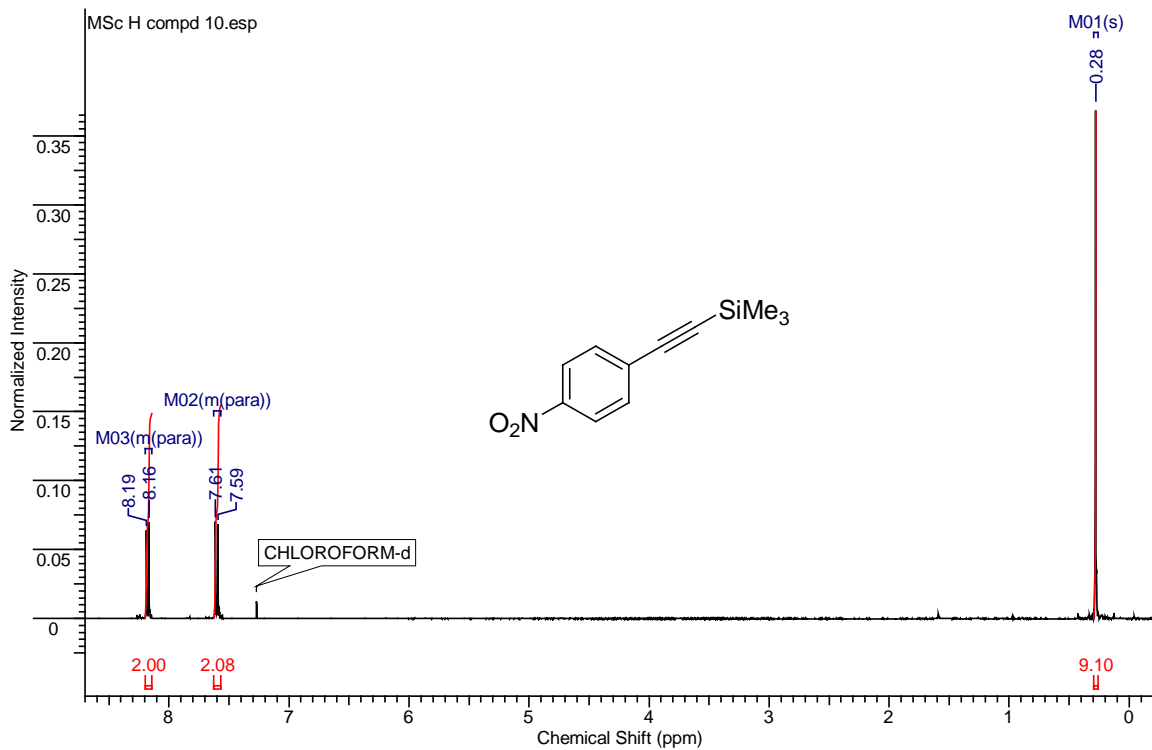
<sup>1</sup> H NMR of compound <b>1</b> .....	86
<sup>1</sup> H NMR of compound <b>2</b> .....	87
<sup>1</sup> H NMR of compound <b>5</b> .....	87
<sup>1</sup> H NMR of compound <b>6</b> .....	88
<sup>1</sup> H NMR and <sup>13</sup> C NMR of compound <b>10</b> .....	89
<sup>1</sup> H NMR and <sup>13</sup> C NMR of compound <b>11</b> .....	90
<sup>1</sup> H NMR and <sup>13</sup> C NMR of compound <b>12</b> .....	91
<sup>1</sup> H NMR and <sup>13</sup> C NMR of compound <b>13</b> .....	92
<sup>1</sup> H NMR and <sup>13</sup> C NMR of compound <b>14</b> .....	93
<sup>1</sup> H NMR and <sup>13</sup> C NMR of compound <b>15</b> .....	94
<sup>1</sup> H NMR of compound <b>16</b> .....	95
<sup>1</sup> H NMR and <sup>13</sup> C NMR of compound <b>17</b> .....	96
<sup>1</sup> H NMR and <sup>13</sup> C NMR of compound <b>18a</b> .....	97
<sup>1</sup> H NMR and <sup>13</sup> C NMR of compound <b>18b</b> .....	98
<sup>1</sup> H NMR for compound <b>18c</b> .....	99
<sup>1</sup> H NMR for compound <b>18d</b> .....	99
<sup>1</sup> H NMR and <sup>13</sup> C NMR of compound <b>18e</b> .....	100
<sup>1</sup> H NMR for compound <b>19a</b> .....	101

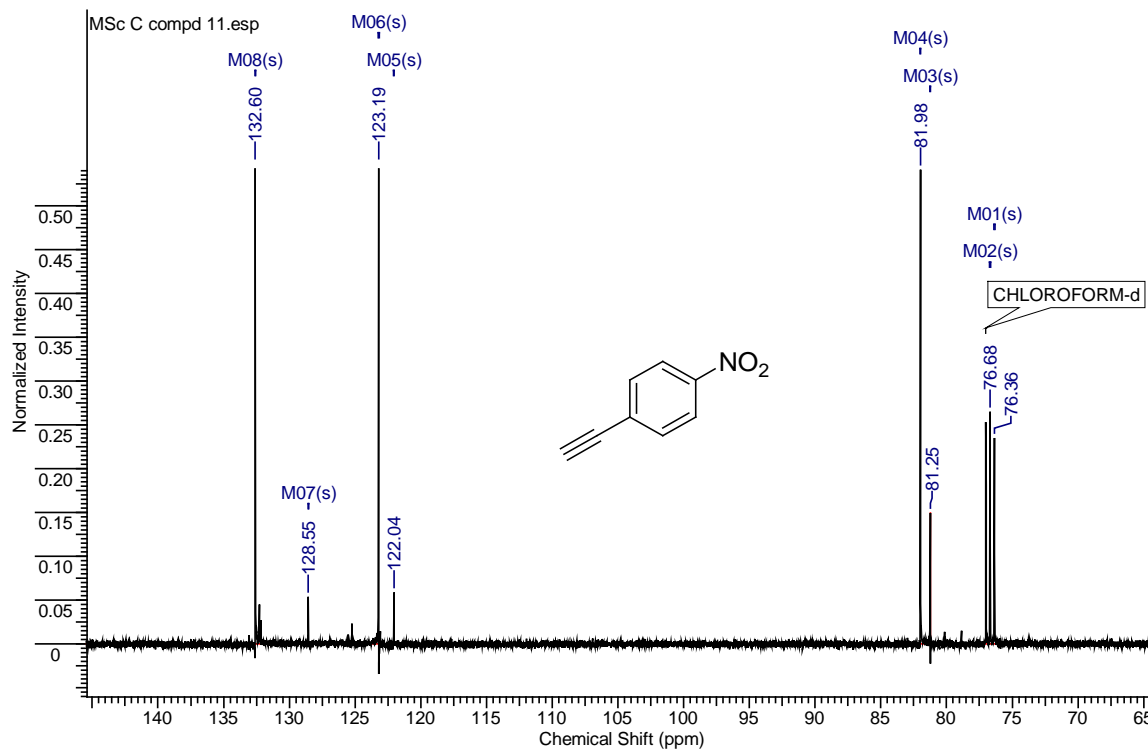
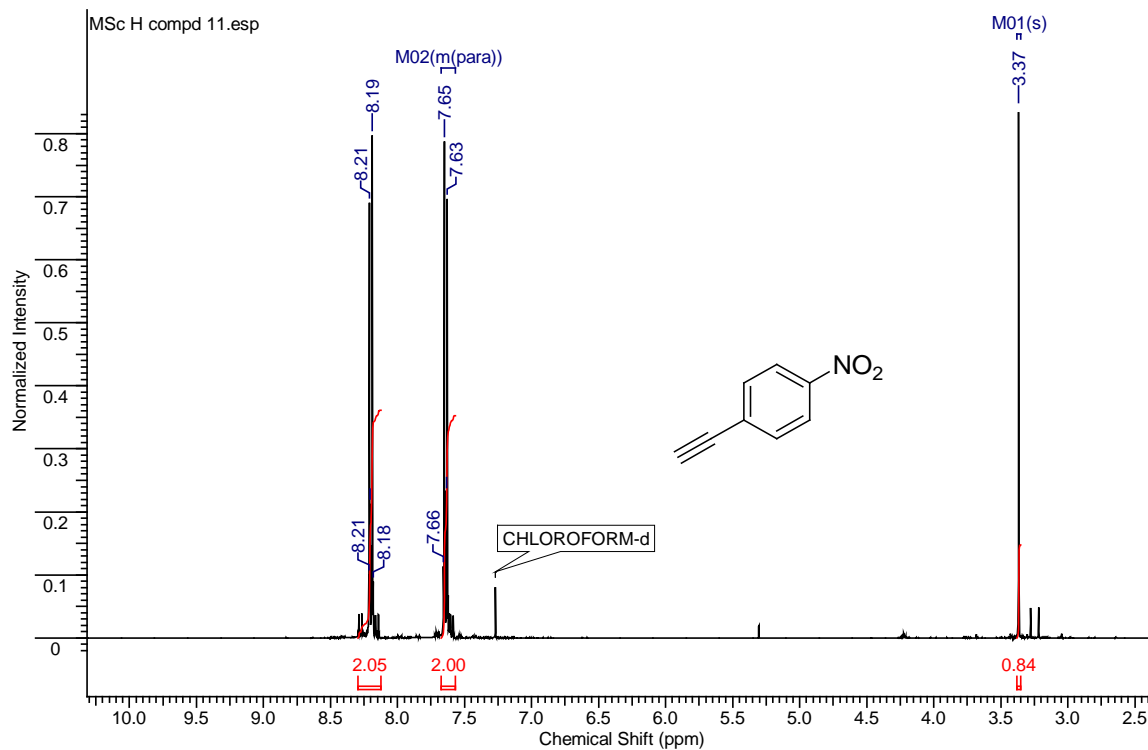


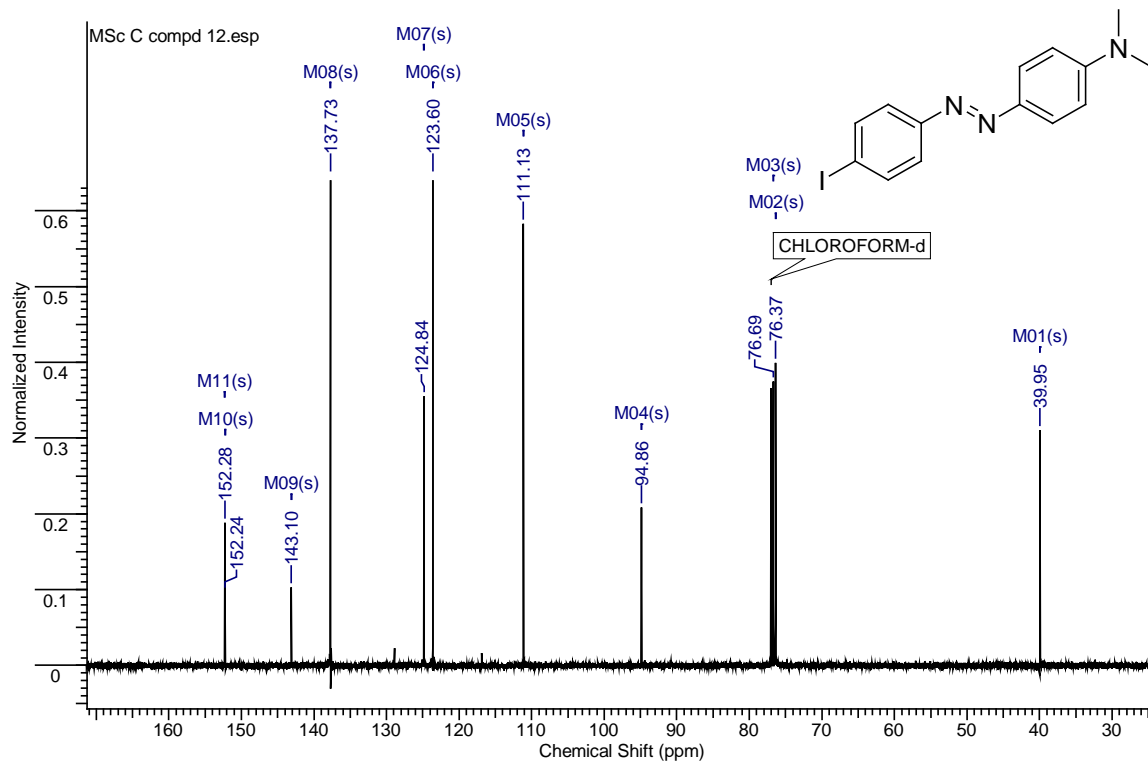
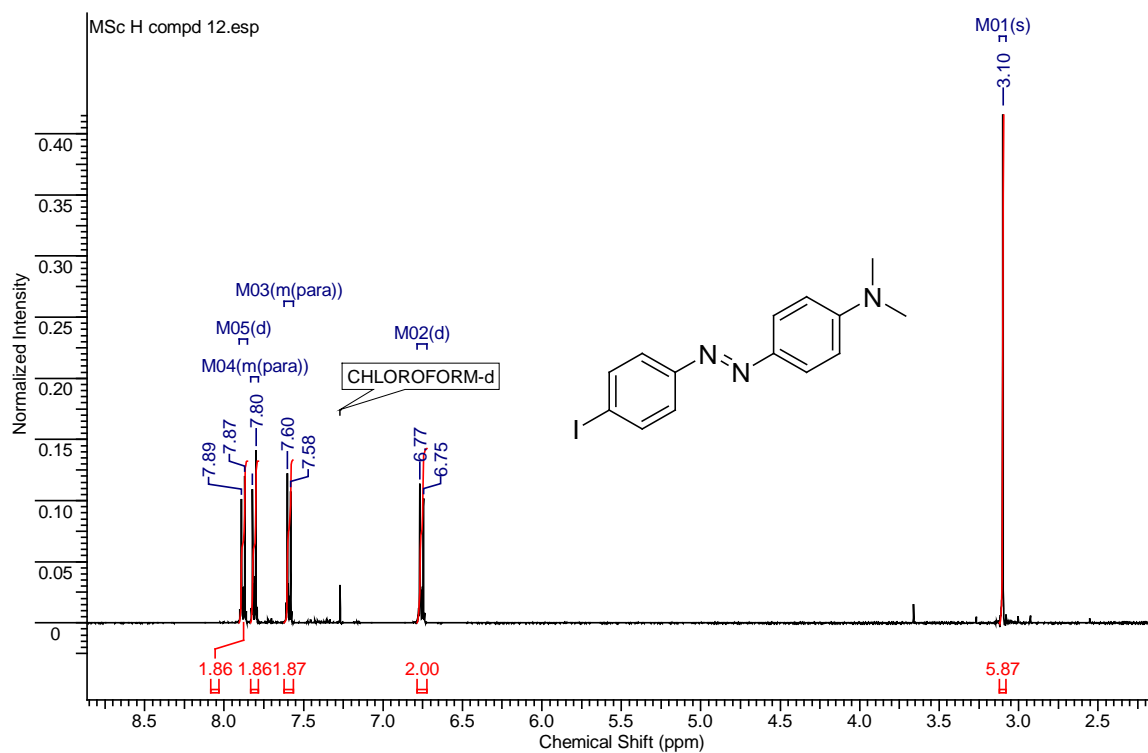


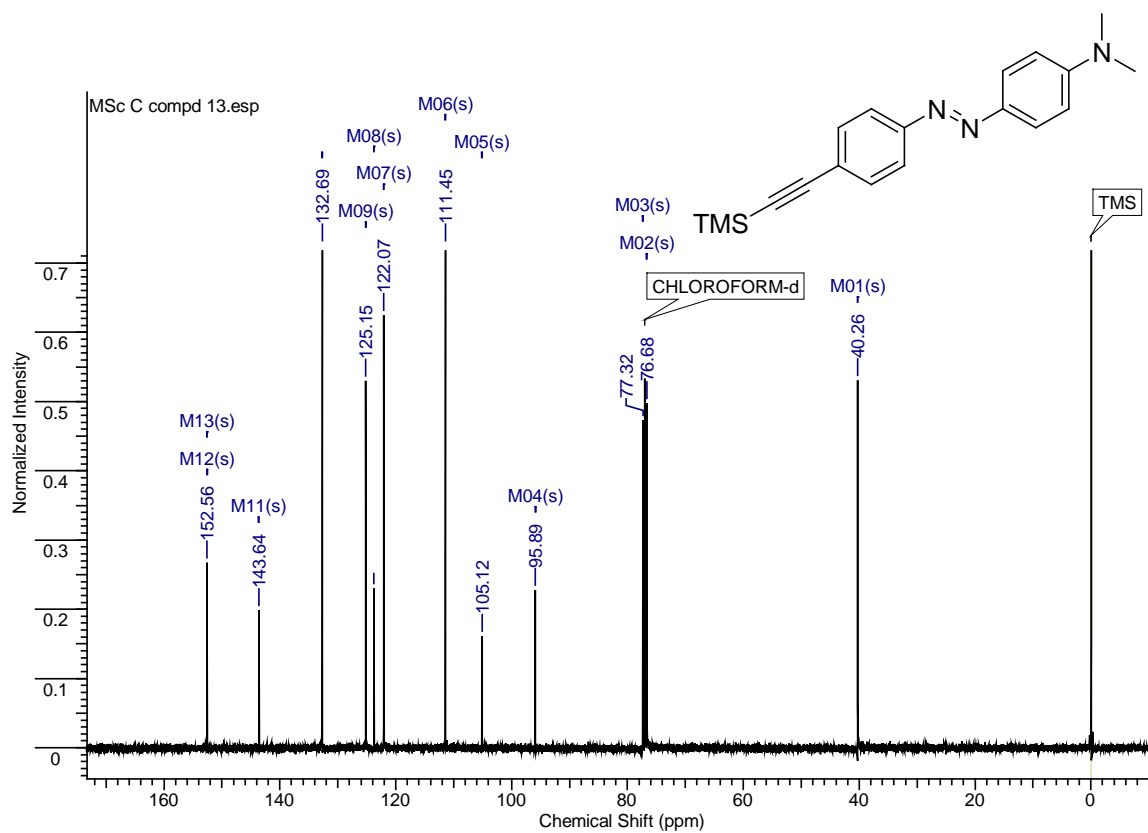
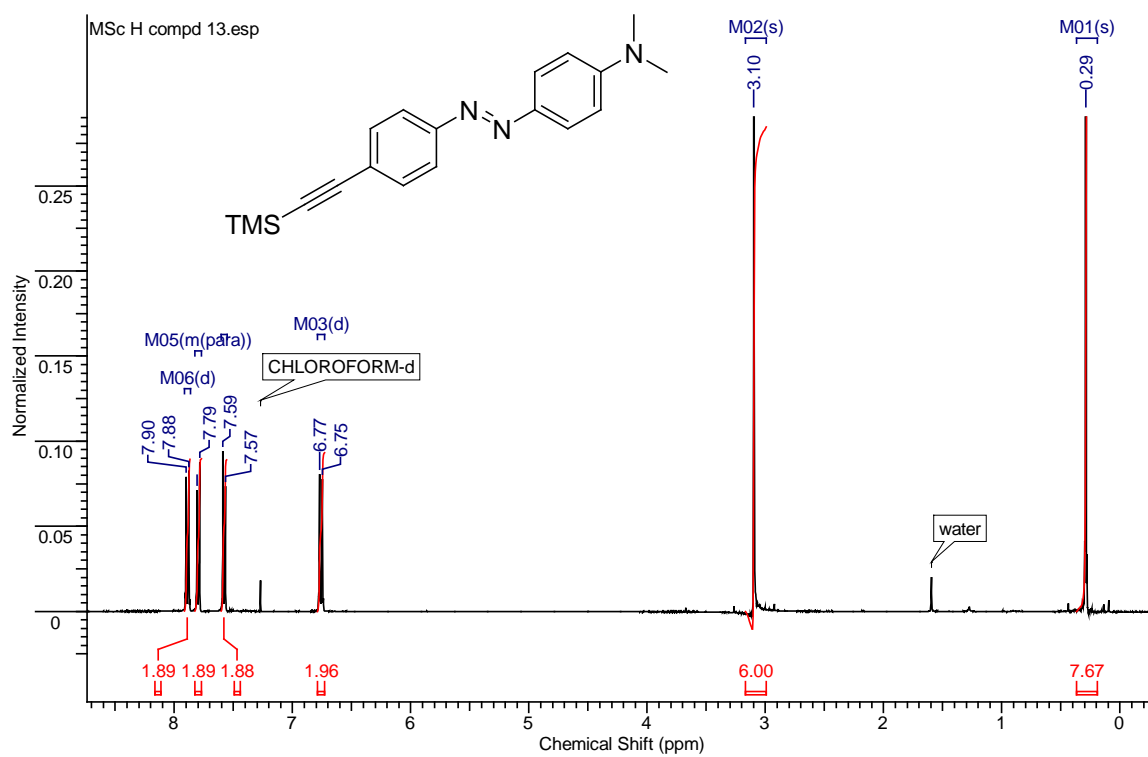


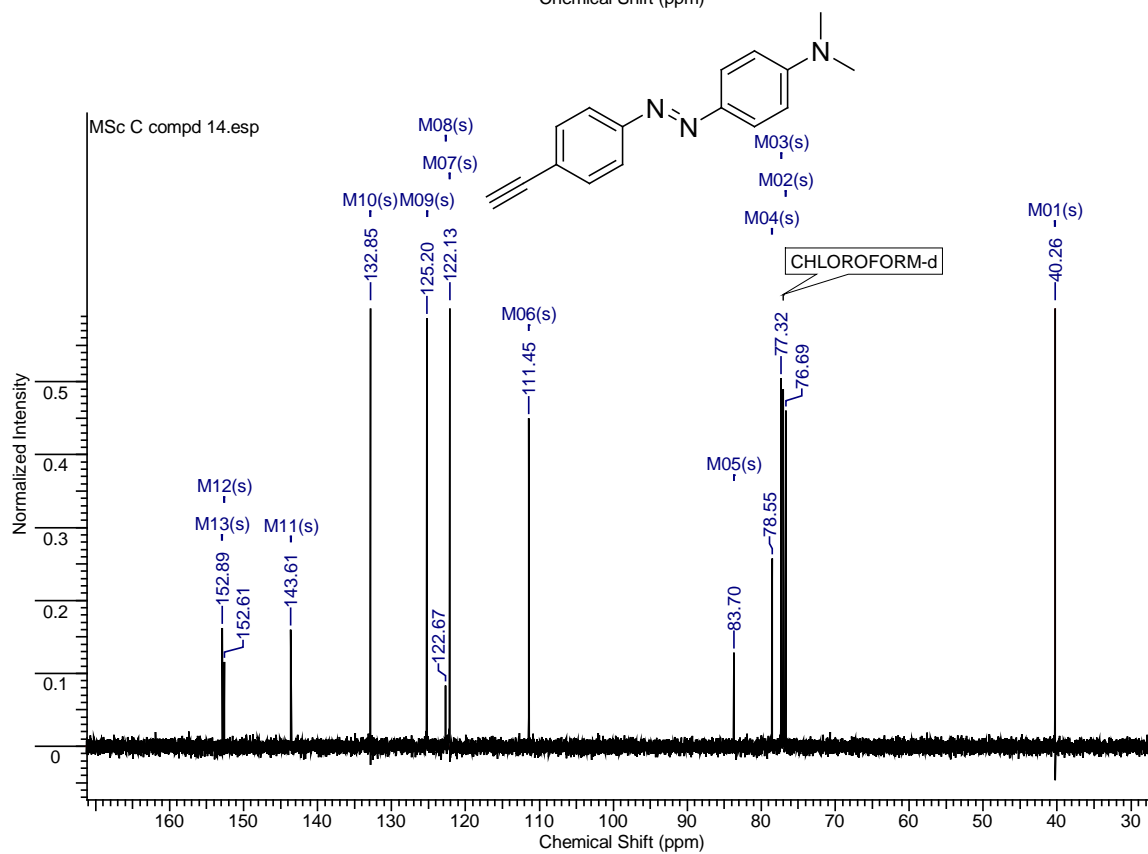
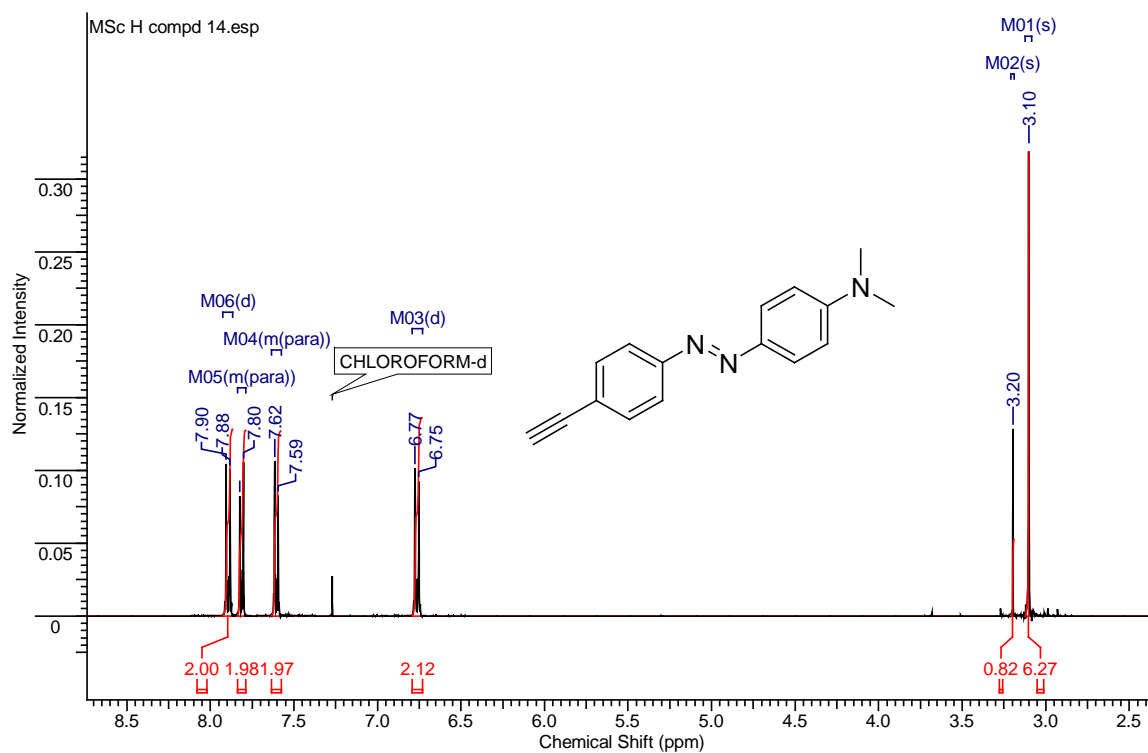


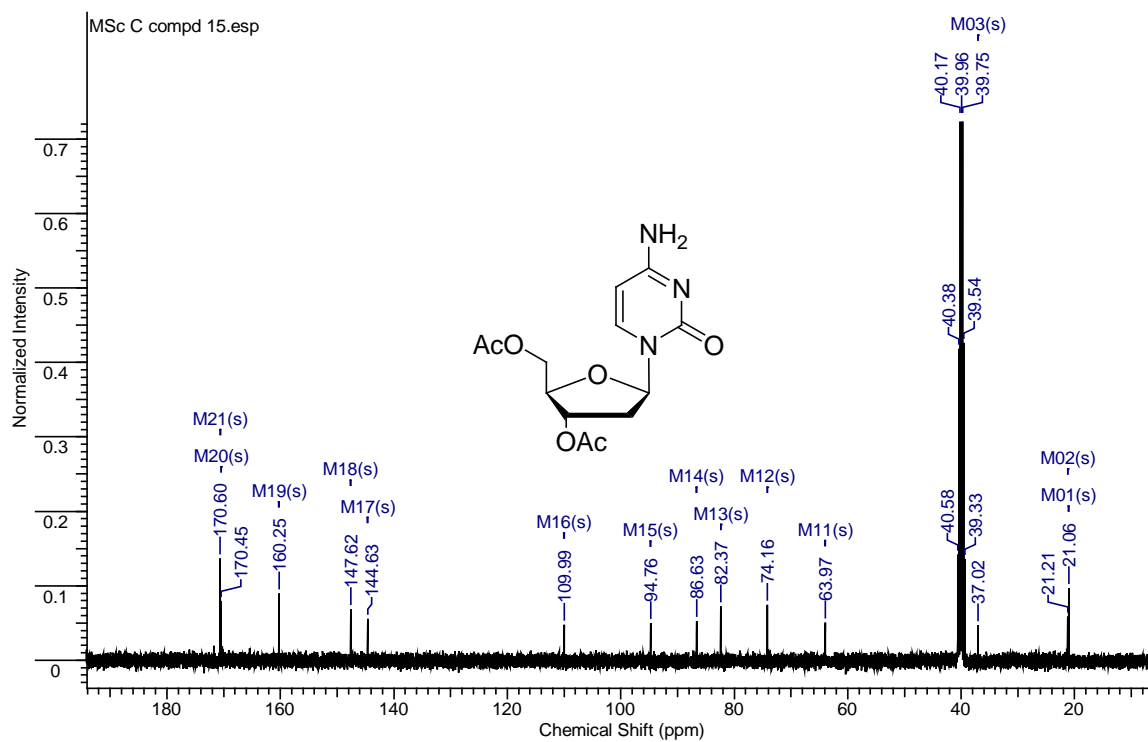
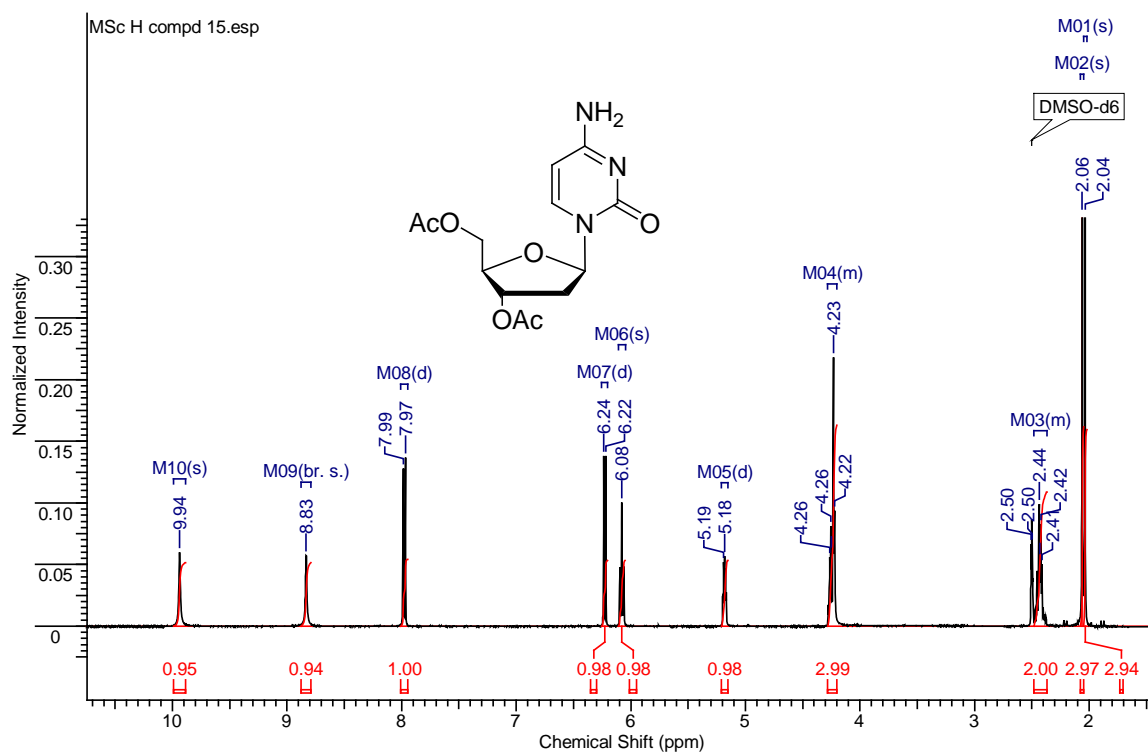




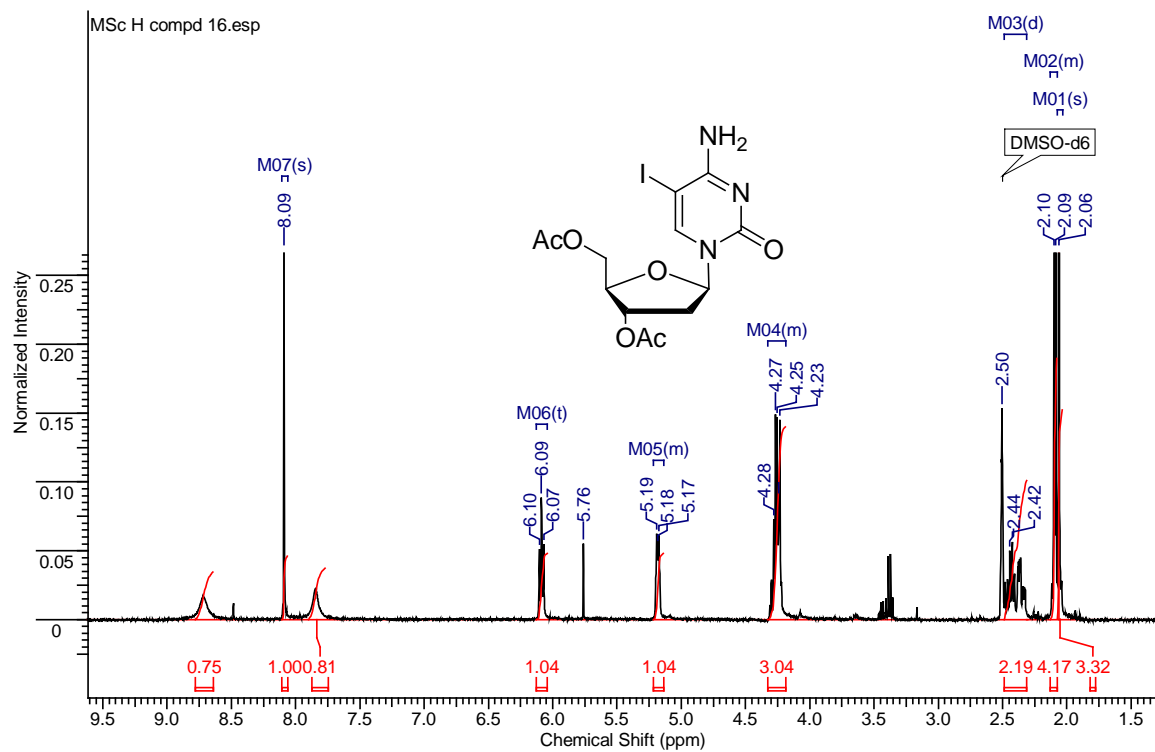


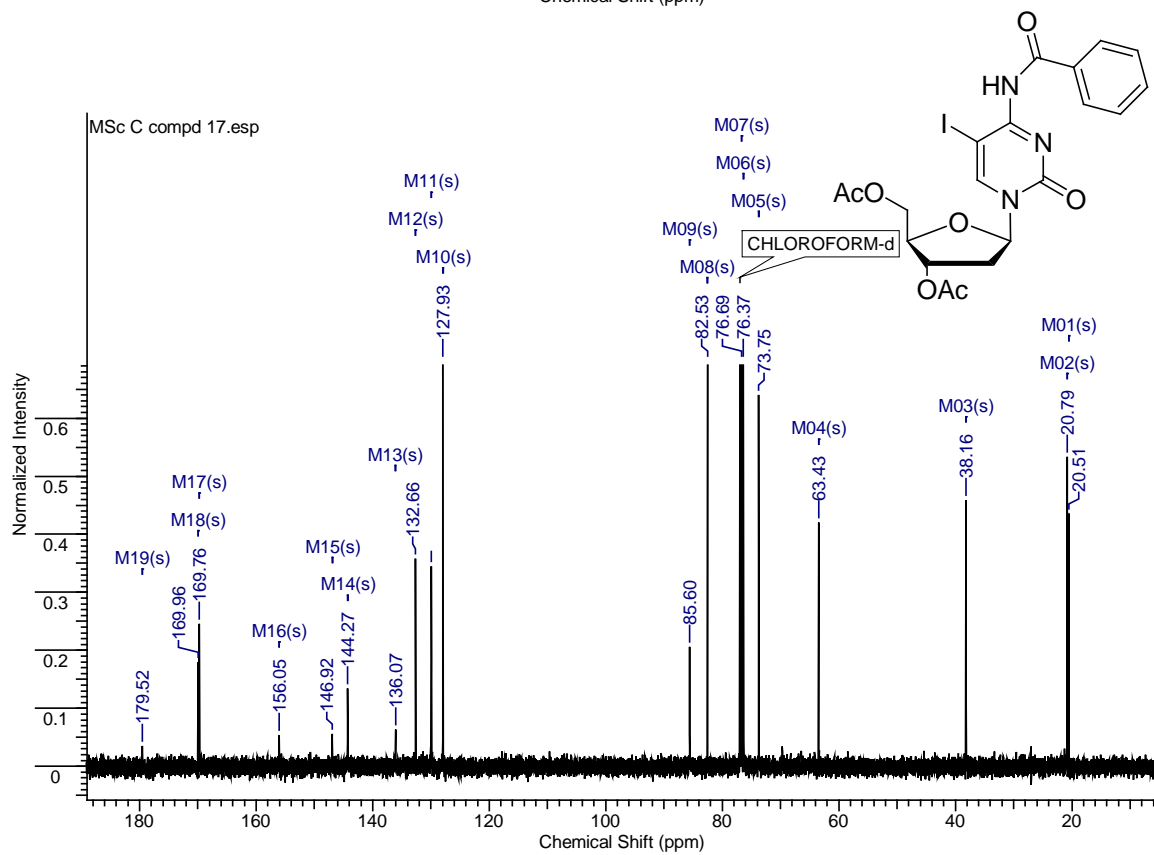
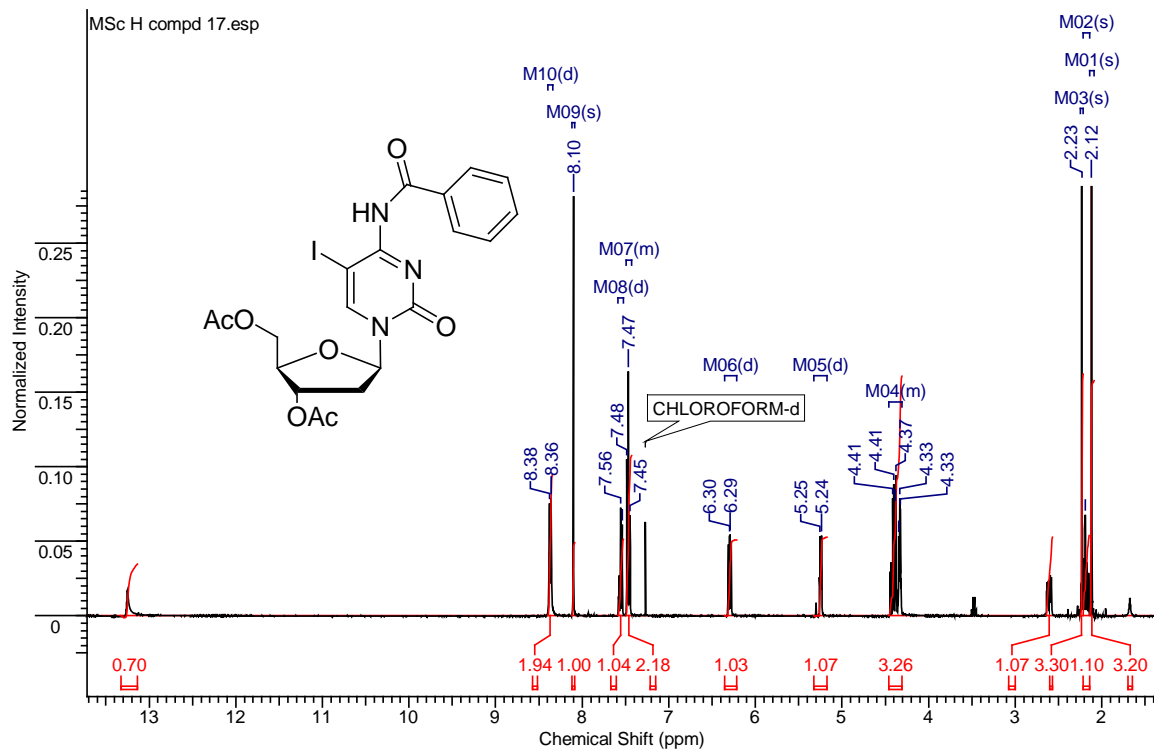


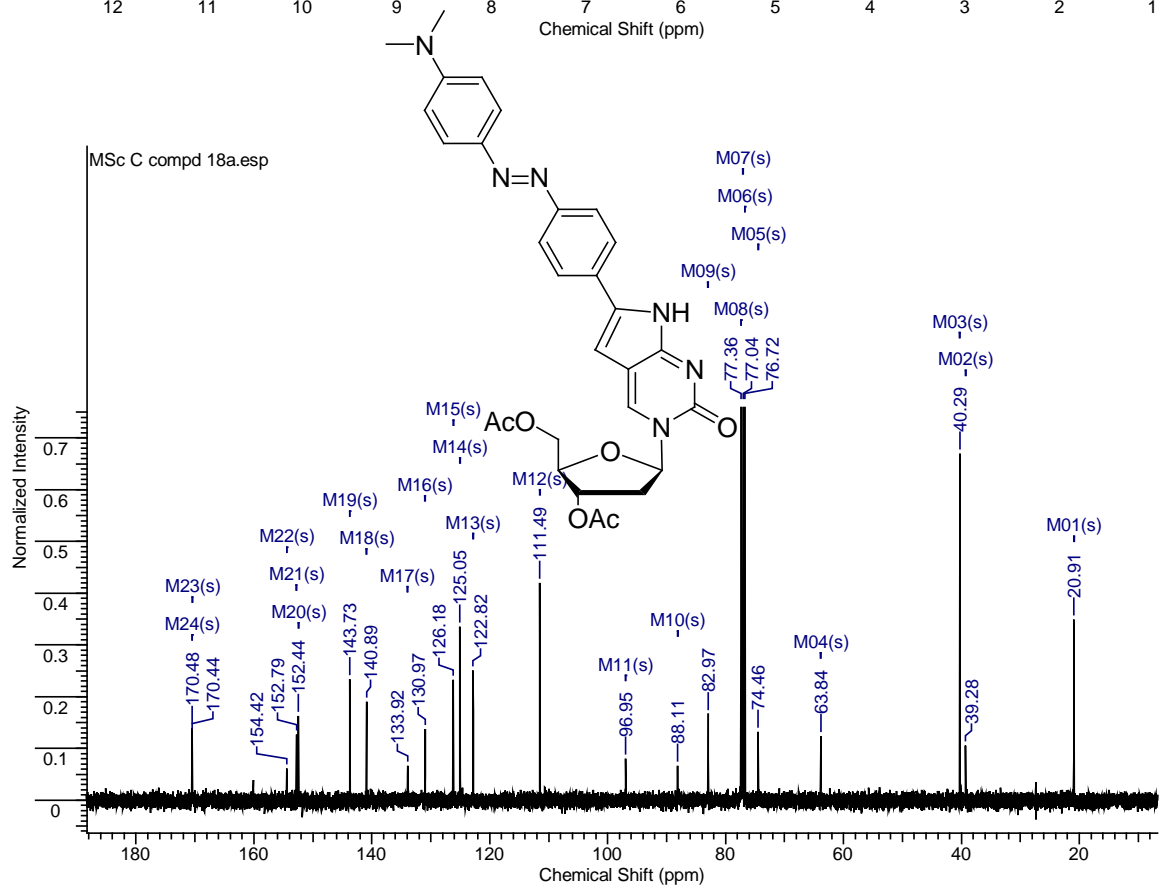
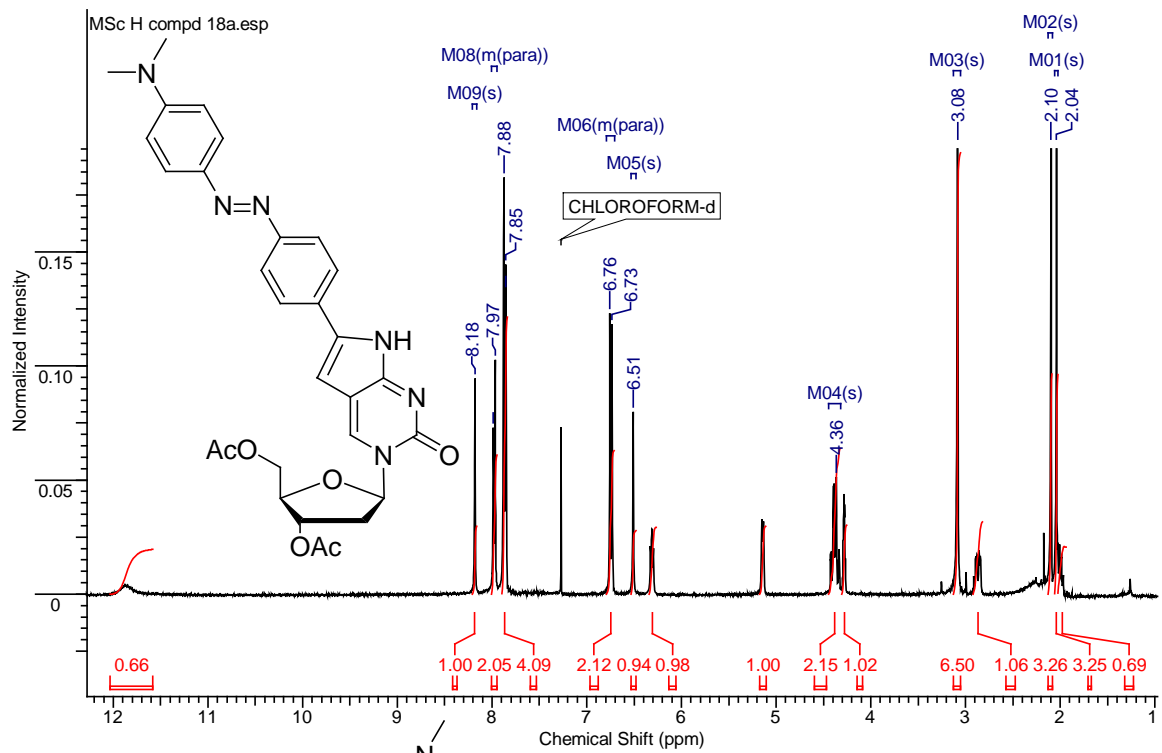


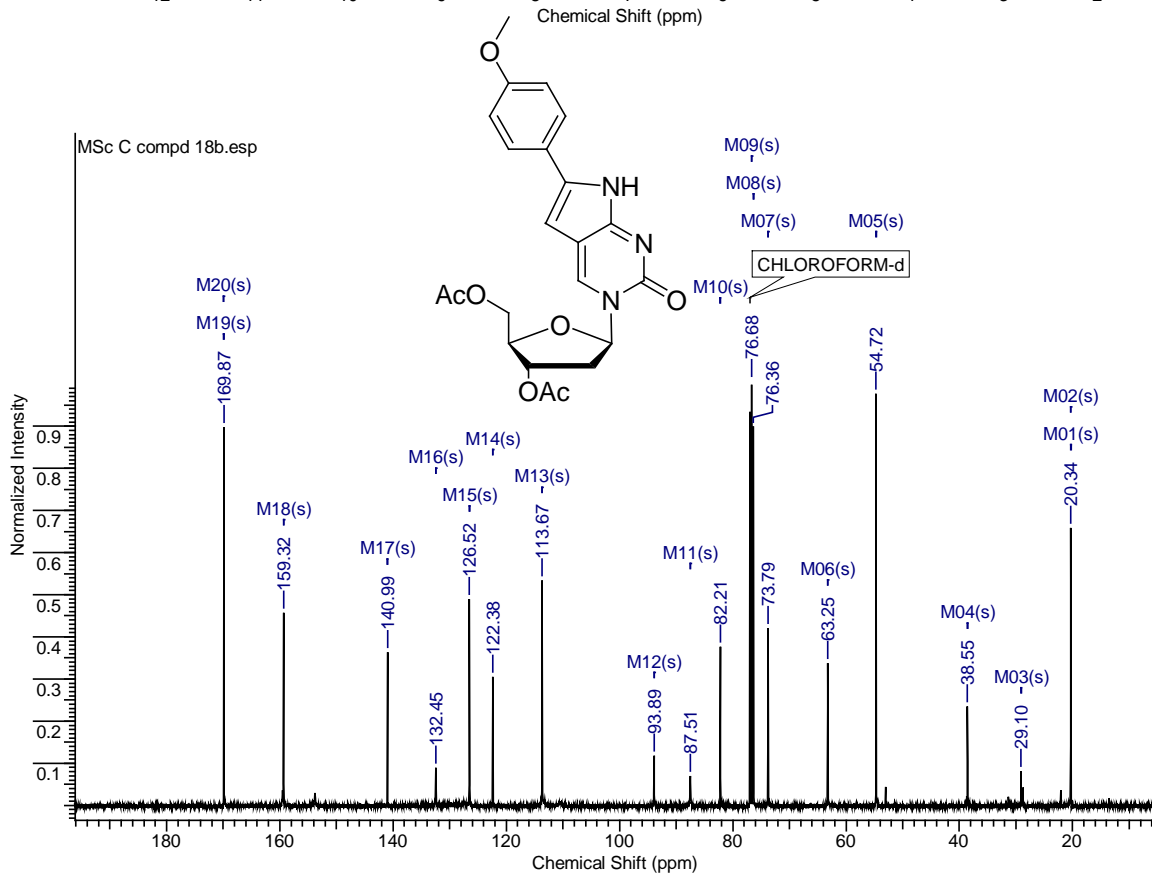
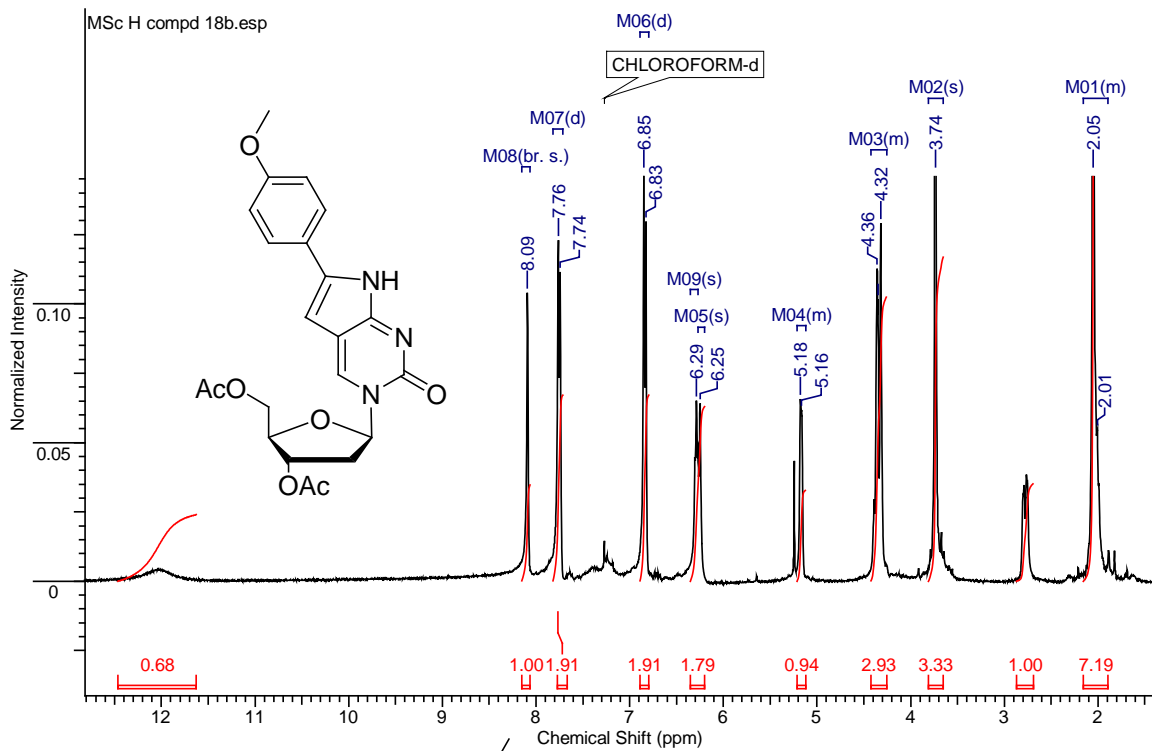


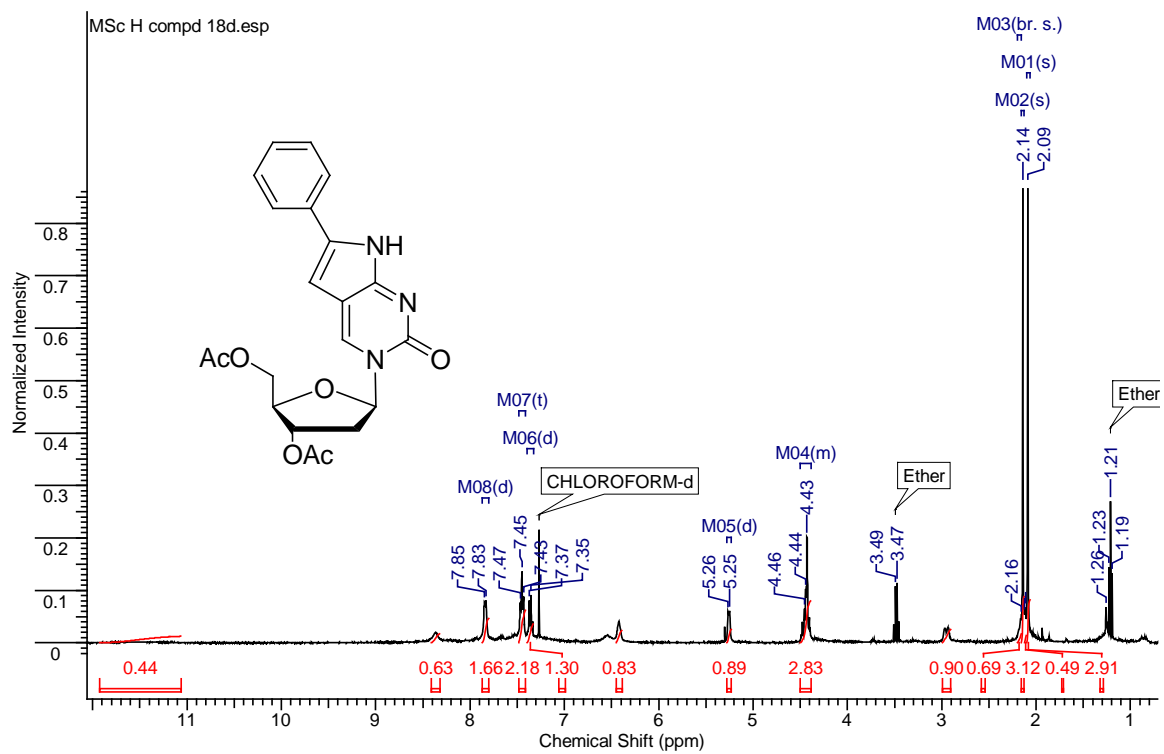
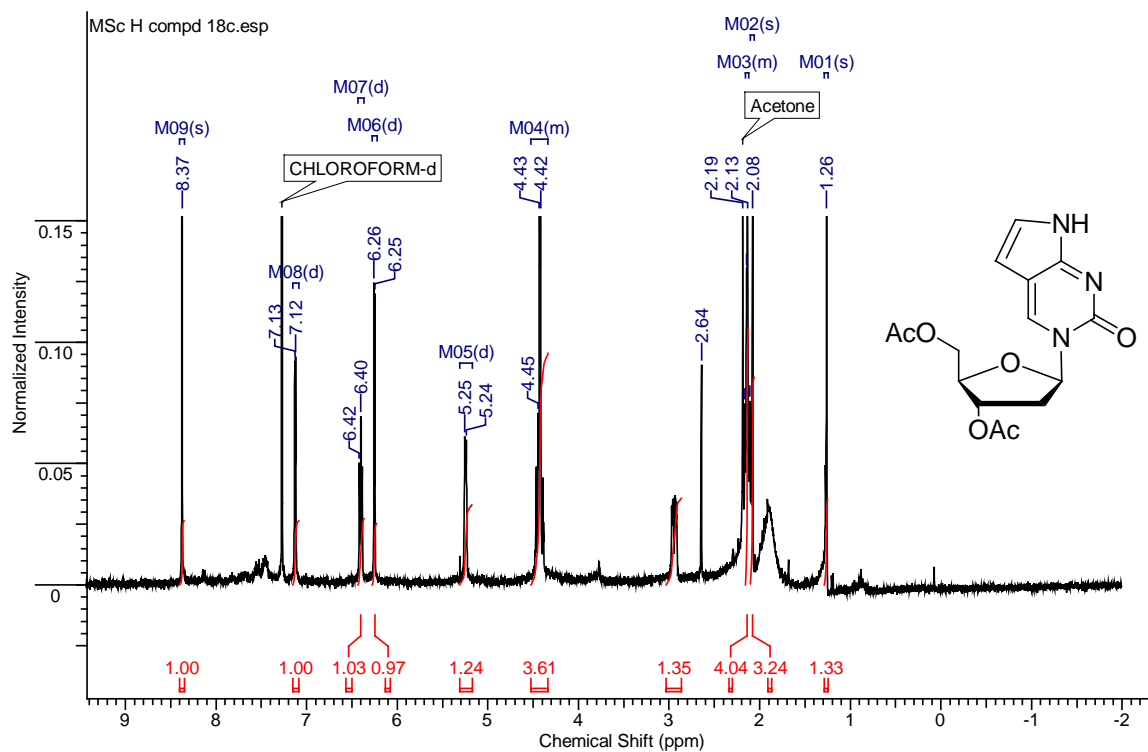


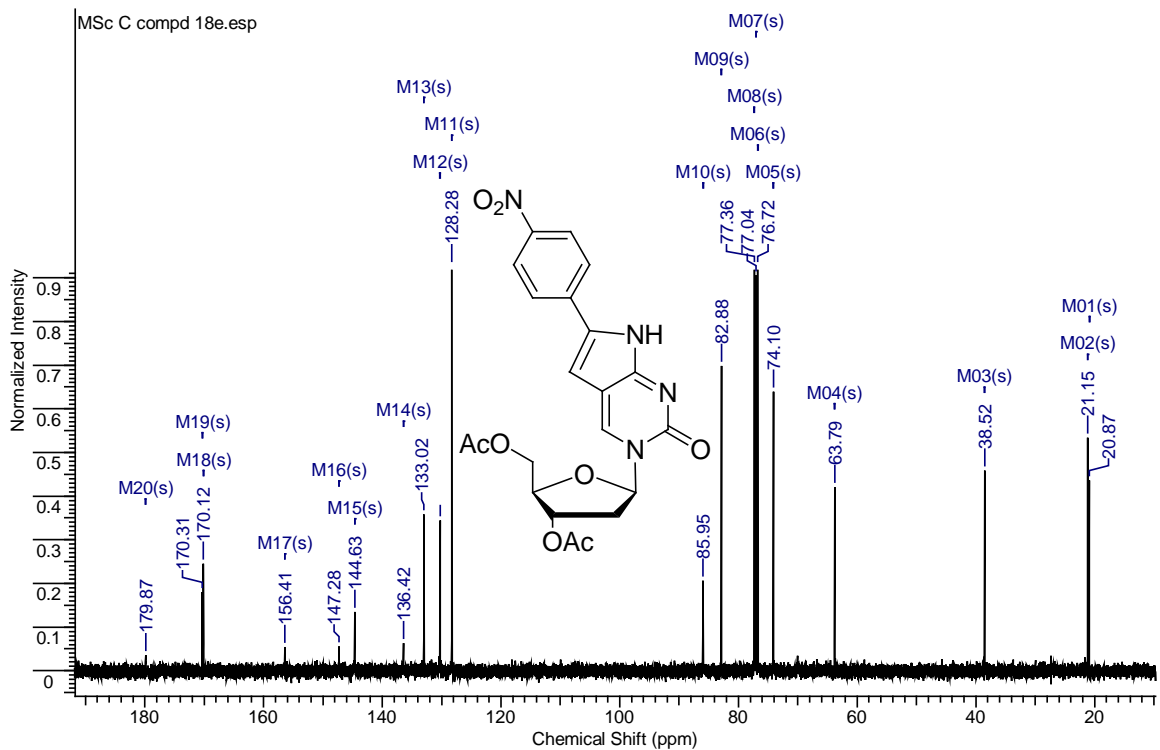
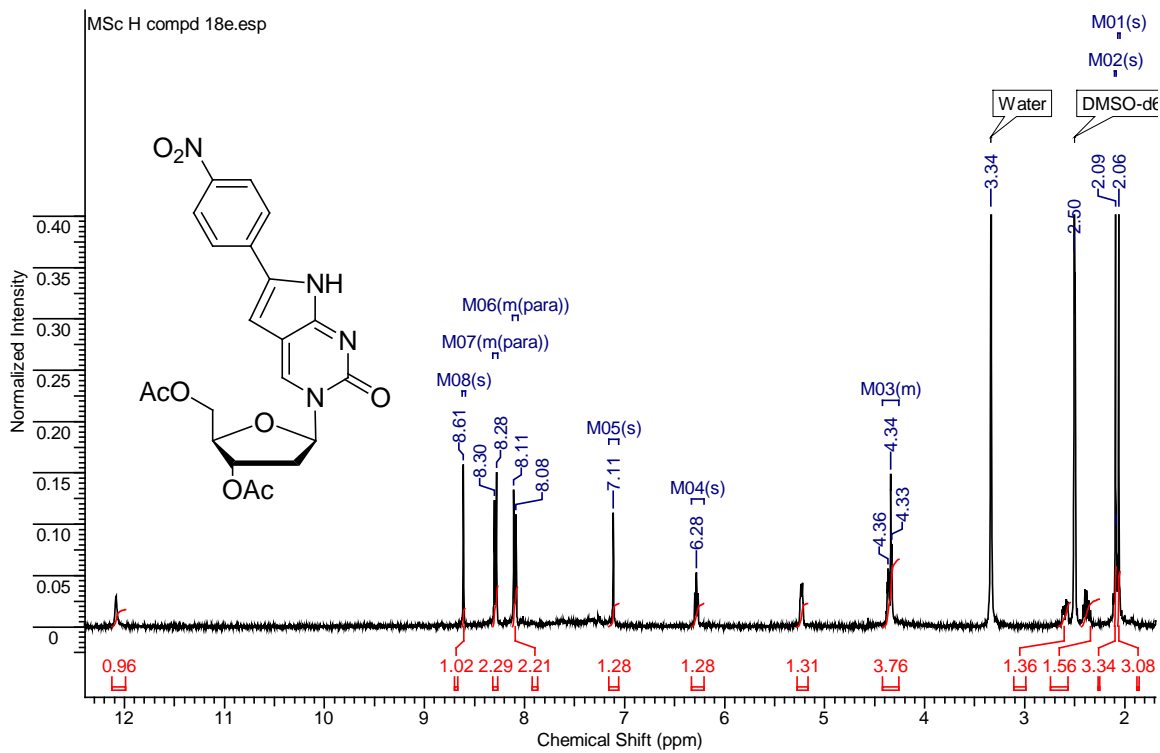


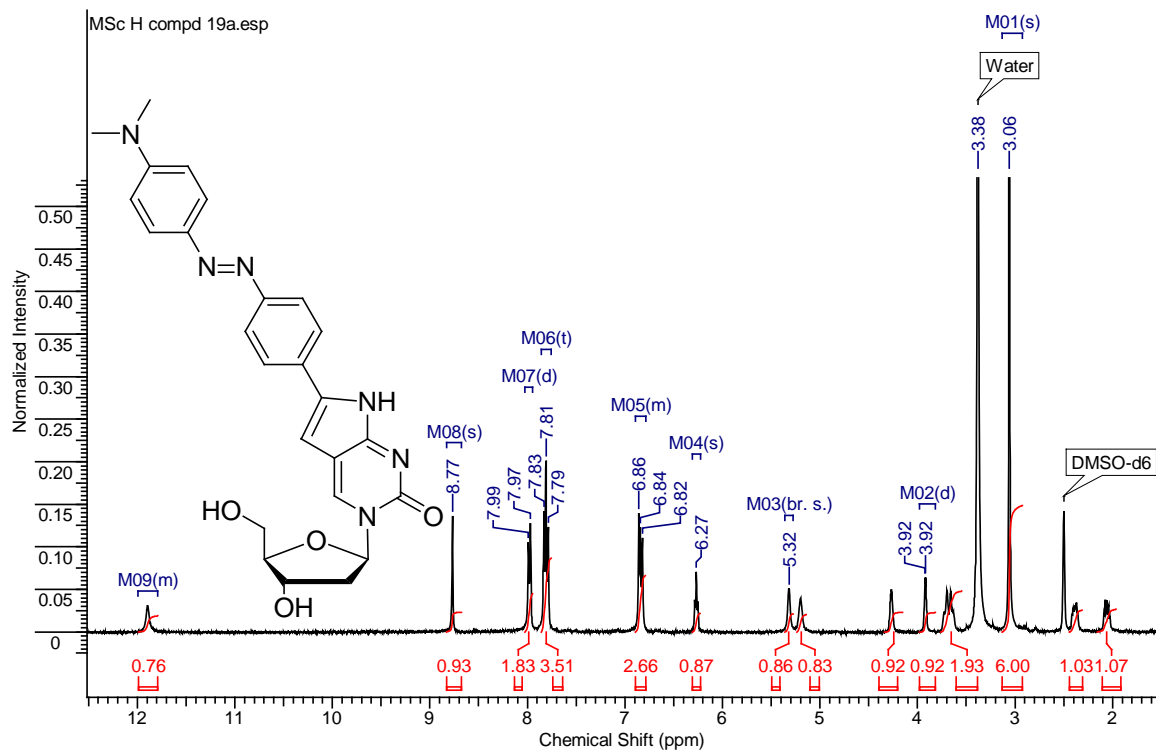












## Curriculum Vitae

**Name:** McKenry Charles

**Post-secondary Education and Degrees:** University of Western Ontario  
London, Ontario, Canada  
1999-2003 and 2009-2010 BSc

**Related Work Experience:** Teaching Assistant  
University of Western Ontario  
2010-2012

**Publications/Presentations:**

- Synthesis project was presented at the Nucleic Acids Chemistry and Biology 5<sup>th</sup> Cambridge Symposium, 31/08/2003, Queens' College, Cambridge, England.
- "*Chemistry for the synthesis of Modified PNA*" oral presentation, 39<sup>th</sup> IUPAC Congress 86<sup>th</sup> Conference of the Canadian Society for Chemistry, Ottawa, ON, oral presentation 08/2003, abstract # OR.3.017

**Volunteer Experience:** Research Assistant 2006 - 2007

LHSC  
London Ontario

**Professional Development:** Graduate student teaching award nominee (2011)

St. John's Ambulance First Aid